Dissertation zur Erlangung des Doktorgrades

der Fakultät für Chemie und Pharmazie

der Ludwig-Maximilians-Universität München

The role of RNA degradation in heterochromatin formation.

Cornelia Michaela Brönner

aus

Dachau, Deutschland

2017

Erklärung

Diese Dissertation wurde im Sinne von § 7 der Promotionsordnung vom 28. November 2011 von Herrn Prof. Dr. Mario Halic betreut.

Eidesstattliche Versicherung

Diese Dissertation wurde eigenständig und ohne unerlaubte Hilfe erarbeitet.

München, 10.3.2017

.....

Cornelia Michaela Brönner

Dissertation eingereicht am 10. März 2017

1. Gutachter: Prof. Dr. Mario Halic

2. Gutachter: Prof. Dr. Klaus Förstemann

Mündliche Prüfung am 10. Mai 2017

To my family

- my best experiment ever -

Part of this thesis has been published:

Brönner, C., Salvi, L., Zocco, M., Ugolini, I., and Halic, M. (2017). Accumulation of RNA on chromatin disrupts heterochromatic silencing. Genome Res. *27*, 1174–1183.

Table of Contents

Summary

Most cellular processes depend on proper transcriptional regulation. To maintain genome stability, large portions of the eukaryotic genome are silenced. This repressive chromatin is also called heterochromatin. Heterochromatin is required for centromere formation, gene silencing, repression of recombination and telomere stability. Long non-coding RNAs (lncRNAs) serve as platform for RNA interference (RNAi)-mediated heterochromatin formation in *Schizosaccharomyces pombe*. At the same time those RNAs are degraded by RNAi to generate siRNA which maintain heterochromatin in a positive feedback loop. That elimination of RNA is also essential to maintain heterochromatic silencing was discovered in this thesis.

The results of this thesis show, that in absence of the two degradation pathways RNAi and Ccr4-Not, heterochromatin is lost specifically at transcribed regions. The nuclease activity of both deadenylases, Ccr4 and Caf1, is required for transcriptional silencing indicating that RNA interferes with heterochromatin organization. In wild type cells, Caf1 and heterochromatic RNA are localized at the chromatin suggesting that heterochromatic transcripts are degraded on the chromatin. If the H3K9 methyltransferase Clr4 is deleted, Caf1 is even more found at heterochromatic regions, demonstrating that the recruitment to chromatin is independent of heterochromatin and it is likely mediated through RNA. Additionally, subtelomeric RNA is more associated with Caf1 in the chromatin fraction than in the soluble fraction. Further data show that heterochromatic transcripts and lncRNA accumulate on the chromatin and form R-loops in *caf1Δdcr1Δ* cells. To test if heterochromatic RNA accumulation might impair heterochromatin formation, an RNA overexpression study was performed. Subtelomeric *tlh* RNA was expressed at a heterochromatic locus under a repressible promoter in wild type cells. The result of this experiment shows that expression of heterochromatic *tlh* RNA, but not euchromatic RNA, abolishes heterochromatin maintenance even in wild type cells in a dose dependent way.

Heterochromatic RNA are targeted by RNAi which recruits the H3K9 methyltransferase to establish heterochromatin, but their uncontrolled accumulation hinders heterochromatin formation. This thesis shows that elimination of heterochromatic transcripts on the chromatin by RNAi and the Ccr4-Not complex is required for heterochromatin assembly. We propose that accumulation of chromatin-bound lncRNA interferes with heterochromatin organization and promotes chromatin opening.

1. Introduction

Deoxyribonucleic acid (DNA) is the carrier of genetic information in all living organisms and even in several viruses. In 1869, Friedrich Miescher was the first identifying a novel substance in the nucleus, which he named “nuclein” (Pray, 2008). Avery et al. proofed in 1944 that instead of proteins it is the, by then called DNA, which contains the heritable information (Avery et al., 1944). In 1953, Watson and Crick solved the double-helix structure of DNA (Watson and Crick, 1953). Since then the knowledge about DNA organization expanded enormously.

1.1 DNA organization within the cell

With evolution, the genomes became bigger, leading to a change in DNA organization. Prokaryotes compact their mostly circular DNA by supercoiling, which is stabilized by several proteins (Thanbichler et al., 2005). The prokaryotic DNA is not separated from the rest of the cell, but it accumulates at a region called nucleoid. With the evolution of the nucleus in eukaryotes, DNA organized in linear chromosomes and also the DNA scaffold became more complex. To compact DNA, but also to improve genome stability and regulate DNA accessibility, eukaryotic DNA is wrapped around protein octamers. This octamer is assembled from two copies each of the histones H2A, H2B, H3 and H4. DNA of approximately 145-147 base pairs (bp) wind around one histone octamer forming the basic unit, called nucleosome (Kornberg, 1974; Luger et al., 1997). This highly conserved pattern is repetitive along the whole DNA strand, building up the chromatin (Figure 1.1). Next to the nucleosomal histones exists another histone, the linker histone H1. The sequence of H1 is the least conserved of all histones and not present in S. *pombe* (Prieto et al., 2012). This histone is located between nucleosomes and its role includes stabilizing higher-order structures of the chromatin (Garcia-Ramirez et al., 1992). More important for the higher-order structure of chromatin are the histone tails of the nucleosome. This large, unstructured N-terminal part of each histone is sticking out from the nucleosome core (Luger et al., 1997) and those amino acids are prone for posttranslational modifications (PTM). The best studied PTMs are methylation, acetylation, phosphorylation, ubiquitination and ADP ribosylation (Strahl and Allis, 2000; Zentner and Henikoff, 2013). These modifications favor or inhibit binding of proteins or change the DNA-histone or nucleosome-nucleosome interaction which influences for example DNA replication, DNA repair, gene regulation and chromosome segregation (Bönisch et al., 2008). As those chromatin modifications are heritable and change the phenotype without changing the

genetic code, PTMs of histones belong to the field of epigenetics and it is important that their regulation works properly for genome stability (Margueron and Reinberg, 2010; Portela and Esteller, 2010).

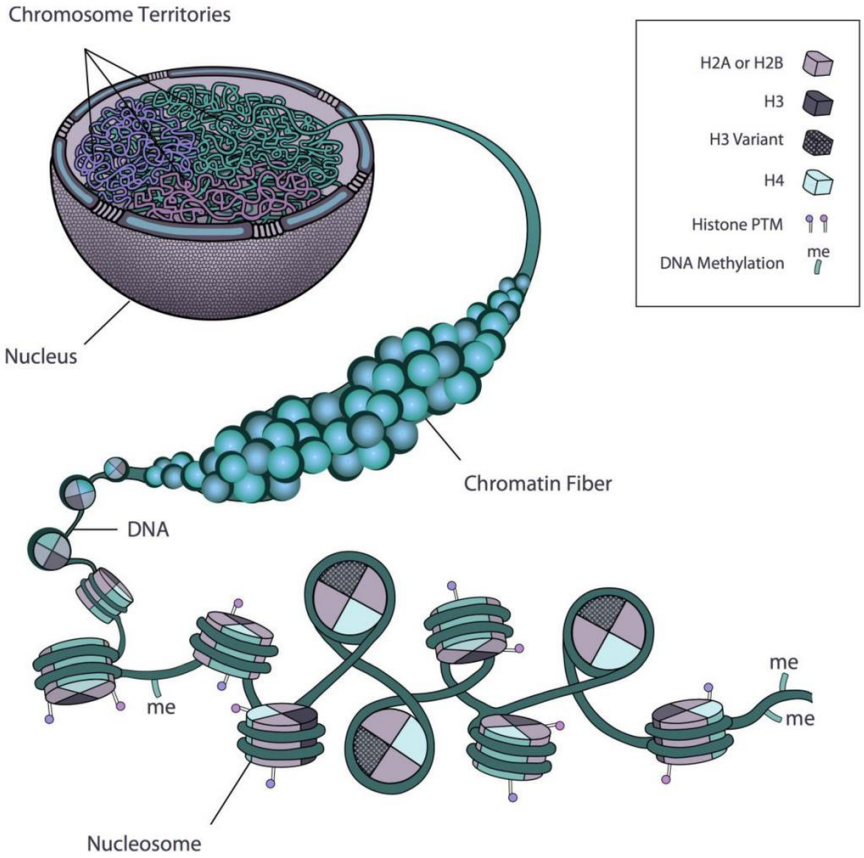

Figure 1.1 Eukaryotic chromatin organization (Rosa and Shaw, 2013)

DNA is wrapped around a histone octamer forming the smallest chromatin unit: the nucleosome. The chromatin fiber gets further compacted to fit into the nucleus. Modifications of DNA and histone tails determine accessibility and compaction of specific regions.

1.1.1 Euchromatin and heterochromatin

Epigenetic, posttranslational histone modifications are for example important to distinguish euchromatin from heterochromatin. Cytogenetically these two major forms of chromatin were identified already in 1928 due to different staining of interphase chromatin by Emil Heitz (Passarge, 1979). This method revealed compact regions, which stain strongly and are located at the periphery of the nucleus, the so called heterochromatin. In contrast the less stainable regions preferentially in the interior of the nucleus were named euchromatin (Passarge, 1979). The suggestions made based on the cytogenetic observations indeed could be confirmed biochemically. Euchromatin is rich in genes and correlates with high transcription levels, while the gene-poor and silent heterochromatin is connected with condensed packaging (Grewal and Moazed, 2003). On molecular level, euchromatin is associated with hyperacetylation of

nucleosomes at lysines, which is recognized by proteins with a bromodomain, like chromatin remodelers and transcriptional modifiers (O'Neill and Turner, 1995; Wang et al., 1997; Zeng and Zhou, 2002). Also methylation of histone 3 lysine 4 (H3K4) is euchromatin specific and is connected with increased transcription (Noma, 2001; Santos-Rosa et al., 2002). On the contrary, hallmarks for heterochromatin in fission yeast, metazoans and higher eukaryotes are hypoacetylated histone tails of H3 and H4, and H3K9 di- or trimethylation, which is bound by HP1 (heterochromatin protein 1) proteins (Bannister et al., 2001; Lachner et al., 2001; Nakayama et al., 2001; Rea et al., 2000; Snowden et al., 2002). These HP1 proteins dimerize and interact with other proteins which leads to condensation and a decreased accessibility of the chromatin (Maison and Almouzni, 2004; Smothers and Henikoff, 2000). Mostly in higher eukaryotes (fission yeast does not encode for a DNA methyltransferase), HP1 proteins recruit for example DNA methyltransferases, which leads to another heterochromatic mark: DNA methylation which also regulates transcription (Maison and Almouzni, 2004; Rountree and Selker, 2010; Xu et al., 1999).

1.1.2 Function of heterochromatin

Heterochromatin can be divided into constitutive and facultative heterochromatin. Constitutive heterochromatin remains throughout the cell cycle and is the same in different cells whereas facultative heterochromatin changes during development according to cellular signals (Trojer and Reinberg, 2007). Constitutive heterochromatin establishes at repetitive elements like the centromeres and subtelomeres (Cam et al., 2005). The overall function of heterochromatin is to maintain genome stability (Grewal and Jia, 2007; Henikoff, 2000): heterochromatin prevents homologous recombination of repetitive elements, which preserves the integrity of chromosomes (Peng and Karpen, 2008); it is important for gene regulation, mainly silencing (Henikoff, 1990), for example silencing of transposable elements (TE) in germline cells (Slotkin and Martienssen, 2007) or regulating gene dosage by X-chromosome inactivation (Heard, 2006; Maxfield Boumil, 2001); centromeric heterochromatin is necessary for correct chromosome segregation (Allshire et al., 1995; Ekwall et al., 1997; Peters et al., 2001; Taddei et al., 2001). For a long time, heterochromatin was considered to be static and transcriptional inert. Instead it was shown that heterochromatin is dynamic and that transcription is necessary for the establishment and maintenance of heterochromatin as described later (Cheutin et al., 2003; Festenstein et al., 2003; Reinhart and Bartel, 2002; Volpe et al., 2002)

1.2 Noncoding RNAs

The Human Genome Project revealed, that only a small fraction of the genome encodes proteins. Originally most noncoding transcripts were described as "junk" or artifacts of an applied method, nowadays it is known that many of those RNAs have a distinct function (Claverie, 2005; Deniz and Erman, 2016; Djebali et al., 2012; Kapranov et al., 2007). There are well known non-coding RNAs (ncRNAs) like ribosomal RNAs (rRNAs) and transfer RNAs (tRNAs), which are both important for translation (Noller, 1993; Wright and Bruford, 2011). rRNAs form together with ribosomal proteins the ribosome, tRNAs recruit sequence specific amino acids to the ribosome-bound messenger RNA (mRNA) to generate proteins (Dahlberg, 1989). Another class of ncRNAs comprises small RNAs (sRNAs), like micro RNAs (miRNAs), endogenous small inhibitory RNAs (siRNAs), or small nucleolar RNAs (snoRNAs) (Deniz and Erman, 2016). snoRNAs play a role in rRNA and tRNA maturation (Maden and Hughes, 1997); Both, miRNAs and siRNAs, are connected with gene silencing, either posttranscriptionally or siRNA for example also due to heterochromatin formation by targeting nascent transcripts (explained more in detail in 1.3). Those nascent transcripts mostly belong to a third class of ncRNAs: long noncoding RNAs (lncRNAs). lncRNAs are longer than 200 nucleotides (nt) in length and mostly display features like mRNA (transcribed by RNA polymerase II, 3' polyadenylation, 5' cap) except that they do not encode proteins (Rutenberg-Schoenberg et al., 2016). Those transcripts originate from antisense transcription, intergenic regions or introns and the function of most lncRNAs remains unknown (Claverie, 2005). Often lncRNAs are associated with regulation of transcription, for example due to chromatin modification. Several lncRNAs, like HOTAIR or *Xist* were proposed to recruit the Polycomb repressive complex 2 (PRC2) to chromatin (Brockdorff, 2013). PRC2 is responsible for trimethylation of lysine 27 on histone H3 (H3K27me3), a repressive chromatin mark important in development and cancer formation (Conway et al., 2015; Müller et al., 2002; Schwartz et al., 2006). H3K27me3 is a mark for facultative heterochromatin and does not exist in yeast. HOTAIR is an **HO**X **t**ranscript **a**ntisense **R**NA, which silences expression of the HOXC locus in *trans* (Rinn et al., 2007). HOX genes encode transcription factors, mainly important for cell differentiation (Barber and Rastegar, 2010). *Xist* is a ~17 kb lncRNA which covers the silenced X-chromosome and is responsible for dosage compensation in female mammals (Brown et al., 1991). Similar to *Xist* but with inverse result, roX lncRNAs increase transcription of the X chromosome in male *D. melanogaster* to adjust the levels similar to female cells. roX RNA is also coating the X

chromosome and it is assembled in a chromatin-modifying complex (called MSL) leading to H4K16 acetylation, which is linked to decondensation of chromatin (Lucchesi et al., 2005; Meller and Rattner, 2002; Smith et al., 2000).

LncRNA can also respond to environmental changes and regulate for example flowering in *Arabidopsis thaliana*. Two lncRNAs, COLDAIR and COOLAIR, are transcripts of the flowering locus (FLC). COOLAIR is an antisense RNA of the FLC, which is highly upregulated and alternatively polyadenylated in cold conditions and correlates with reduced H3K4 methylation and silencing (Ietswaart et al., 2012). In extended cold periods, COLDAIR, an intronic sense lncRNA of FLC, is proposed to repress transcription additionally to COOLAIR in a Polycomb-dependent way, leading to H3K27me3 (Heo and Sung, 2011).

These are few examples demonstrating the importance of lncRNAs. Their exact pathways remain elusive, but they suggest a role for ncRNAs in regulating chromatin changes. It is however still a controversial topic if lncRNA can directly recruit chromatin modifying proteins or if this mechanism is indirect (Davidovich and Cech, 2015).

1.3 Heterochromatin in *Schizosaccharomyces pombe*

The unicellular, rod-shaped, haploid eukaryote *Schizosaccharomyces pombe* (*S. pombe*) belongs to the kingdom of fungi (Mitchison, 1990; Piel and Tran, 2009). As it divides by medial fission, *S. pombe* is also called fission yeast (Piel and Tran, 2009). The genome consists of three chromosomes with a total size of 13.8 Mb (Wood et al., 2002). *S. pombe* is an ideal model organism to study heterochromatin due to easy genetics, a fast replication time and especially because of its similarities to higher eukaryotes, but with less redundant genes (Bähler et al., 1998; Goto and Nakayama, 2012; Wixon, 2002). Heterochromatic features like H3K9 methylation, heterochromatic proteins (e.g. HP1 proteins, methyltransferase, RNAi) and also telomeric proteins (proteins of the Shelterin complex) are conserved from fission yeast to higher eukaryotes (Goto and Nakayama, 2012; de Lange, 2005; Martienssen et al., 2005). Constitutive heterochromatin in *S. pombe* is located at the pericentromeric repeats, the mating type locus and at the subtelomeres (Allshire, 1995; Cam et al., 2005). Low levels of H3K9 methylation are also found at meiotic genes (Hiriart et al., 2012; Marasovic et al., 2013; Zofall et al., 2012).

1.3.1 Centromeres

All three chromosomes contain regional centromeres which are flanked by inverted repeats similar to plants and metazoans. The central core is surrounded by the innermost repeats (*imr*), which are unique on each chromosome. The outer repeat region (*otr*) consists mainly of the two repetitive elements *dg* and *dh*, which are present in different copy numbers at each centromere (Allshire, 1995; Martienssen et al., 2005; Wood et al., 2002). Heterochromatin establishes at the *imr* and *otr* repeats and silences reporter genes inserted into these regions (Allshire et al., 1994, 1995; Fishel et al., 1988). Crucial for establishment and maintenance of centromeric heterochromatin is the RNA interference (RNAi) pathway (Volpe et al., 2002).

1.3.2 RNAi dependent heterochromatin formation

RNAi is mostly connected with posttranscriptional gene silencing and defending the cell from external RNA, like viruses (Hannon, 2002). It was also shown that RNAi is important for regulating chromatin in different organisms (Moazed, 2009). In *S. pombe*, the RNAi dependent heterochromatin formation is well studied. The pathway is initiated by primal small RNAs (priRNAs), which are generated from degradation products from bidirectional transcribed repeats (Halic and Moazed, 2010). These single stranded degradation products bind Argonaute (Ago1) and they are trimmed by the CAF1 family of 3'-5' exonuclease Triman (Tri1) to mature priRNAs with the length of small interfering RNAs (siRNAs), 22-23 nucleotides (Marasovic et al., 2013). Together with the chromodomain protein Chp1 and the GW protein Tas3, siRNA-loaded Ago1 forms the **R**NA **i**nduced **t**ranscriptional **s**ilencing (RITS) complex (Verdel et al., 2004). RITS targets siRNA-complementary nascent RNA and is responsible for the recruitment of the **R**NA-**d**irected **R**NA polymerase **c**omplex (RDRC) to those transcripts (Bühler et al., 2006; Motamedi et al., 2004; Sugiyama et al., 2005). RDRC generates the complementary strand of the targeted transcript, leading to double stranded RNA, which is further processed by the RNase III Dicer (Dcr1) into siRNA duplexes (Colmenares et al., 2007; Reinhart and Bartel, 2002; Volpe et al., 2002). Additionally, RDRC and RITS associate with the **Cl**r4-**R**ik1-**C**ul4 (CLRC) complex, leading to methylation of H3K9 by the methyltransferase Clr4 (Bayne et al., 2010; Gerace et al., 2010; Nakayama et al., 2001; Zhang et al., 2008). The HP1 proteins Swi6 and Chp2 bind methylated H3K9, leading to the assembly of heterochromatin and silencing (Bannister et al., 2001; Motamedi et al., 2008; Sugiyama et al., 2007). Heterochromatin is maintained by the positive feedback loop continued by the newly formed siRNA duplexes. The **Ar**gonaute siRNA **c**haperone (ARC) complex loads the siRNA onto Ago1, which slices one strand

and generates a new RITS complex (Holoch and Moazed, 2015) (Figure 1.2). Once established, H3K9 methylation can also be maintained and spread by Clr4 itself over several cell cycles. Clr4 can bind methylated H3K9 by its chromodomain and then it propagates this methylation mark to adjacent nucleosomes (Al-Sady et al., 2013; Audergon et al., 2015; Ragunathan et al., 2015).

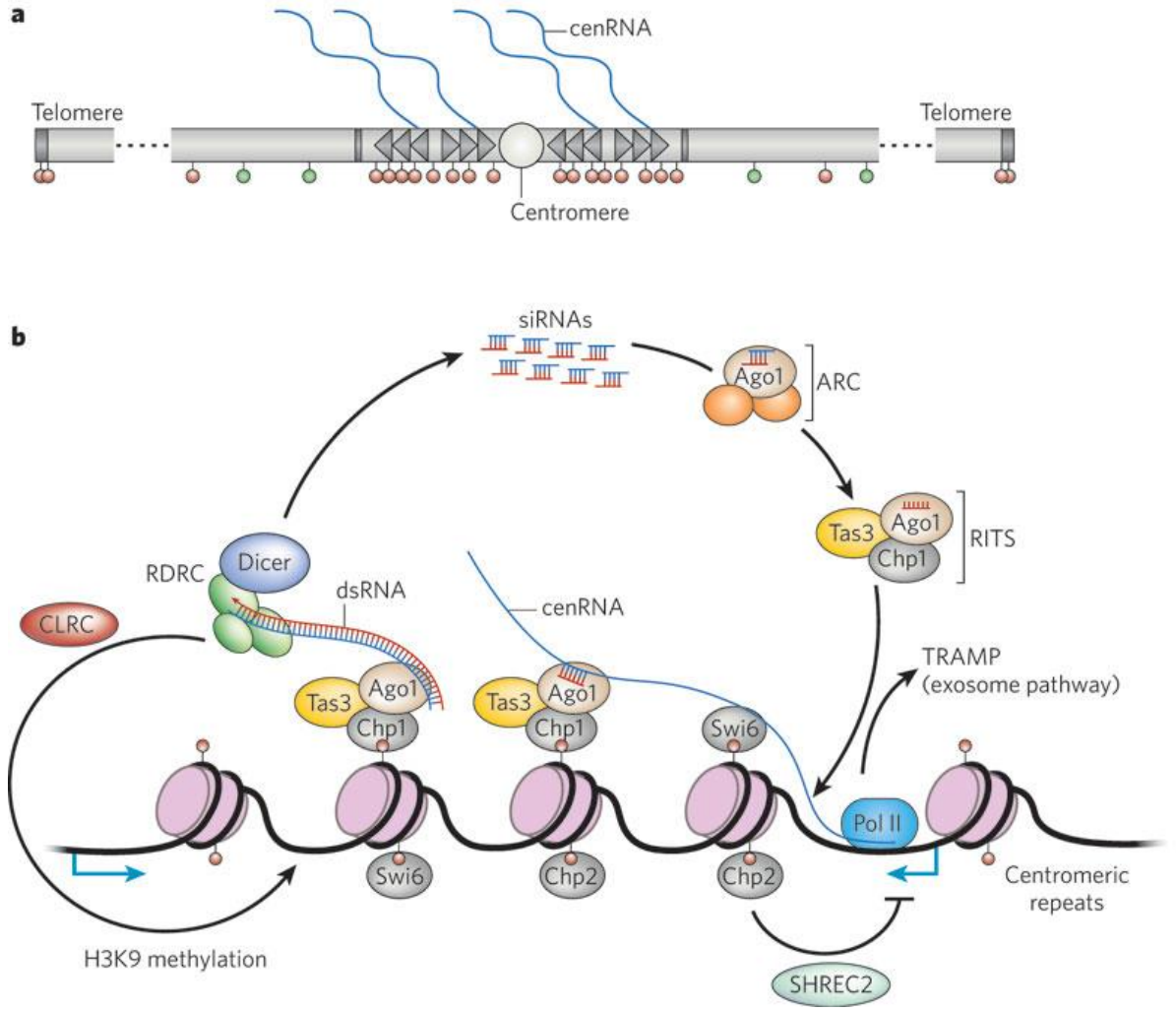

Figure 1.2 RNAi dependent heterochromatin formation

a) Presentation of chromosome 1 in *S. pombe*. Red dots indicate H3K9 methylation, at centromeric repeats and subtelomeres. Although centromeric repeats are silenced with heterochromatin, there is still transcription. b) This transcription is necessary for heterochromatin formation by RNAi. Ago1, a subunit of the RITS complex, is loaded with siRNA which target nascent complementary RNA. Recruitment of RDRC leads to double stranded RNA which is sliced by Dcr1 into new siRNA. Those siRNA are loaded onto Ago1 with the ARC complex starting the feedback loop again. Furthermore, CLRC is recruited to the chromatin by RDRC and RITS and methylates H3K9, where HP1 proteins (Swi6 and Chp2) bind to establish heterochromatin.

The mechanism, that small RNA establish heterochromatin is conserved. Similar to siRNAs in *S. pombe,* piRNAs (PIWI interacting RNA) silence mainly transposable elements in animal germline cells (Tóth et al., 2016). PIWI proteins belong to a subclass of Argonaute proteins and bind piRNAs, which are slightly larger than siRNAs. This complex silences either posttranscriptionally or regulates transcription by depositing repressive histone marks or DNA methylation (Aravin et al., 2008; Kuramochi-Miyagawa et al., 2008; Sienski et al., 2012). Also in plants, siRNAs are responsible for silencing by induction of DNA methylation (Matzke et al., 2004).

1.3.3 Mating type locus

On the right arm of chromosome 2 is the position of the mating type (*mat*) locus, consisting in homothallic h90 strains of three main components: *mat1*, *mat2-P* and *mat3-M* (Klar, 2007) (Figure 1.3). According to which sequence (M for minus or P for plus) is integrated at *mat1*, the mating type is determined. Only cells with different mating type can mate, which happens under stress conditions (Klar et al., 2014). At *mat2-P* and *mat3-M* are the sequences for M and P encoded additionally, which are used for switching the mating type via transposition to *mat1* (Klar, 2007). Expression of the *mat1* locus only occurs if cells initiate mating, for example under nitrogen starvation (Kelly et al., 1988; Thon and Klar, 1992). *mat2-P* and *mat3-M* are in general silenced, but if heterochromatin is lost and cells starve they are also expressed (Thon and Klar, 1992).

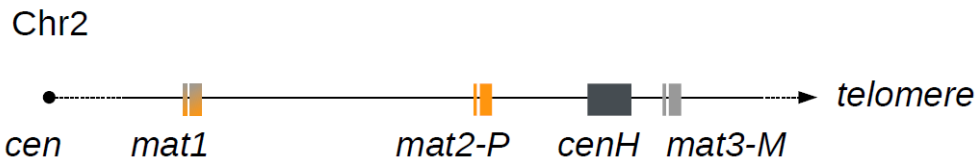

Figure 1.3 Scheme for the mating type locus.

The *mat* locus is encoded on the right arm of chromosome 2. *mat1* expresses either P or M and determines the mating type of a cell. *mat2*-P and *mat3*-M are silenced and are used for switching through homologous recombination. The *cenH* element is important for RNAi dependent heterochromatin establishment.

In h90 strains equal amounts of M and P cells are found, but the mating type locus can rearrange, leading to heterothallic strains (Beach and Klar, 1984). Heterothallic strains (h^+, h^-) in general do not switch, but especially h^+ strains are able to revert their mating type (Beach and Klar, 1984). Between *mat2-P* and *mat3-M* lies the 4.3 kb *cenH* element. *cenH* shares 96%

homology with the centromeric *dg* and *dh* repeats and is essential for heterochromatin establishment involving the RNAi pathway (Grewal and Klar, 1997; Hall et al., 2002). RNAi is however dispensable for heterochromatin maintenance (Hall et al., 2002). Between *cenH* and *mat3-M* are binding sites for the ATF/CREB transcription factors Atf1/Pcr1 (Jia et al., 2004a). Those transcription factors are conserved and regulate gene expression during sexual development and environmental stress (Takeda et al., 1995; Watanabe and Yamamoto, 1996; Wilkinson et al., 1996). Atf1 and Pcr1 recruit the histone deacetylases Clr3 and Clr6 as well as the HP1 protein Swi6 to maintain silencing (Kim et al., 2004a; Yamada et al., 2005). Once established, Clr4 can propagate H3K9 methylation itself (Al-Sady et al., 2013; Audergon et al., 2015; Ragunathan et al., 2015) but also Atf1 and Pcr1 were shown to nucleate heterochromatin independently of RNAi (Jia et al., 2004a). Heterochromatin at the *mat* locus is especially important for directional mating type switching (Jia et al., 2004b; Lorentz et al., 1992).

1.3.4 Subtelomeres

The subtelomeric region is highly homologous on both arms of chromosome 1 and 2 with at least 4 copies of *tlh* present (Hansen et al., 2006; Mandell et al., 2005a). On chromosome 3, ribosomal DNA (rDNA) repeats are inserted between coding genes and telomeres with H3K9 methylation between the rDNA open reading frames (ORFs) (Cam et al., 2005). The Shelterin complex binds telomeres and recruits the CLRC methyltransferase and the SHREC deacetylase complexes (Snf2-histone deacetylase repressor complex) (Kanoh et al., 2005; Motamedi et al., 2008; Sugiyama et al., 2007; Tadeo et al., 2013; Wang et al., 2016). Subsequently, CLRC and SHREC spread from the telomeric repeats into the subtelomeric region to establish heterochromatin. Next to the Shelterin complex, also RNAi can establish subtelomeric heterochromatin, which is only lost if both redundant establishment pathways are depleted (Hansen et al., 2006; Kanoh et al., 2005; Mandell et al., 2005b) (Figure 1.4). Also depletion of the telomeric repeats (where Shelterin binds) up to the subtelomeres including *tlh* leads to loss of heterochromatin (Kanoh et al., 2005), indicating that both pathways are recruited to these regions. *tlh* shares a homologous region with *cenH* were small amounts of siRNA map in wild type cells (Cam et al., 2005), assuming that with loss of *tlh*, RNAi recruitment is impaired. Although several stress induced genes are located at the subtelomeric region, *tlh* expression is not influenced by either nitrogen starvation or growth in stationary phase (Hansen et al., 2006). Overexpression of *tlh* was shown to increase viability of telomerase deficient cells but

the function of the annotated RecQ type helicase is not known (Mandell et al., 2005a). Subtelomeric heterochromatin is important to maintain genome stability by prevention of inter- and intrachromosomal recombination or end fusion (Kanoh et al., 2005).

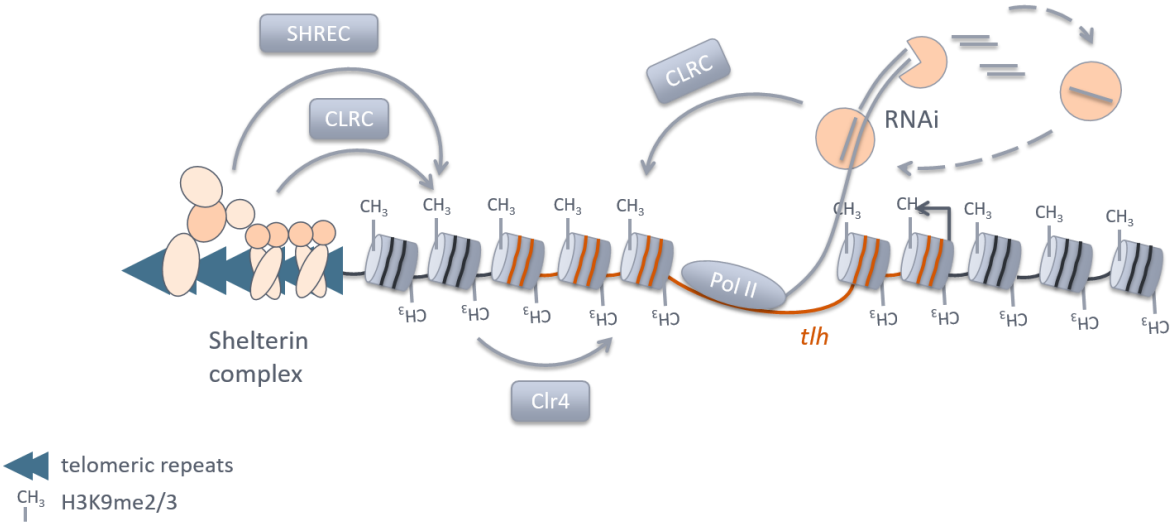

Figure 1.4 Heterochromatin establishment at subtelomeres.

The Shelterin complex is located at the telomeric repeats and recruits the SHREC deacetylase complex as well as CLRC with the H3K9 methyltransferase Clr4. If the Shelterin complex is depleted, RNAi is recruited to the subtelomeres to establish heterochromatin. Clr4 is able to spread heterochromatin, once it is established.

1.4 The role of the Ccr4-Not complex in RNA degradation

1.4.1 Eukaryotic RNA degradation pathways

To increase their stability, most RNA polymerase II-transcribed mRNAs have a 5' 7-methyl guanosine cap and a non-templated 3' poly adenosine stretch, called poly(A) tail (Garneau et al., 2007; Mangus et al., 2003; Moore and Proudfoot, 2009; Zhang et al., 2010). Posttranscriptionally, the RNA is cleaved at the polyadenylation site to release it from the polymerase followed by adenylation (Murthy and Manley, 1995; Sheets and Wickens, 1989). Shortening of this poly(A) tail is mostly the first step of RNA degradation, with three complexes, Ccr4-Not, PAN and PARN, known to be deadenylases (Parker and Song, 2004). The Ccr4-Not complex is the predominant deadenylase complex (Daugeron et al., 2001; Tucker et al., 2001). PAN controls the length of poly(A) tails of individual mRNA species (Brown and Sachs, 1998) and is suggested to initiate deadenylation in the cytosol (Yamashita et al., 2005). The *in vivo* role of PARN in mRNA degradation is not completely solved (Yamashita et al., 2005). In *S. pombe*, its homologue Triman was shown to process small RNA to generate priRNAs

(Marasovic et al., 2013). Deadenylation of mRNA is either followed by decapping of the protective 5’ cap with consecutive 5’-3’ digestion by the exonuclease Xrn1 (= Exo2 in *S. pombe*) (Beelman et al., 1996; Stevens and Maupin, 1987) or by 3’-5’ degradation through the exosome (Anderson and Parker, 1998) (Figure 1.5). Next to this main degradation pathways also deadenylation independent 5’-3’ or 3’-5’ decay as well as endonucleolytic digest control RNA levels in the cell (Garneau et al., 2007).

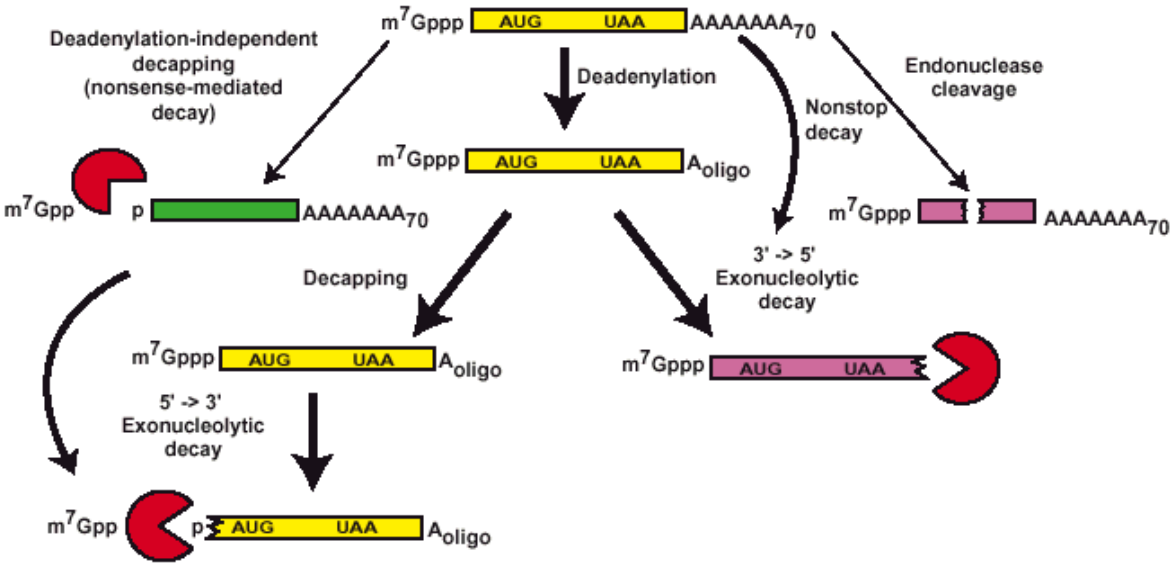

Figure 1.5 RNA degradation pathways.

Degradation of polyadenylated RNA starts mostly by deadenylation which is either followed by decapping and subsequent 5’-3’ exonucleolytic digest or by 3’-5’ degradation. RNA degradation can also start with decapping or endonucleolytic cleavage.

1.4.2 The Ccr4-Not complex

The **C**arbon **c**atabolite **r**epressor protein 4 **n**egative **o**n **T**ATA (Ccr4-Not) complex is a multifunctional, essential complex, consisting of up to 10 subunits. The complex is conserved in all eukaryotes and was reported to be involved in all steps from RNA transcription to protein turnover (Collart, 2016). It used to be described as a transcription regulator, however only two enzymatic functions were detected so far: deadenylation and ubiquitination (Collart and Panasenko, 2012). There exist two low resolution structures of the whole complex (Nasertorabi et al., 2011; Ukleja et al., 2016) (Figure 1.6) but due to several co-immunoprecipitations, yeast-2-hybrid experiments and high resolution X-ray structures of individual subunits, it is known that Not1 builds the essential scaffold protein to which the

other subunits bind (Xu et al., 2014). Next to Not1, also Not2, Not3/5, Rcd1 (= Caf40, CNOT9), and the deadenylases Ccr4 and Caf1 (**C**cr4p **a**ssociated **f**actor 1; *S. cerevisiae:* Pop2) belong to the highly conserved core proteins. Not4 (= Mot2 in S. *pombe*) is a conserved RING finger E3 ubiquitin ligase, which is a stable subunit of the Ccr4-Not complex in yeast but not in human and *D. melanogaster* (Albert et al., 2002; Bhaskar et al., 2015; Hanzawa et al., 2001; Lau et al., 2009; Temme et al., 2010). Another, not stable associated subunit is the putative ABC ATPase Caf16, which interacts with Ccr4 (Liu et al., 2001). S. *cerevisiae* Caf130, which resembles D. *melanogaster* Not10 and human Cnot10, and Cnot11 is not a subunit of the Ccr4-Not complex in *S. pombe* (Ukleja et al., 2016). In *S. pombe* Mmi1, a protein regulating the decay of meiotic transcripts, was also found to stably interact with the complex (Ukleja et al., 2016).

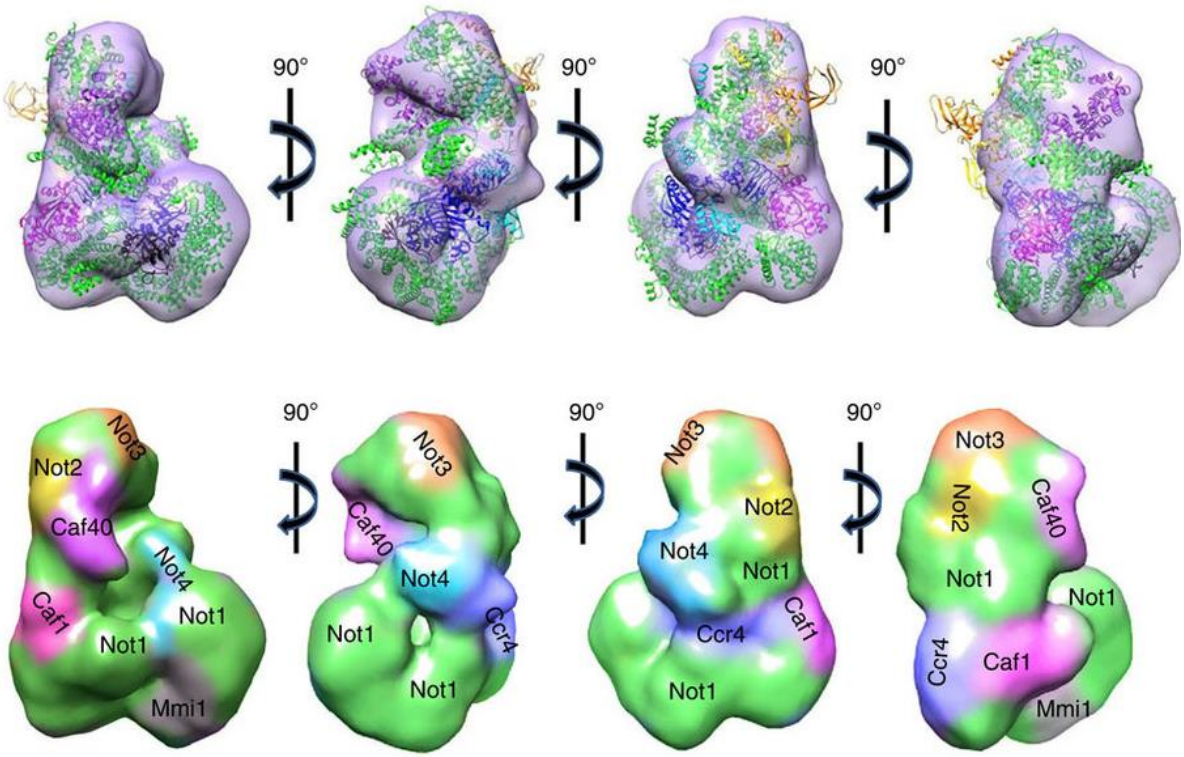

Figure 1.6 Model for subunit organization of the Ccr4-Not complex in *S. pombe* (Ukleja et al., 2016)

3D reconstitution of the Ccr4-Not complex and indication of possible subunit localization of the Ccr4-Not complex. The Ccr4-Not complex is L-shaped and consists of the core proteins Not1, Not2, Not3, Rcd1 (= Caf40), Caf1, and Ccr4. In *S. pombe*, Not4 (= Mot2) and Mmi1 are also stably associated with the complex.

1.4.3 Function of the Ccr4-Not complex

The main function of the Ccr4-Not complex is RNA degradation. In higher eukaryotes it is suggested that the BTG/TOB family of proteins direct the complex to mRNAs for generic digest (Winkler, 2010). These proteins are not conserved in yeast, proposing another general recruitment mechanism (Collart, 2016). Furthermore, the Ccr4-Not complex is connected to specific RNA decay. In higher eukaryotes, RNAi targets particular mRNA using sRNA called micro RNA (miRNA) (Huntzinger and Izaurralde, 2011). Via the interaction of CNOT9 (Rcd1 in *S. pombe*) with the GW182 protein (Tas3 in *S. pombe*) of the RITS complex, the Ccr4-Not complex is recruited to degrade those transcripts (Chen et al., 2014; Mathys et al., 2014). Additionally, Tristetraprolin (TTP) was published to mediate Ccr4-Not dependent decay of specific, AU rich element (ARE) containing mRNAs (Fabian et al., 2013; Sandler et al., 2011) and also the germline specific protein Nanos was shown to interact with the Ccr4-Not complex (Suzuki et al., 2010). Besides deadenylation, the Ccr4-Not complex is connected with protein turnover by the E3 ubiquitin ligase Not4 (*S. pombe* Mot2) (Dimitrova et al., 2009; Laribee et al., 2007; Matsuda et al., 2014; Mersman et al., 2009). Additionally, the Ccr4-Not complex is associated with regulation of transcription (Collart, 2016; James et al., 2007; Kruk et al., 2011; Lenssen et al., 2005), but the precise role remains elusive.

1.4.1 Ccr4 and Caf1 – the deadenylases of the Ccr4-Not complex

Ccr4 and Caf1 are the major deadenylases in the cell (Daugeron et al., 2001; Tucker et al., 2001). Caf1 binds Not1 at the N-terminus and is required for recruitment of Ccr4 to the complex (Bai et al., 1999; Basquin et al., 2012; Dupressoir et al., 2001; Liu et al., 1998). Ccr4 is an endonuclease-exonuclease-phosphatase (EEP) type nuclease with high poly(A) affinity and it is the primary deadenylase in *S. cerevisiae* (Chen et al., 2002; Tucker et al., 2002). Caf1 belongs to the DEDD-family of exonucleases because of the conserved Asp and Glu motif in the active center (Horiuchi et al., 2009; Jonstrup et al., 2007; Thore et al., 2003). In mammalian cells and in *S. pombe*, also Caf1 displays enzymatic activity to shorten poly(A) tails (Mauxion et al., 2008; Sandler et al., 2011; Stowell et al., 2016). Although, Caf1 and Ccr4 deadenylate RNA *in vitro* without the addition of other components of the complex (Jonstrup et al., 2007; Thore et al., 2003; Tucker et al., 2002), efficient RNA decay *in vivo* requires the assembly of the deadenylases with Not1 (Basquin et al., 2012; Petit et al., 2012).

1.5 Aim of this study

Heterochromatin is an efficient way to silence large regions of the genome due to reduced accessibility. In small RNA mediated heterochromatin formation, long non-coding RNAs serve as a template for Argonaute targeting, siRNA generation, and recruitment of the H3K9 methyltransferase complex CLRC (Moazed, 2009). To maintain the RNAi feedback loop, the lncRNA is degraded to form new sRNA. If elimination of this lncRNA, besides the generation of sRNA, is important for heterochromatin formation was the topic of this thesis.

As removing the RNase Dicer or its activity would inhibit the whole RNAi pathway including heterochromatin establishment, the goal was to find an RNase which would contribute to heterochromatin formation and also analyze why RNA needs to be degraded. In *S. pombe*, establishment of heterochromatin largely depends on the RNAi pathway. To distinguish heterochromatin maintenance from establishment, the focus was on subtelomeres, as deletion of proteins from the RNAi pathway does not prevent heterochromatin establishment there. Still the other constitutive heterochromatin loci were important to analyze as well.

If RNA degradation is important for heterochromatin formation, the question arises why heterochromatic RNA is needed to be eliminated. How could RNA influence heterochromatin? And is there a difference to euchromatic RNA? Genome wide data analysis was performed to address these questions.

2. Material and Methods

2.1 Material

2.1.1 *S. pombe* strains

Table 2.1 *S. pombe* strains used in this study

Number	Genotype of *S. pombe* strain	Origin
65	h90 otr1R(SphI)::ura4+ ura4-DS/E leu1-32 ade6-M210 natMX6::3xFLAG-*ago1*	SPY797
80	h+ leu1-32 ade6-210 ura4DS/E otrR(SPhI)::ura4+ *clr4*Δ::kanMX6	SPY815
34	h90 otr1R(SphI)::ura4+ ura4-DS/E leu1-32 ade6-M210 natMX6::3xFLAG-*ago1 dcr1*Δ::hphMX6	
260	h+ otr1R(SphI)::ura4+ ura4-DS/E leu1-32 ade6-M210 *ago1*Δ::kanMX6	SPY418
510	h90 otr1R(SphI)::ura4+ ura4-DS/E leu1-32 ade6-M210 natMX6::3xFLAG-*ago1 caf1*Δ::kanMX6	
521/522	h90 otr1R(SphI)::ura4+ ura4-DS/E leu1-32 ade6-M210 natMX6::3xFLAG-*ago1 caf1*Δ::kanMX6 *dcr1*Δ::hphMX6	
523/524	h90 otr1R(SphI)::ura4+ ura4-DS/E leu1-32 ade6-M210 natMX6::3xFLAG-*ago1*Δ::hphMX6 *caf1*Δ::kanMX6	
544	h90 otr1R(SphI)::ura4+ ura4-DS/E leu1-32 ade6-M210 natMX6::3xFLAG-*ago1 ccr4*Δ::hphMX6	
577	h90 otr1R(SphI)::ura4+ ura4-DS/E leu1-32 ade6-M210 natMX6::3xFLAG-*ago1 ccr4*Δ::hphMX6 *dcr1*Δ::kanMX6	
1023	h90 otr1R(SphI)::ura4+ ura4-DS/E leu1-32 ade6-M210 natMX6::3xFLAG-*ago1 mot2*Δ::kanMX6	
997	h90 otr1R(SphI)::ura4+ ura4-DS/E leu1-32 ade6-M210 natMX6::3xFLAG-*ago1 dcr1*Δ::hphMX6 *mot2*Δ::kanMX6	
651	h90 otr1R(SphI)::ura4+ ura4-DS/E leu1-32 ade6-M210 natMX6::3xFLAG-*ago1 not2*Δ::kanMX6	

Number	Genotype of *S. pombe* strain	Origin
654	h90 otr1R(SphI)::ura4+ ura4-DS/E leu1-32 ade6-M210 natMX6::3xFLAG-*ago1 not2*Δ::kanMX6 *dcr1*Δ::hphMX6	
728	h90 otr1R(SphI)::ura4+ ura4-DS/E leu1-32 ade6-M210 natMX6::3xFLAG-*ago1 rcd1*Δ::kanMX6	
729	h90 otr1R(SphI)::ura4+ ura4-DS/E leu1-32 ade6-M210 natMX6::3xFLAG-*ago1 rcd1*Δ::kanMX6 *dcr1*Δ::hphMX6	
735	h90 otr1R(SphI)::ura4+ ura4-DS/E leu1-32 ade6-M210 natMX6::3xFLAG-*ago1 caf16*Δ::kanMX6	
736	h90 otr1R(SphI)::ura4+ ura4-DS/E leu1-32 ade6-M210 natMX6::3xFLAG-*ago1 caf16*Δ::kanMX6 *dcr1*Δ::hphMX6	
633	h90 otr1R(SphI)::ura4+ ura4-DS/E leu1-32 ade6-M210 natMX6::3xFLAG-*ago1 taz1*Δ::kanMX6	
636	h90 otr1R(SphI)::ura4+ ura4-DS/E leu1-32 ade6-M210 natMX6::3xFLAG-*ago1 taz1*Δ::kanMX6 *dcr1*Δ::hphMX6	
588	h90, ade6-D1, his3-D1, leu1-3, ura4-D18, otr1R(SphI)::ade6+, TAS-his3+-tel1(L), TAS-ura4+-tel2(L)	FY1862
591	h90, ade6-D1, his3-D1, leu1-3, ura4-D18, otr1R(SphI)::ade6+, TAS-his3+-tel1(L), TAS-ura4+-tel2(L), *caf1*Δ::kanMX6	
599	h90, ade6-D1, his3-D1, leu1-3, ura4-D18, otr1R(SphI)::ade6+, TAS-his3+-tel1(L), TAS-ura4+-tel2(L), *dcr1*Δ::hphMX6	
600	h90, ade6-D1, his3-D1, leu1-3, ura4-D18, otr1R(SphI)::ade6+, TAS-his3+-tel1(L), TAS-ura4+-tel2(L), *caf1*Δ::kanMX6, *dcr1*Δ::hphMX6	
955	h90, ade6-D1, his3-D1, leu1-3, ura4-D18, otr1R(SphI)::ade6+, TAS-his3+-tel1(L), TAS-ura4+-tel2(L) *caf1*Δ::natMX6, *taz1*Δ::kanMX6	
301	h90, mat3::ura4, ura4-DS/E, leu1-32, ade6-M210, *swi6*Δ::natMX6	
999	h90, 301 x 599, *swi6*Δ::natMX6, *dcr1*Δ::hphMX6	
1002	h90, 301 x 591, *swi6*Δ::natMX6, *caf1*Δ::kanMX6	

Number	Genotype of *S. pombe* strain	Origin
63	h+ otr1R(SphI)::ura4+ ura4-DS/E leu1-32 ade6-M210	
773	h+ otr1R(SphI)::ura4+ ura4-DS/E leu1-32 ade6-M210 natMX6::3xFLAG-3xHA-*caf1*	
848	h+ otr1R(SphI)::ura4+ ura4-DS/E leu1-32 ade6-M210 natMX6::3xFLAG-3xHA-*caf1 clr4*Δ::kanMX6	
1038	h90 otr1R(SphI)::ura4+ ura4-DS/E leu1-32 ade6-M210 natMX6::3xFLAG-*ago1* SPNCRNA.70Δ::ade6-2xbla-hph-nmt1-5'*tlh*-adh1T	L. Salvi
1039	h90 otr1R(SphI)::ura4+ ura4-DS/E leu1-32 ade6-M210 natMX6::3xFLAG-*ago1* SPNCRNA.70Δ::ade6-2xbla-hph-nmt1-3'*tlh*-adh1T	L. Salvi
1040	h90 otr1R(SphI)::ura4+ ura4-DS/E leu1-32 ade6-M210 natMX6::3xFLAG-*ago1* SPNCRNA.70Δ::ade6-2xbla-hph-nmt1-*LEU2*-adh1T	L. Salvi
746	h90 otr1R(SphI)::ura4+ ura4-DS/E leu1-32 ade6-M210 natMX6::3xFLAG-*ago1 caf1*Δ::kanMX6 *ccr4*Δ::hphMX6	
530	h90 otr1R(SphI)::ura4+ ura4-DS/E leu1-32 ade6-M210 natMX6::3xFLAG-*ago1 exo2*Δ::kanMX6	
558	h90 otr1R(SphI)::ura4+ ura4-DS/E leu1-32 ade6-M210 natMX6::3xFLAG-*ago1 mlo3*Δ::hphMX6	
708	h90 otr1R(SphI)::ura4+ ura4-DS/E leu1-32 ade6-M210 kanMX6::3xFLAG-*ago1 cid14*Δ::natMX6	P. Pisacane
581	h90 ade6-M210 leu1-32 ura4-D18 *taz1*+: HA-ura4+	SPTN327
602	h90 ade6-M210 leu1-32 ura4-D18 *taz1*+: HA-ura4+ *caf1*Δ::kanMX6 *dcr1*Δ::hphMX6	
1073	h+ otr1R(SphI)::ura4+ ura4-DS/E leu1-32 ade6-M210 *caf1*Δ::kanMX6 *dcr1*Δ::hphMX6	

Number	Genotype of *S. pombe* strain	Origin
1082	h+ otr1R(SphI)::ura4+ ura4-DS/E leu1-32 ade6-M210 natMX::*caf1* promoter *caf1*, *dcr1*Δ::hphMX6	
1084	h+ otr1R(SphI)::ura4+ ura4-DS/E leu1-32 ade6-M210 natMX::*caf1* promoter *caf1*, *dcr1*Δ::hphMX6 nat::*caf1*promoter-*caf1*D53AD243AD174A	
1141	h+ otr1R(SphI)::ura4+ ura4-DS/E leu1-32 ade6-M210 natMX::*caf1*, *ccr4*H664A-*ccr4*Terminator::hphMX6 *dcr1*Δ::hphMX6	
1143	h+ otr1R(SphI)::ura4+ ura4-DS/E leu1-32 ade6-M210 *dcr1*Δ::hphMX6, *ccr4*H664A-*ccr4*Terminator::hphMX6, nat::*caf1*promoter-*caf1*D53AD243AD174A	

Number: internal number for strains in the lab, Origin: Numbers are the original numbers from the labs they were produced in. All other strains were done for this study, by either Mario Halic, Mirela Marasovic or Manuel Zocco if the number is smaller than 700, or by myself > 700 (if not indicated differently).

2.1.2 Oligonucleotides

Table 2.2 Oligonucleotides used in this study

Number	Binding site	Sequence 5'-3'	Usage
289F	3'*tlh*	AACCCAGACACAGAAATTCG	
289R	3'*tlh*	AGCCCATGACCTACAGTCAG	NB / RT
179F	5'*tlh*	CCAGCTCTTTCGTTCAGGAC	
179R	5'*tlh*	AGTTGACGCTCCTTGGAAGA	NB / RT
559F	middle *tlh*	CAGAGCACAAGAGATGGTGT	
559R	middle *tlh*	ATTGGCTTTTCAGCAAACTT	NB / RT
113D	28S rRNA	AACACCACTTTCTGGCCATC	NB
110a F	tdh1	CCAAGCCTACCAACTACGA	
110a R	tdh1	AGAGACGAGCTTGACGAA	RT
110f F	Cen *dg*	CTGCGGTTCACCCTTAACAT	

Number	Binding site	Sequence 5'-3'	Usage
110f R	Cen *dg*	CAACTGCGGATGGAAAAAGT	RT
655F	Intergenic *SPAC212.10* and *SPAC212.09c*	GGACAGTCGGGAACAAC	
655R	Intergenic *SPAC212.10* and *SPAC212.09c*	CGGGCTATGCTATCCTCTAC	NB
648F	e*tlh* F	TCTTCCCATTTTTCCTCCTA	
648R	e*tlh* R	TTTTGAAGCGACTTTAGCA	
219F	act1	GATTCTCATGGAGCGTGGTT	
219R	act1	CTCATGAATACCGGCGTTTT	RT
170T		TTTTTTTTTTTTTTTTT	RT

Number: Internal primer number of the lab, Usage: Primers used for ChIP and qRT-PCR if no specification, RT: reverse transcription, NB: Northern Blot

DNA oligonucleotides were synthetized by Metabion (Martinsried, Germany) and BioTez (Berlin, German)

2.1.1 Consumables and Chemicals.

Consumables were used from Sarstedt AG & Co. (Nümbrecht, Germany), Biozym Scientific GmbH (Oldendorf), 4titude Ltd (Berlin, Germany) and Mettler Toledo (Gießen).

Standard chemicals mentioned in "Material and Methods" were ordered from Sigma Aldrich (Steinheim, Germany), Roth (Karlsruhe, Germany), New England Biolabs (NEB, Frankfurt, Germany), Thermo Scientific (Waltham, USA), Formedium (Hunstanton, UK), VWR (Darmstadt, Germany), Merck (Darmstadt, Germany), Promega (Mannheim, Germany) or Biozym Scientific GmbH (Oldendorf, Germany).

2.1.2 Media

Table 2.3 Composition of different media used for this study.

Name	Composition
LB (*E. coli*)	10 g/l tryptone, 5 g/l Yeast extract, 10 g/l NaCl, pH 7.0
YES (*S. pombe*)	5 g/l Yeast extract, 30 g/l glucose, 0.226 g/l of each: leucine, adenine, histidine, lysine, uracil
YE (*S. pombe*)	5 g/l Yeast extract, 30 g/l glucose
EMMC (*S. pombe*)	20 g/l glucose, 12.4 g/l EMM without dextrose, 0.226 g/l adenine, 0.226 g/l uracil, 0.226 g/l leucine
EMMC low ade plates (*S. pombe*)	20 g/l glucose, 12.4 g/l EMM without dextrose, 10 mg/l adenine, 0.226 g/l uracil, 0.226 g/l leucine, 20 g/l agar

All media were also used to make solid plates by adding 20 g/l agar. Plates were supplemented with antibiotics if necessary:

Geneticindisulfat (G 418) 0.2 g/l (*kan* resistant cells grow), Nourseothricin (NTC) 0.1 g/l (*nat* expressing cells grow), Hygromycin 0.1 g/l (*hph* gene causes resistance).

2.1.3 Strains used for sequencing

Table 2.4 Methods and strains used for sequencing

Small RNA-seq:
wild type (65); *caf1*Δ (510); *caf1*Δ*dcr1*Δ (521); *ccr4*Δ (544); *ccr4*Δ*dcr1*Δ (557); *taz1*Δ (633); *taz1*Δ*dcr1*Δ (636); *exo2*Δ (530); rrp6Δ (GEO: GSE3863); *mlo3*Δ (558); *cid14*Δ (708); dis3-54Δ (GEO: GSE19734); leo1Δ (GEO: GSE66940); swi6Δ (GEO: GSE70945)
RNA-seq:
wild type (65); *caf1*Δ*dcr1*Δ (521); *clr4*Δ (80)
p(A)RNA-seq:
wild type (65); *dcr1*Δ (34); *caf1*Δ (510); *caf1*Δ*dcr1*Δ (521)
RNA PolII- RNA IP-seq:
wild type (65, 63); *caf1*Δ*dcr1*Δ (521, 1073); *dcr1*Δ (1082); *caf1*ccr4*dcr1*Δ (1143)
H3 ChIP-seq:
wild type (65); *caf1*Δ*dcr1*Δ (521)

H3 RNA IP-seq:
wild type (65); *caf1*Δ*dcr1*Δ (521); *caf1*Δ (510); *dcr1*Δ (34); mock
Caf1 ChIP & **Caf1 ChIPexo-seq:**
Untagged; 3xFLAG-*caf1* (773); 3xFLAG-*caf1 clr4*Δ (848)
Caf1 RNA IP-seq:
Untagged; 3xFLAG-*caf1* (773); 3xFLAG-*caf1 clr4*Δ (848)
H3K9me2 ChIP:
wild type (65); *caf1*Δ*dcr1*Δ (521); *caf1*Δ (510); *caf1*ccr4*dcr1*Δ (1143)
PolII ChIP-seq:
wild type (65)

All sequencing data have been deposited in the NCBI Gene Expression Omnibus with the accession number GSE94129.

2.2 Experimental Procedures

2.2.1 Strain construction

All *S. pombe* strains used in this study are listed in Table 2.1. The strains were constructed by electroporation (Biorad MicroPulser program ShS) with a PCR-based gene targeting product leading to deletion or epitope-tagging of specific genes (Bähler et al., 1998). Plasmids were cloned by enzyme digestion and subsequent DNA-ligation. Point mutations were introduced with inverse PCR (Ulrich et al., 2012). The point mutations for Caf1D53AD243AD174A were chosen according to Jonstrup et al. (Jonstrup et al., 2007). D50A corresponds to D53A according to a new pombase annotation. The Ccr4 activity mutant, Ccr4H665A, was taken corresponding to the homologous Ccr4H818A mutant in *S. cerevisiae* (Chen et al., 2002). For genomic integration of the point mutants, a PCR with long overhang primers according to Bähler et al. was performed from the plasmid and the product transformed (Bähler et al., 1998). Positive transformants were selected on YES plates containing 100 – 200 mg/ml antibiotics and were confirmed by PCR and sequencing by GATC Biotech.

For generation of the overexpression strains one half of *tlh1* (5'*tlh*: 1-2800 bp) or *LEU2* (from *S. cerevisiae*; from start codon to stop codon, without 3' UTR) was cloned into pFA6a-kanMX6-nmt3-Tadh (*adh* Terminator). To improve the recombination efficiency, upstream of kanMX6

and downstream of Tadh ~700 bp of the sequence upstream and downstream of SPNCRNA.70 were cloned, respectively. The PCR product spanning "620 bp up SPNCRNA.70 – kanMX6 – Pnmt1 – ½ *tlh* or *LEU2* – Tadh – 759 bp down SPNCRNA.70" was transformed into a wild type *S. pombe* strain. To insert the *ade6* reporter (done by Luca Salvi), the strains were transformed with a PCR construct harboring 80 nt overhangs complementary to the sequence upstream of *SPNCRNA.70* and to the *nmt* promoter, respectively. In between was the *ade6* gene, a 1.7 kb long spacer spanning two *bla* sequences without start codon and promoter, and the *hphMX6* cassette. A PCR was performed and sequenced with the forward primer binding upstream of *SPNCRNA.70* and a reverse primer.

2.2.2 Ago1-bound siRNA sequencing

Endogenous 3xFLAG-tagged Ago1 was purified from different mutants by protein affinity purification. The pellet of a 2.5 l culture with OD_{600} between 2.0 – 2.5 was resuspended 1:1 in lysis buffer (50 mM HEPES (pH 7.5), 1.5 M NaOAc, 5 mM MgCl2, 2 mM EDTA pH 8, 2 mM EGTA pH8, 0.1% Nonidet P-40, 20% Glycerol) containing 1 mM PMSF, 0.8 mM DTT and Complete EDTA free Protease Inhibitor Cocktail (Roche). Cells were lysed with 0.25-0.5 mm glass beads (Roth) using the BioSpec FastPrep-24 bead beater (MP-Biomedicals) (4 cycles of 30 s at 6.5 m/s then 5 min on ice). The lysate was spun at 13000 x g for 15 min to remove cell debris. The supernatant was incubated with 30 µl Flag-M2 affinity gel (Sigma, A2220) for 1.5 h at 4°C. The resin was washed 5 times with lysis buffer. Ago1 was eluted with 1% SDS, 300 mM NaOAc. The protein-bound RNA was recovered by phenol-chloroform-isoamylalcohol (25:24:1, Roth) extraction and ethanol precipitation. Small RNAs with the length 20-30 nt were excised from an 18% acrylamide urea gel. 2 pmol of a preadenylated 3' adaptor oligonucleotide (miRNA Cloning Linker-1 from IDT, 5'-App CTG TAG GCA CCA TCA AT/ddC/-3') were ligated in a 10 µl reaction with 5 U T4 RNA ligase (TaKaRa), ligation buffer without ATP and 5 U RNasin (Promega) at 20°C for 2 hours. The 3' ligated products were purified on an 18% acrylamide urea gel with subsequent phenol-chloroform purification and ethanol purification. The 5' adaptor ligation was performed in a 10 µl reaction with 2 pmol 5' adaptor oligonucleotide (5'-GUU CAG AGU UCU ACA GUC CGA CGA UC-3'), 5 U RNasin (Promega), 0.06 µg BSA, 5 U T4 RNA ligase (Thermo Scientific) and 1x ligation buffer with ATP (Thermo Scientific) for 2 h at 20°C. The ligated products were gel purified and reverse transcribed with 10 pmol primer (RT primer: 5'- GTG ACT GGA GTT CAG ACG TGT GCT CTT CCG ATC GAT TGA TGG TGC CTA CAG-3') and the

SuperScript III First Strand Synthesis System (Thermo Scientific). The cDNA was PCR-amplified with Q5 High-Fidelity 2x Master Mix (NEB) for 14-20 cycles using the Illumina P5 5' primer (5' -AAT GAT ACG GCG ACC ACC GAG ATC TAC ACT CTT TCC CTA CAC GAC G -3') and the Illumina P7 3' primer with inserted barcode (5'-CAA GCA GAA GAC GGC ATA CGA GAT XXXXXX GTG ACT GGA GTT CAG ACG TG -3'). Single end sequencing was performed on an Illumina GAIIX sequencer at the LAFUGA core facility of the Gene Center, Munich. The Galaxy platform was used to demultiplex the obtained reads with Je-Demultiplex-Illu (Goecks et al., 2010).

2.2.3 Total RNA isolation

Total RNA was isolated from a 2 ml (qRT-PCR) or 10 ml (Northern Blot) yeast culture with OD_{600} of 1.0 applying the hot phenol method (Wecker, 1959). The pellet was resuspended in 500 µl lysis buffer (300 mM NaOAc pH 5.2, 10 mM EDTA, 1% SDS) and 500 µl phenol-chloroform-isoamylalcohol (25:24:1, Roth) and incubated at 65°C for 10 min with constant mixing. The organic and aqueous fractions were separated by centrifugation at 20 000 x g for 10 min. Nucleic acids in the aqueous fraction were precipitated with ethanol and then treated with DNase I (Thermo Scientific) for 1 h or 2 h at 37°C. DNase was removed by a second phenol-chloroform-isoamylalcohol extraction and ethanol precipitation.

2.2.4 Reverse Transcription and quantitative Real-Time PCR (qRT-PCR)

50 ng of total RNA was reverse transcribed with SuperScript III First Strand Synthesis System (Thermo Scientific) and 0.2 pmol of either specific primers if not stated in the figure legend, or a poly(dT) primer (Table 2.2). Real-time PCR was performed with 1 ng of cDNA, DyNamo Flash SYBR Green qPCR Master Mix (Thermo Scientific), and specific primers in the Toptical thermocycler (Biometra), according to the manufacturer's instructions. qRT-PCR was performed in duplicate or triplicate for each cDNA sample and primer. A non-reverse-transcribed sample was used as control for DNA contamination.

2.2.5 Total RNA and poly(A) RNA sequencing

rRNA of 1 µg total RNA was degraded with Terminator nuclease (Epicentre) in buffer A at 30°C for 2 h. For p(A) RNA sequencing, poly-adenylated RNA was extracted from total RNA with oligo d(T)25 magnetic beads (NEB). The RNA library was obtained using the NEBNext Ultra Directional RNA Library Prep Kit for Illumina (NEB). Single end sequencing was performed on

an Illumina GAIIX sequencer at the LAFUGA core facility of the Gene Center, Munich. The Galaxy platform was used to demultiplex the obtained reads with Je-Demultiplex-Illu (Goecks et al., 2010).

2.2.6 Northern Blot

10 µg of total RNA were run on a 0.8% agarose MOPS gel and transferred to a positively charged nylon membrane according to GE Healthcare Amersham Hybond N+ instructions for Northern blotting with capillary transfer. The RNA was UV-cross-linked to the membrane with Spectrolinker XL-1500 (Spectroline, "optimal crosslink"). Prehybridization was performed with Church Buffer (0.5 M NaH2PO4/ Na2HPO4 pH 7.2, 1 mM EDTA, 7% SDS) at 40°C for at least 8 hours. 10 pmol of DNA probes were labeled with T4 PNK (NEB) and 10 pmol [γ-32P]-ATP (Hartmann Analytic) at 37°C for 60 min. The labeled probes were purified with an Illustra MicroSpin G-25 column (GE Healthcare), mixed with 5 ml Church Buffer, and incubated with the membrane for at least 2 h at 40°C. The membrane was rinsed twice with 2x SSC buffer (0.3 M NaCl, 0.03 M sodium citrate, pH 7.0) and then washed three times with 2x SSC buffer for 15 min at 40°C each. The membrane was wrapped in cling film and exposed to a storage phosphor screen (BAS MS 2025 - Fujifilm Corporation) overnight up to 2 days at -80°C. The screen was scanned with a Typhoon FLA 9500 (GE Healthcare). For a second labeling of the same membrane, the membrane was stripped in boiling 0.1% SDS for 5 min with subsequent prehybridization.

2.2.7 Growth assay and ade6 reporter spot assay

Tenfold serial dilutions of cultures with OD_{600} between 0.7 and 1.5 were made so that the highest density spot contained 10^5 cells. Cells were spotted on not supplemented, non-selective medium YE (low adenine) medium or EMMC low adenine (10 mg/l adenine). The plates were incubated at 32°C for 2-3 days and imaged. Cells with a silenced *ade6* gene are red, cells expressing ade6 are white. In pink colonies the *ade6* gene is partially de-repressed. For investigating maintenance of heterochromatin at the *ade6* gene in the overexpression strains, a 50 ml culture of one red colony in YES was grown to an OD_{600} of 1-2 and ca. 200 - 500 cells were plated on a YE (low adenine, thiamine +) and an EMMC 10 mg/l adenine (low adenine, thiamine -) plate. The plates were grown at 32°C until the color of the colonies was clearly visible. The plates were imaged and different cell colors were quantified by counting.

2.2.8 Chromatin immunoprecipitation (ChIP)

50 ml yeast cultures with an OD_{600} of 1.2 were cross-linked with 1% formaldehyde (Roth) for 15 min at room temperature. The reaction was quenched with 125 mM glycine for 5 min. The frozen pellet was resuspended in 500 µl lysis buffer (250 mM KCl, 1x Triton-X, 0.1% SDS, 0.1% Na-Desoxycholate, 50 mM HEPES pH 7.5, 2 mM EDTA, 2 mM EGTA, 5 mM MgCl2, 0.1% Nonidet P-40, 20% Glycerol) with 1 mM PMSF and Complete EDTA free Protease Inhibitor Cocktail (Roche). Lysis was performed with 0.25-0.5 mm glass beads (Roth) and the BioSpec FastPrep-24 bead beater (MP-Biomedicals), 8 cycles at 6.5 m/s for 30s and 3 min on ice. DNA was sheared by sonication (Bioruptor, Diagenode) 35 times for 30 s with a 30 s break. Cell debris was removed by centrifugation at 13 000 x g for 15 min. The crude lysate was normalized based on the RNA and Protein concentration (Nanodrop, Thermo Scientific) and incubated with 1.2 µg immobilized (Dynabeads Protein A or G, Thermo Scientific) antibody against dimethylated H3K9 (H3K9me2, abcam AB1220), H3 (ab1791, abcam), H3S10P (ab5176, abcam), anti-FLAG M2-Magnetic Beads (Sigma-Aldrich) or 5 µl agarose conjugated Pierce HA Epitope Tag Antibody (#26181, Thermo Scientific) for at least 2 h at 4°C. The resin with immunoprecipitates was washed five times with each 1 ml of lysis buffer and eluted with 150 µl of elution buffer (50 mM Tris HCl pH 8.0, 10 mM EDTA, 1% SDS) at 65°C for 15 min. Cross-linking was reversed at 95°C for 15 min and subsequent RNase A (Thermo Scientific) digest for 30 min followed by Proteinase K (Roche) digest for at least 2 h at 37°C or ON at 65°C. DNA was recovered by phenol-chloroform-isoamylalcohol (25:24:1, Roth) extraction with subsequent ethanol precipitation. DNA levels were quantified by qRT-PCR and normalized to *tdh1* background levels. Oligonucleotides used for quantification are listed in Table 2.2. For sequencing, a ChIPseq library was made using the NEBNext Ultra II DNA Library Prep Kit for Illumina kit (NEB). Single end sequencing was performed on an Illumina GAIIX sequencer at the LAFUGA core facility of the Gene Center, Munich. The Galaxy platform was used to demultiplex the obtained reads with Je-Demultiplex-Illu (Goecks et al., 2010).

2.2.9 RNA immunoprecipitation (RNA IP)

RNA IP was performed like ChIP but without RNase A digest, with anti-RNA polymerase II CTD repeat YSPTSPS antibody [8WG16] (ab817, abcam) or anti-H3 antibody (ab1791, abcam). Cells were also crosslinked with 1% Formaldehyde for 15 min. After phenol-chloroform-

isoamylalcohol extraction, DNA was digested with DNase I (Thermo Scientific) for 2 h at 37°C. RNA was recovered with a second phenol-chloroform-isoamylalcohol purification and ethanol precipitation. RNA was either taken for making a sequencing library using the NEBNext Ultra Directional RNA Library Prep Kit for Illumina (NEB) or it was reverse transcribed into cDNA with specific primers with subsequent qRT-PCR.

2.2.10 ChIP-exo sequencing

ChIP-exo was performed similarly as described before with minor modifications (Rhee and Pugh, 2012; Serandour et al., 2013). Starting material was the frozen pellet of a 100 ml yeast culture with an OD_{600} of 1.2, cross-linked with 1% formaldehyde (Roth) for 30 min. Sonication was performed with the Branson Sonifier, 40.4 setting, five times for 30 s. For immunoprecipitation 6 µl anti-FLAG M2-Magnetic Beads (Sigma-Aldrich) or anti-RNA polymerase II CTD repeat YSPTSPS antibody [8WG16] (ab817, abcam) coupled to Protein G Dynabeads (Thermo Scientific) were used overnight. The salt buffers written in the protocol were only used for washing after immunoprecipitation and adaptor ligation. Otherwise washing was done twice with a general wash buffer (10 mM Tris HCl pH 8, 2 mM EDTA pH 8, 300 mM NaCl, 0.1% Triton X-100) and once with TE. Elution was also done with a different Elution buffer (25 mM Tris HCl pH 8, 10 mM EDTA pH 8, 200 mM NaCl, 1% SDS). PCR amplification was performed with NEBNext® Q5® Hot Start HiFi PCR Master Mix, NEB. Single end sequencing was performed on an Illumina GAIIX sequencer at the LAFUGA core facility of the Gene Center, Munich. The Galaxy platform was used to demultiplex the obtained reads with Je-Demultiplex-Illu (Goecks et al., 2010).

2.2.11 Chromatin fractionation

The frozen pellet of a 10 ml culture with an OD_{600} of 1.0 was resuspended in 250 µl lysis buffer (250 mM KCl, 1x Triton-X, 0.1% SDS, 0.1% Na-Desoxycholate, 50 mM HEPES pH 7.5, 2 mM EDTA, 2 mM EGTA, 5 mM MgCl2, 0.1% Nonidet P-40, 20% Glycerol) and lysed with 0.25-0.5 mm glass beads (Roth) and the BioSpec FastPrep-24 bead beater (MP-Biomedicals), 8 cycles at 6.5 m/s for 30s and 3 min on ice. (Under the microscope it was analyzed that 99% of the cells were broken.) The lysate was spun at 21,000 x g for 20 min. 200 µl of the supernatant were taken as “unbound” fraction. Residual supernatant was removed by washing twice with 800 µl lysis buffer and centrifugation at 21,000 x g for 10 min. The pellet was resuspended in 250 µl lysis

buffer. 200 µl of the suspension built the "chromatin" fraction. The fractions were divided in half, respectively, to separate between RNA and DNA. The DNA samples were treated with RNaseA and Proteinase K before Phenol-Chloroform-Isoamylalcohol treatment and Ethanol precipitation. qRT-PCR was performed without normalization of DNA amount to analyze if chromatin fractionation worked. RNA was recovered by Phenol-Chloroform-Isoamylalcohol treatment, Ethanol precipitation and DNase digest like described for total RNA isolation. Reverse transcription was performed with 100 ng RNA for each sample and specific primers for *tlh* and *tdh*. qRT-PCR was performed using also non-reverse transcribed sample as control to be sure that no DNA was amplified. In each fraction, *tlh* RNA was normalized to *tdh1* RNA and presented as fold change compared to "wild type unbound".

2.2.12 3xFLAG-Caf1 RNA IP with chromatin fractionation

Caf1-associated RNA in the chromatin and the non-chromatin fraction were isolated like the RNA IP described before. Just before sonication, the sample was centrifuged for 20 min at 21 000 x g at 4°C. The supernatant was taken as "soluble fraction", the pellet was washed twice with lysis buffer, then resuspended in lysis buffer, which formed the "chromatin fraction". IP was performed with anti-FLAG M2-Magnetic Beads (Sigma-Aldrich).

2.2.13 Analysis of sequencing data

Single end sequencing of libraries was performed on an Illumina GAIIX sequencer at the LAFUGA core facility of the Gene Center, Munich. The Galaxy platform was used to demultiplex the obtained reads with Je-Demultiplex-Illu (Goecks et al., 2010). Demultiplexed Illumina reads were mapped to the *S. pombe* genome, allowing 2 nucleotides mismatch to the genome using Novoalign (htttp://www.novocraft.com). h90 *S. pombe* genome was assembled using the *mat* sequence from Pombase and imported it in IGV. Small RNA reads mapping to multiple locations were randomly assigned. By using Perl scripts, the datasets were normalized to the number of reads per million (rpm) sequences for small RNAseq or reads per million mapping to coding sequences for total RNAseq, p(A) RNAseq, Caf1-RIPseq and H3RIPseq. ChIP data were either normalized by rpm if variation in read amounts was low, if centromeric heterochromatin was lost for example, ChIP-seq data were normalized to regions which were not changed in different mutants. Caf1 ChIP reads were summed in a window of 100 nt and divided by a corresponding control to display the fold-change using the Integrative Genomics Viewer (IGV)

(http://www.broad.mit.edu/igv). Sequencing data were done in two replicates or the data were confirmed by another method like qRT-PCR. Sequenced strains are listed in Table 2.4.

2.2.14 Box plot generation

Box plot generation of wild type H3-RIP-seq over PolII-RIP-seq, or *caf1*Δ*dcr1*Δ H3RIP-seq over wild type H3RIP-seq: The fold change of reads of every gene from sample 1 (e.g. wild type H3-RIP-seq) over sample 2 (e.g. wild type PolII-RIP-seq) was calculated using Perl. Genes were classified based on their annotation: "lncRNA": euchromatic noncoding RNA with annotation SPNCRNA. "mRNA": all protein coding genes without genes in heterochromatic areas. "heterochromatic": Genes which are located in constitutive heterochromatic regions (except for tRNA and rRNA: Chr1 0 -37 kb, 3753 – 3790 kb, 5532 kb – end; Chr2: 0 – 15 kb, 1600 – 1645 kb, 2114 – 2122 kb, 2129 kb – 2137 kb, 4497 kb – end; Chr3: 1068 kb – 1140 kb) were extracted with a script written in Perl. Overlaps between classifications were in general excluded. Euchromatic genes exclude all heterochromatic genes as well as rRNA transcripts.

2.2.15 Statistical analysis

Two sided *t*-test for two independent datasets with high variance was used to calculate the p-value. The p-value was displayed with stars: P-value < 0.05 *, < 0.01 **, < 0.001 ***.

3. Results

3.1 Caf1 and RNAi are required for heterochromatin formation

The RNAi pathway is important for heterochromatin establishment at the centromeres, at the same time it degrades nascent RNA to start a positive feedback loop with sRNAs. To analyze if additional RNA degradation is important for heterochromatin formation, we deleted several nucleases and sequenced Argonaute-bound small RNAs. In *caf1Δ* cells, a high amount of small RNAs was generated from subtelomeric repeats (Figure 3.1 A and B). In wild type cells, less than 1% of Argonaute-bound small RNAs map to the subtelomeric region, indicating that RNAi is not the major contributor to silencing at the subtelomeric repeats (Figure 3.1 B). On the contrary, in *caf1Δ* cells more than 30% of Argonaute-bound small RNAs map to the subtelomeric repeats (Figure 3.1 B). These small RNAs are Dcr1-dependent and show all features of siRNAs like a 5' uridine and an average length between 21-23 nt (Figure 3.1 A, C and D) (Halic and Moazed, 2010; Marasovic et al., 2013). Subtelomeric siRNAs are generated from *tlh1*, *SPAC212.10*, and *SPAC212.09c*, covering a region from 0 kb to 9 kb on the left arm of chromosome 1 (Figure 3.1 A) and the homologous regions on both arms of chromosomes 1 and 2. A similar pattern was detected in deletion of Ccr4, the second deadenylase of the Ccr4-Not complex, but lower amounts of siRNAs were generated from the subtelomeric region in *ccr4Δ* cells (Figure 3.1 A and B). In *caf1Δ* or *ccr4Δ* cells, no defect in length of Argonaute-bound small RNAs could be observed, indicating that Caf1 or Ccr4, in contrast to Triman, are not directly processing small RNAs (Figure 3.1 D) (Marasovic et al., 2013). These data suggest that the Caf1 and Ccr4 nucleases degrade subtelomeric transcripts, and in their absence, RNAi acts as a redundant degradation mechanism.

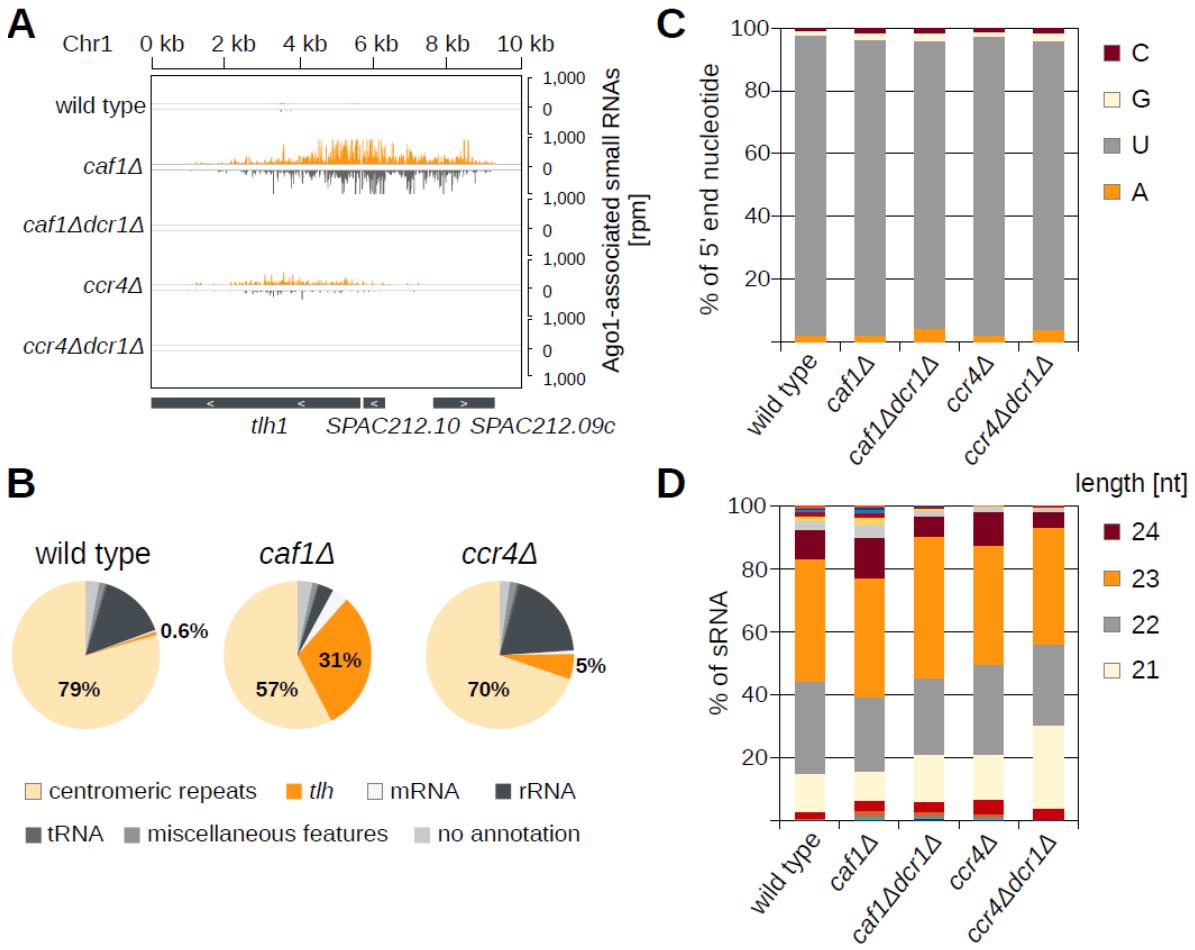

Figure 3.1 Argonaute-bound small RNAs at subtelomeres

A) Endogenously tagged Argonaute-bound sRNA sequencing reads in indicated cells were plotted over the subtelomeric region. The location of genes is indicated as grey boxes below the small RNA peaks. Reads from + and - strands are depicted in orange and grey, respectively. Scale bars on the right denote small RNA read numbers normalized per one million reads. *caf1Δ* and *caf1Δdcr1Δ* experiment done by Mario Halic.

B) Classification of Argonaute-bound small RNAs from wild type, *caf1Δ* and *ccr4Δ* cells. Pie charts illustrate percentages for the individual small RNA classes relative to the total number of reads for each strain. Argonaute-bound subtelomeric siRNAs are increased more than 50-fold in *caf1Δ* cells compared to wild type.

C) 5' nucleotide preference of Argonaute-associated small RNAs in indicated cells. Strong preference for 5' U indicates Argonaute association.

D) Length distribution of siRNAs that are associated with Argonaute in indicated cells. 20-27 nucleotide long small RNAs were analyzed by high-throughput sequencing.

Centromeric siRNAs were generated near wild type levels at *dg* and *dh* repeats but were strongly reduced at the IRC3 element in *caf1Δ* cells (Figure 3.2) (Halic and Moazed, 2010). Similarly to the subtelomeric region, higher amounts of siRNAs were generated at the *mat* locus in *caf1Δ* cells (Figure 3.2).

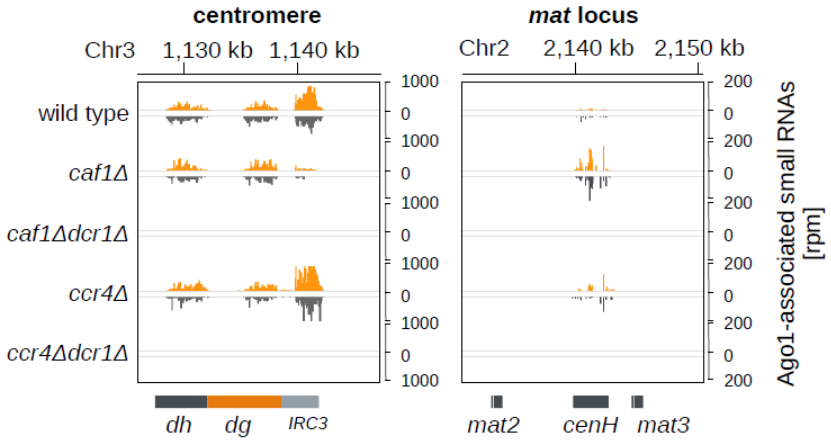

Figure 3.2 sRNAs at centromeres and *mat* locus

Small RNA reads in indicated cells were plotted over the centromeric region and the *mat* locus. The location of genes is indicated as grey boxes below the alignment. Reads from + and - strands are depicted in orange and grey, respectively. Scale bars on the right denote small RNA read numbers normalized per one million reads. For the *mat* locus, only unique mapping reads are shown to exclude reads also mapping to the centromere.

We observed a partial loss of silencing in *caf1Δ* cells at subtelomeric and centromeric repeats (Figure 3.3 A and B). Centromeric *dg* and subtelomeric *tlh* transcripts were 4-5 fold up-regulated, and silencing of a centromeric *ade6* reporter was reduced with pink colonies appearing (Figure 3.3 A , B and C). When grown on low adenine medium, cells which express *ade6* are white, when *ade6* is repressed, cells accumulate a red intermediate of the adenine pathway.

Next, we generated *caf1Δdcr1Δ* and *caf1Δago1Δ* double mutants in several genetic backgrounds to remove both degradation pathways, RNAi and Ccr4-Not. While single deletions of *caf1* and *ago1*/*dcr1* had a small impact on expression in the subtelomeric region, deletion of both pathways completely de-repressed subtelomeric transcripts (*tlh1*, *SPAC212*.10 and *SPAC212*.09c) to the level of deletion of the H3K9 methyltransferase Clr4 (Figure 3.3 A). Centromeric silencing is lost already in *dcr1Δ* cells, so *caf1Δdcr1Δ* cells do not show much additional effect (Figure 3.3 C, D). At *cenH* of the *mat* locus, silencing is only lost in *caf1Δdcr1Δ* cells (Figure 3.3 D). All heterochromatic transcripts are polyadenylated (Figure 3.3 D), which suggests that they can be targeted by the Ccr4-Not complex. Our data show that in the absence of Caf1 and RNAi components, silencing of heterochromatic transcripts is lost.

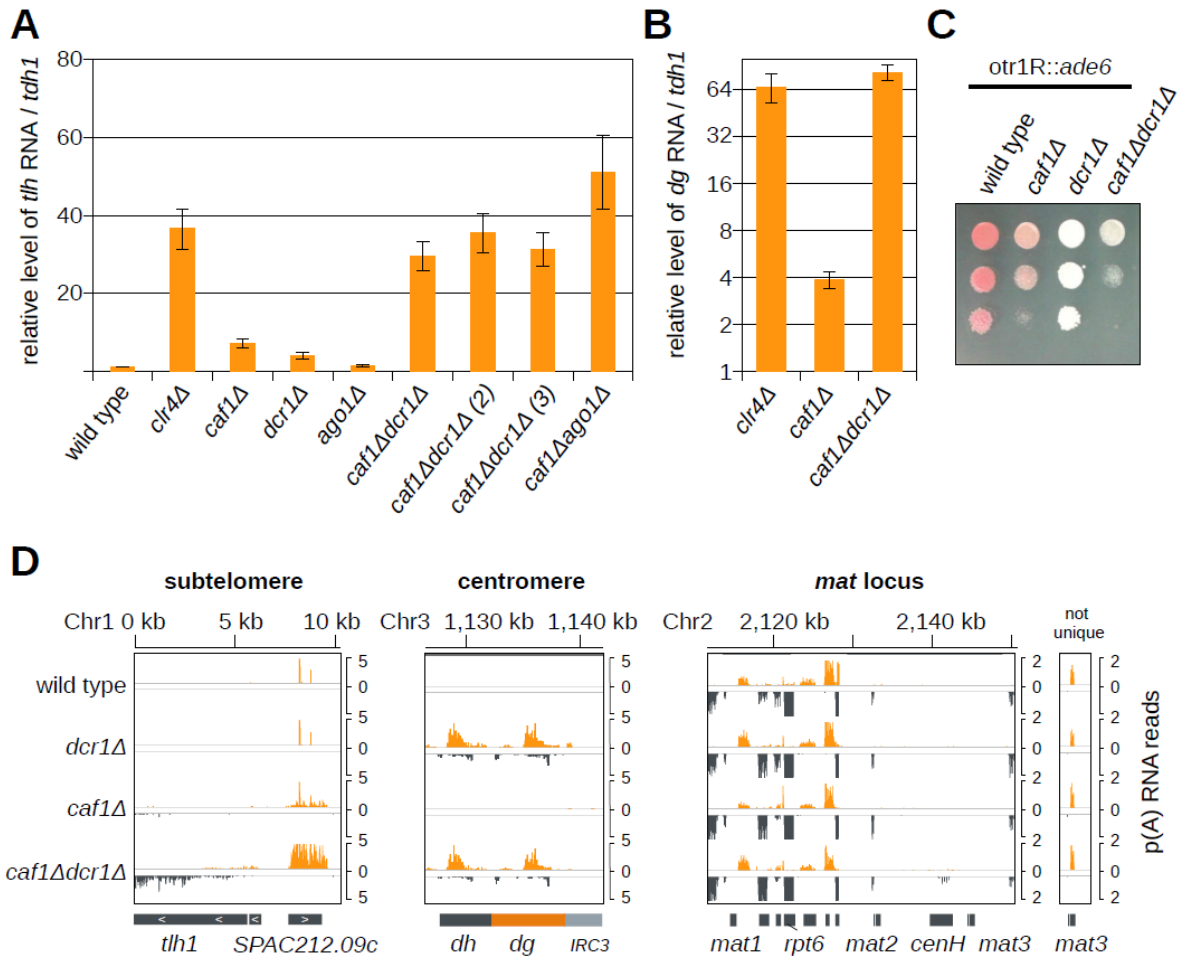

Figure 3.3 Heterochromatic silencing is lost in *caf1Δ*RNAiΔ cells

A) Quantification of subtelomeric *tlh* transcripts in indicated strains by RT-qPCR. In *caf1Δdcr1Δ* and *caf1Δago1Δ* cells, silencing of subtelomeric repeats is lost. Error bars indicate the standard error of more than seven independent experiments (several experiments were performed by Manuel Zocco). For *caf1Δdcr1Δ* and *caf1Δago1Δ*, experiments of two independent colonies were averaged, respectively. Reverse transcription was performed with specific primers, wild type was set to 1. *caf1Δdcr1Δ* (2) and (3) are strains with different genetic background.

B) Quantification of centromeric *dg* transcripts in indicated strains by RT-qPCR. Wild type RNA levels are set to 1, logarithmic scale. Error bars indicate standard error of more than five independent experiments (several experiments done by Manuel Zocco).

C) Growth assay on YE (low adenine) showing reduction in centromeric silencing at the *ade6* reporter gene in indicated mutants compared to wild type. Cells were plated in 10-fold dilutions starting with 10^5 cells.

D) Polyadenylated RNA sequencing reads in indicated cells are plotted over heterochromatic regions. Reads from + and - strands are depicted in orange and grey, respectively. Heterochromatic transcripts are polyadenylated. Scale bars on the right denote RNA read numbers per one million normalized to all protein coding reads. For *mat* locus, only unique mapping reads are presented (left), to exclude reads also mapping to the centromere. *mat1* and *mat3* share the same sequence in this annotation, the right panel shows reads randomly distributed.

H3K9me2 ChIP revealed that H3K9me2 was reduced at *tlh* and centromeric *dg* in single mutants (Figure 3.4 A and B). At centromeres, *dcr1*Δ or *ago1*Δ single mutants already show a strong reduction of H3K9me2 as RNAi is the only establishment pathway there (Figure 3.4 B) (Halic and Moazed, 2010; Volpe et al., 2002). In *caf1*Δ*dcr1*Δ and *caf1*Δ*ago1*Δ cells, H3K9me2 was lost at subtelomeric and centromeric repeats, and at the *mat* locus (Figure 3.4 A, B, C and D), which shows that H3K9me2 and heterochromatic silencing cannot be maintained in these mutants at all constitutive heterochromatic loci.

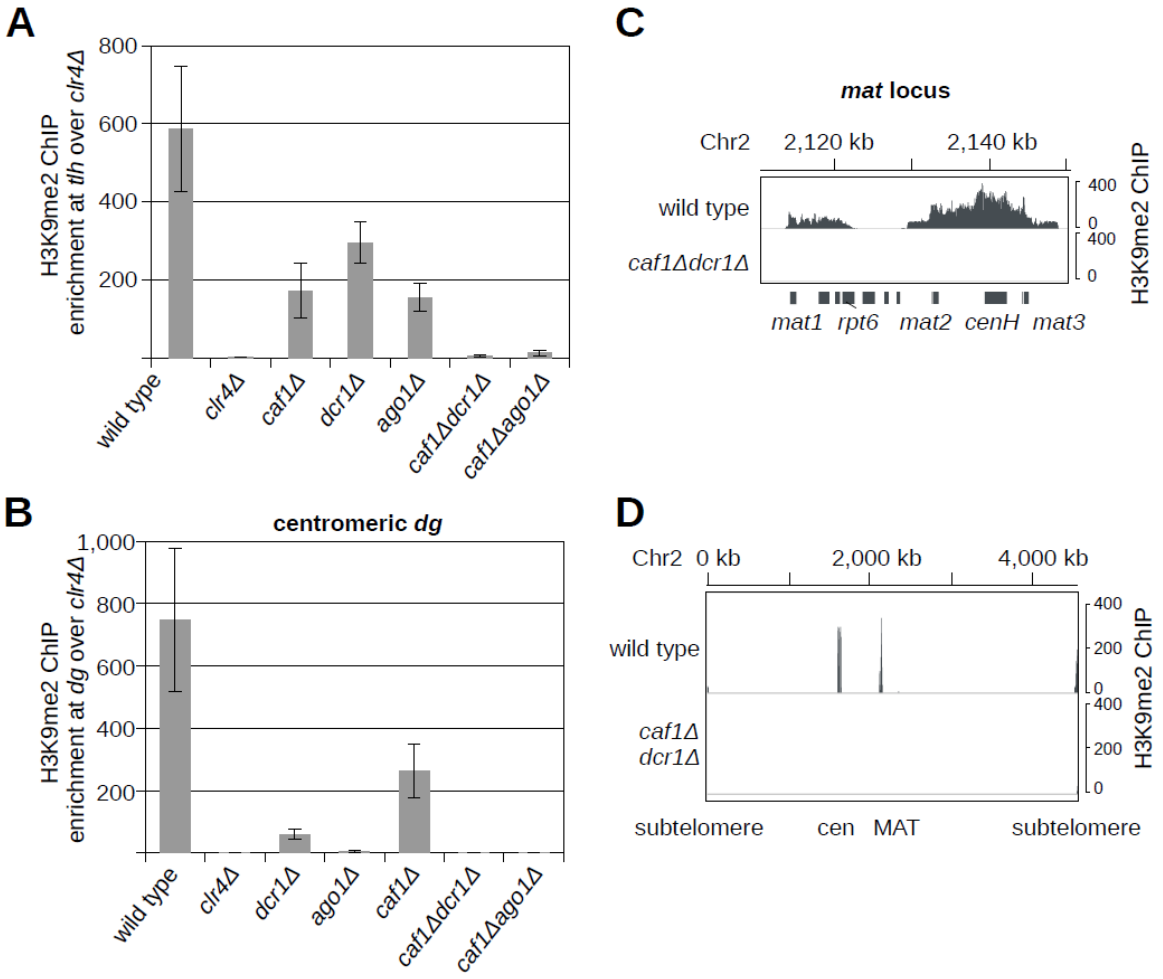

Figure 3.4 H3K9me2 levels at all constitutive heterochromatin loci.

A-B) qRT-PCR ChIP. H3K9me2 is lost at subtelomeric *tlh* repeats (A) and centromeric *dg* repeats (B) in *caf1Δdcr1Δ* and *caf1Δago1Δ* cells. Error bars indicate the standard error of at least three independent experiments (Several experiments done by Manuel Zocco). For *caf1Δdcr1Δ* and *caf1Δago1Δ,* data of two independent colonies were averaged, respectively. *clr4Δ* was set to 1.

C-D) ChIP-seq experiment showing that H3K9me2 is lost in *caf1Δdcr1Δ* cells at all heterochromatic loci (D). Scale bars on the right denote read numbers per million reads normalized to the TAS region (Chr2 4,534 kb – 4,538 kb). (C) Zoomed in version of D) for the *mat* locus.

Additional to *caf1* and RNAi deletion mutants, double mutants of *caf1* and the HP1 protein *swi6* also showed a strong defect in subtelomeric heterochromatin formation and silencing (Figure 3.5 A and B). To the contrary, *swi6Δdcr1Δ* cells do not lead to additional loss of heterochromatic silencing compared to *swi6Δ* mutants. This suggests, that opening of the chromatin due to loss of HP1, with additional loss of RNA degradation by the Ccr4-Not complex is enough to lose silencing. Furthermore it seems that Swi6 and Dcr1 are rather in the same pathway of heterochromatin establishment.

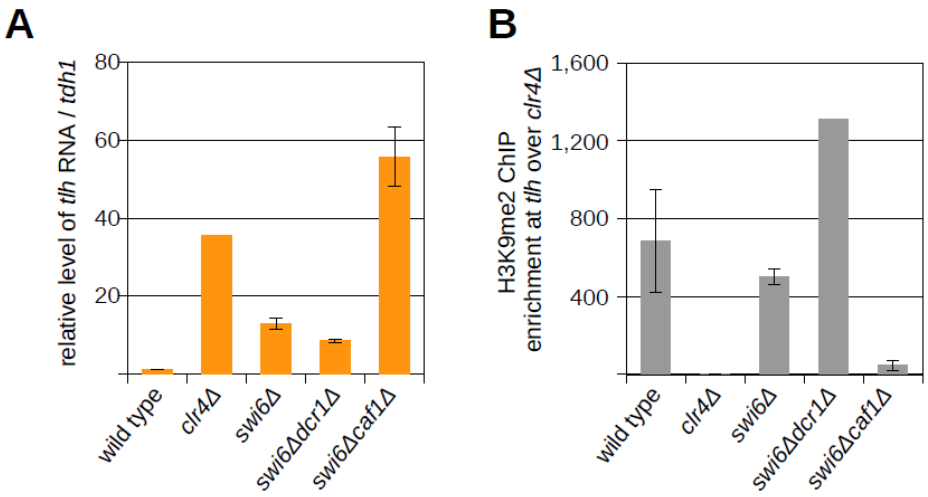

Figure 3.5 Effect of HP1 protein Swi6 on subtelomeric heterochromatin

A) Quantification of subtelomeric *tlh* transcripts in indicated strains by RT-qPCR. In *swi6Δcaf1Δ* cells, silencing of subtelomeric repeats is lost. Error bars indicate the standard error of two independent experiments. Reverse transcription was performed with specific primers, wild type was set to 1.

B) ChIP qRT-PCR experiment showing that H3K9me2 is lost at subtelomeric *tlh* repeats in *swi6Δcaf1Δ* cells. Error bars indicate standard error of two independent experiments. *clr4Δ* was set to 1.

3.2 Subtelomeric heterochromatin is lost at transcribed regions

The Shelterin complex recruits the methyltransferase complex CLRC and the histone deacetylation complex SHREC to telomeres from where they spread to establish subtelomeric heterochromatin (Kanoh et al., 2005; Sugiyama et al., 2007; Wang et al., 2016). In *caf1*Δ*dcr1*Δ cells, Taz1, a DNA binding protein of the Shelterin complex, is still recruited to the telomeric repeats (Figure 3.6 A). This indicates that the Shelterin complex could still recruit CLRC to establish heterochromatin. In *taz1*Δ cells we observe a small increase in subtelomeric siRNAs and consistent with previous studies, in *taz1*Δ*dcr1*Δ cells, when both CLRC recruitment pathways are eliminated, *tlh* transcripts accumulate (Figure 3.6 B, C and D) (Hansen et al., 2006; Kanoh et al., 2005). In *caf1*Δ*taz1*Δ cells, we did not observe additional loss of H3K9me2 at *tlh* compared to *caf1*Δ (Brönner et al., 2017).

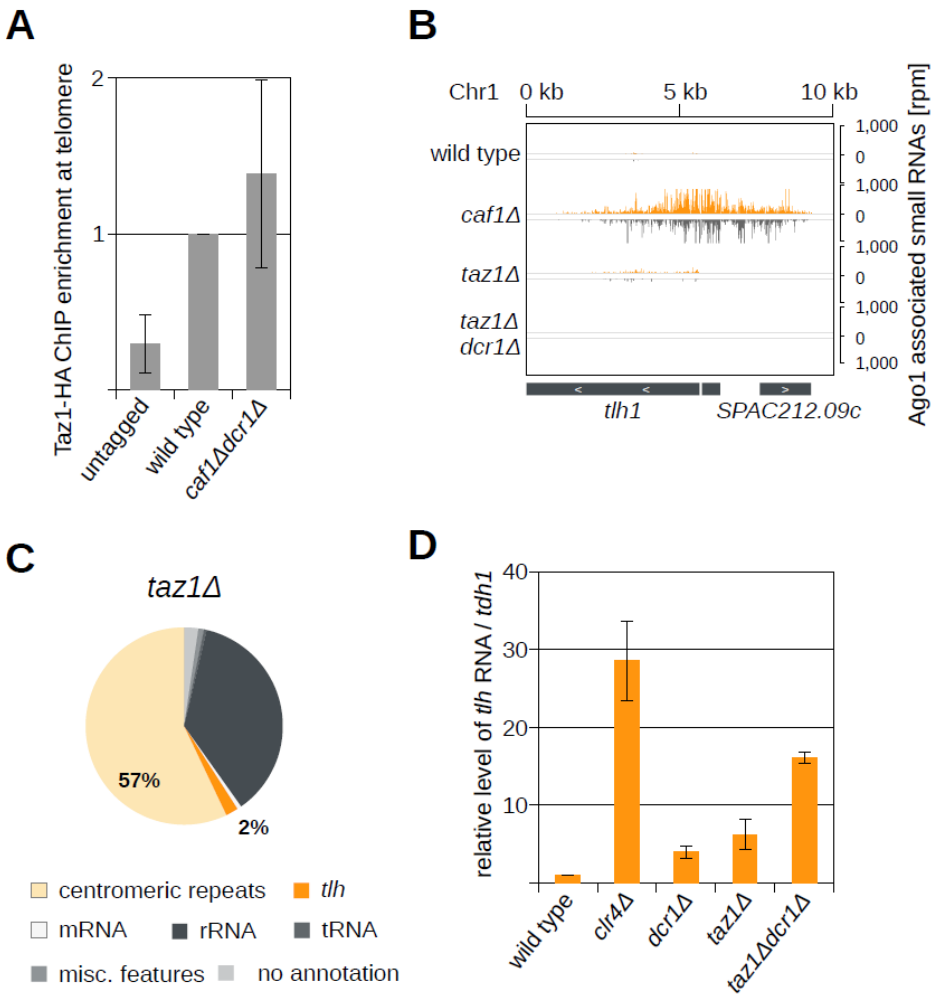

Figure 3.6 Shelterin complex is still localized at telomeric repeats

A) ChIP experiment showing that endogenously tagged Taz1-HA is found at the TERRA-transcription site, close to telomeric repeats, in both wild type and *caf1Δdcr1Δ* cells. Error bars indicate standard error of three independent experiments.

B) Small RNA sequencing. Argonaute-associated small RNA reads in indicated cells were plotted over the subtelomeric region. The location of genes is indicated as grey boxes below the small RNA alignment. Reads from + and - strands are depicted in orange and grey, respectively. Scale bars on the right denote small RNA read numbers normalized per one million reads.

C) Classification of Argonaute-bound small RNAs from *taz1Δ* cells. Pie chart illustrates percentages for the individual small RNA classes relative to the total number of reads.

D) Quantification of subtelomeric *tlh* transcripts in indicated strains by RT-qPCR (RT with specific primers). Subtelomeric *tlh* transcripts accumulate in *taz1Δdcr1Δ* cells, although less than in *clr4Δ* cells. Error bars indicate standard error of four independent experiments.

Consistent with Taz1 localization (Figure 3.6 A), H3K9me2 was not lost at the telomere associated sequence (TAS) in *caf1Δdcr1Δ* cells, indicating that the Shelterin complex can still establish heterochromatin at the telomeric borders, which can spread until the transcribed *tlh* locus (Figure 3.7). These data also indicate that Caf1 is not essential for heterochromatin establishment and spreading until the transcribed *tlh* region. When both degradation pathways, RNAi and Caf1, were eliminated, heterochromatin was lost at the transcribed *tlh* region and the region upstream of *tlh* towards the centromere (Figure 3.7). This indicates that heterochromatin cannot spread over the transcribed *tlh* gene in *caf1Δdcr1Δ* cells.

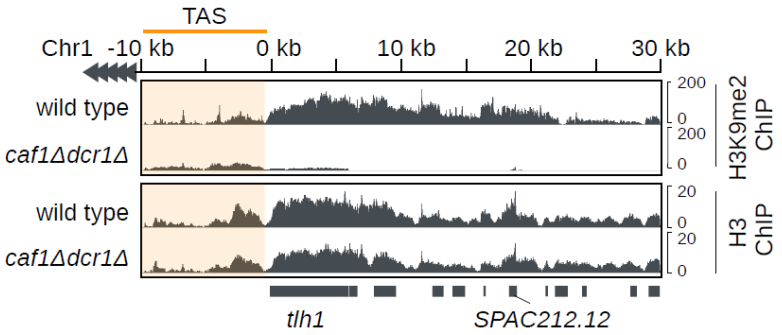

Figure 3.7 Heterochromatin is only lost at transcribed regions

H3K9me2 ChIP-seq reads blotted over the subtelomeric region of chromosome 1 left arm in indicated strains. H3 ChIP reads are blotted below as control. The *S. pombe* genome assembly is incomplete in the subtelomeric region, but additional insert clones from the telomere plasmid library with the sequence of the telomere associated region (TAS) are available on www.pombase.com. Scale bars on the right denote DNA read numbers normalized per one million reads. In *caf1Δdcr1Δ* cells, H3K9me2 is not lost at regions between telomeric repeats and the transcribed *tlh* gene (highlighted in orange). H3 ChIP reads show that this region is in general reduced in amount of nucleosomes compared to *tlh.* Grey triangles symbolize telomeric repeats.

Small RNA sequencing data in *caf1*Δ cells show, that siRNAs are generated from *tlh*, *SPAC212.10*, *SPAC212.09c* and their intergenic regions (Figure 3.1 A). We sequenced RNA from *caf1*Δ*dcr1*Δ cells and found reads in the intergenic region (Figure 3.8 A). Also sequencing of RNA Polymerase II (PolII) associated nascent RNA showed increased transcriptional activity in the intergenic region in *caf1*Δ*dcr1*Δ cells, but not in wild type cells (Figure 3.8 A). This is consistent with the nucleosome positioning data that show a nucleosome free region between *SPAC212.10* and *SPAC212.09c* in *caf1*Δ*dcr1*Δ (Figure 3.8 A) and *clr4*Δ cells (Garcia et al., 2010). This indicates chromatin changes and the opening of a second *tlh* promoter. Northern blot analysis confirms that *tlh* RNA is longer in *caf1Δdcr1Δ* and *caf1Δago1Δ* cells than in *ago1*Δ or *caf1*Δ cells (Figure 3.8 B). *tlh* probes from the 3' end as well as from the 5' intergenic region hybridized to the longer transcript, indicating that in *caf1*Δ*dcr1*Δ cells transcripts start 2 kb upstream of the annotated *tlh* promoter and terminate at the *tlh* terminator (Figure 3.8 B). The extended *tlh* (*etlh*) transcript is polyadenylated and is enriched in *caf1*Δ, but not in *ago1*Δ cells, and is completely de-repressed in *caf1*Δ*dcr1*Δ and *caf1*Δ*ago1*Δ cells (Figure 3.8 C). The *etlh* transcript was also accumulating in *clr4*Δ, *taz1Δdcr1*Δ and to lower levels in *ccr4*Δ*dcr1*Δ cells (Figure 3.8 D). Tas3 is the GW182 protein in the RITS complex, which is important for recruitment of the Ccr4-Not complex to miRNA targeted mRNA in higher eukaryotes (Chen et al., 2014; Mathys et al., 2014). If Tas3 is the protein recruiting RNAi and the Ccr4-Not complex to subtelomeric *tlh*, deletion will show the same defect like *caf1*Δ*dcr1*Δ cells. Northern blot analysis of *tas3*Δ RNA only displayed the lower *tlh* band similar to *ago1*Δ cells, which excludes that Tas3 recruits Caf1 to heterochromatin.

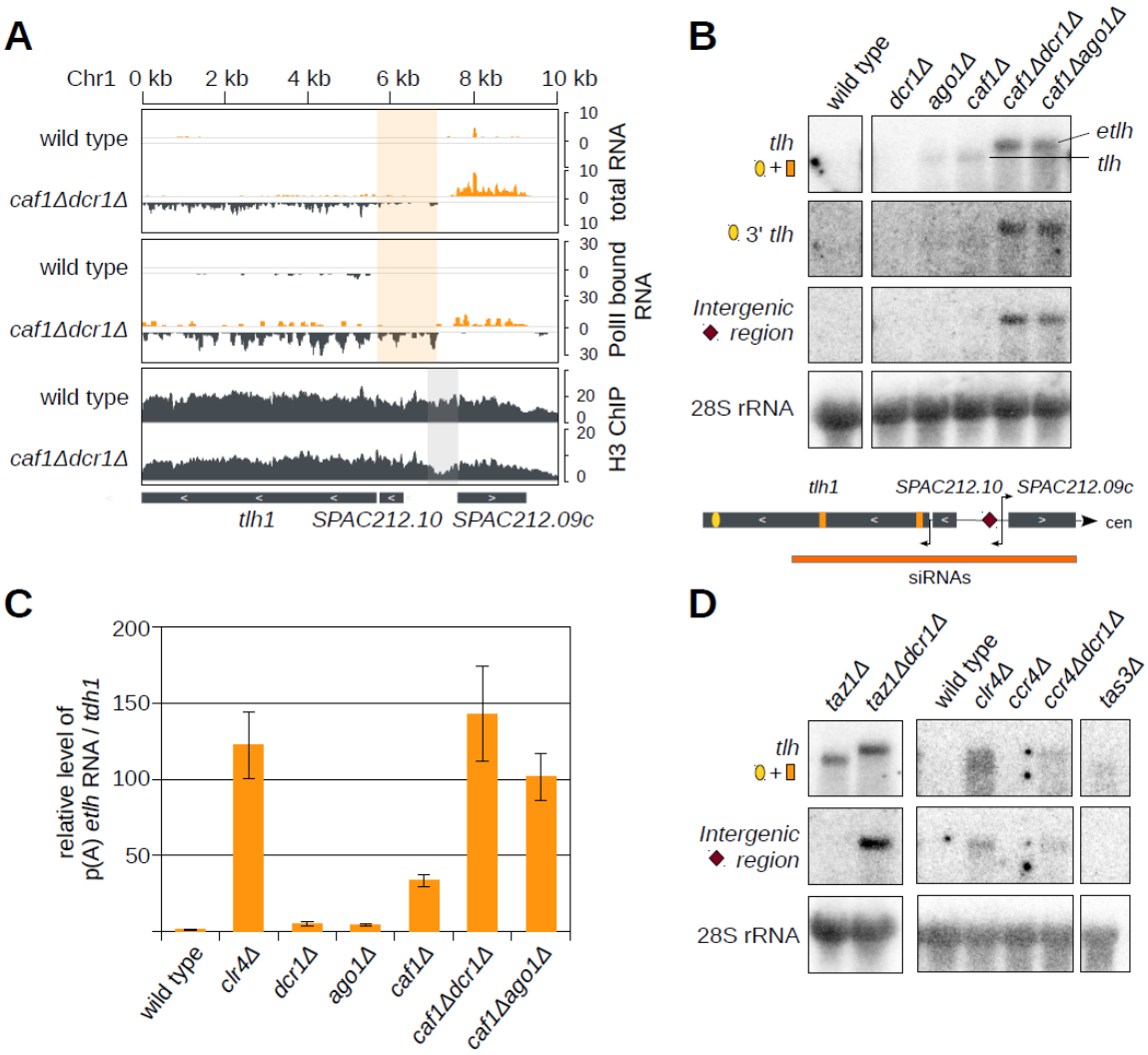

Figure 3.8 Transcriptional and chromatin changes in *caf1Δdcr1Δ* cells

A) Sequencing reads in indicated cells are plotted over the subtelomeric region.

Top and middle panel: Total RNA (top) and RNA Polymerase II (PolII)-associated RNA reads. Reads from + and - strands are depicted in orange and grey, respectively. Scale bars on the right denote RNA read numbers normalized to total number of reads mapping to protein coding genes. Highlighted in orange are reads, which map upstream of *tlh1*.

Bottom panel: H3 ChIP-seq, showing a nucleosome free region (highlighted in grey) upstream of the PolII-associated RNA *tlh* reads. Scale bars on the right denote reads per million.

B) Northern blot analysis showing accumulation of two distinct *tlh* products. Top panel ("*tlh*"): three probes mapping to the annotated *tlh* sequence. Second panel ("3' *tlh*"): one probe mapping to the 3' end of *tlh*. Third panel ("Intergenic region"): one probe hybridizing between SPAC212.10 and SPAC212.09c. Last panel: 28S rRNA probe as loading control. In *caf1Δdcr1Δ* and *caf1Δago1Δ* cells a longer transcript (*etlh*) accumulates.

C) Quantification of subtelomeric *etlh* transcripts in indicated strains by RT-qPCR. In *caf1Δ* cells, *etlh* silencing is strongly reduced. In *caf1Δdcr1Δ* and *caf1Δago1Δ* cells, silencing of the *etlh* transcript is lost. Error bars indicate the standard error of > three independent experiments. Reverse transcription was performed with oligo(dT) primer, qRT-PCR was performed with primers specific for *etlh*. Wild type was set to 1.

D) Northern blot showing accumulation of two distinct products of *tlh*. In *taz1Δdcr1Δ* and *ccr4Δdcr1Δ* cells, *etlh* accumulates. In *tas3Δ* cells only the smaller product, *tlh*, is detected.

3.3 Caf1 and Ccr4 activity is required for heterochromatin assembly

In order to analyze if other subunits of the Ccr4-Not complex are required for subtelomeric silencing, *tlh* RNA levels were determined in single and *dcr1*Δ double mutants. In the double mutant of the second deadenylase Ccr4 and RNAi (*ccr4*Δ*dcr1*Δ), subtelomeric transcripts were accumulating, but H3K9me2 was not completely lost at the subtelomeric *tlh* region (Figure 3.9 A and B). *not2*Δ*dcr1*Δ, *rcd1*Δ*dcr1*Δ (RQCD1, Caf40) and *caf16*Δ*dcr1*Δ cells showed no or little effect on *tlh* RNA levels (Figure 3.9 C), in *mot2*Δ*dcr1*Δ cells, *tlh* transcripts were de-repressed (Figure 3.9 A, and B). Also H3K9me2 was strongly reduced at *tlh* and *dg* repeats in *mot2*Δ*dcr1*Δ cells (Figure 3.9 D). Our data indicate that the Ccr4-Not complex subunits Caf1, Ccr4 and Mot2 are involved in silencing and heterochromatin formation at constitutive heterochromatic loci. At the most distal region (towards centromeres), subtelomeric H3K9me2 was lost already in *caf1*Δ, *ccr4*Δ and *mot2*Δ cells (Cotobal et al., 2015).

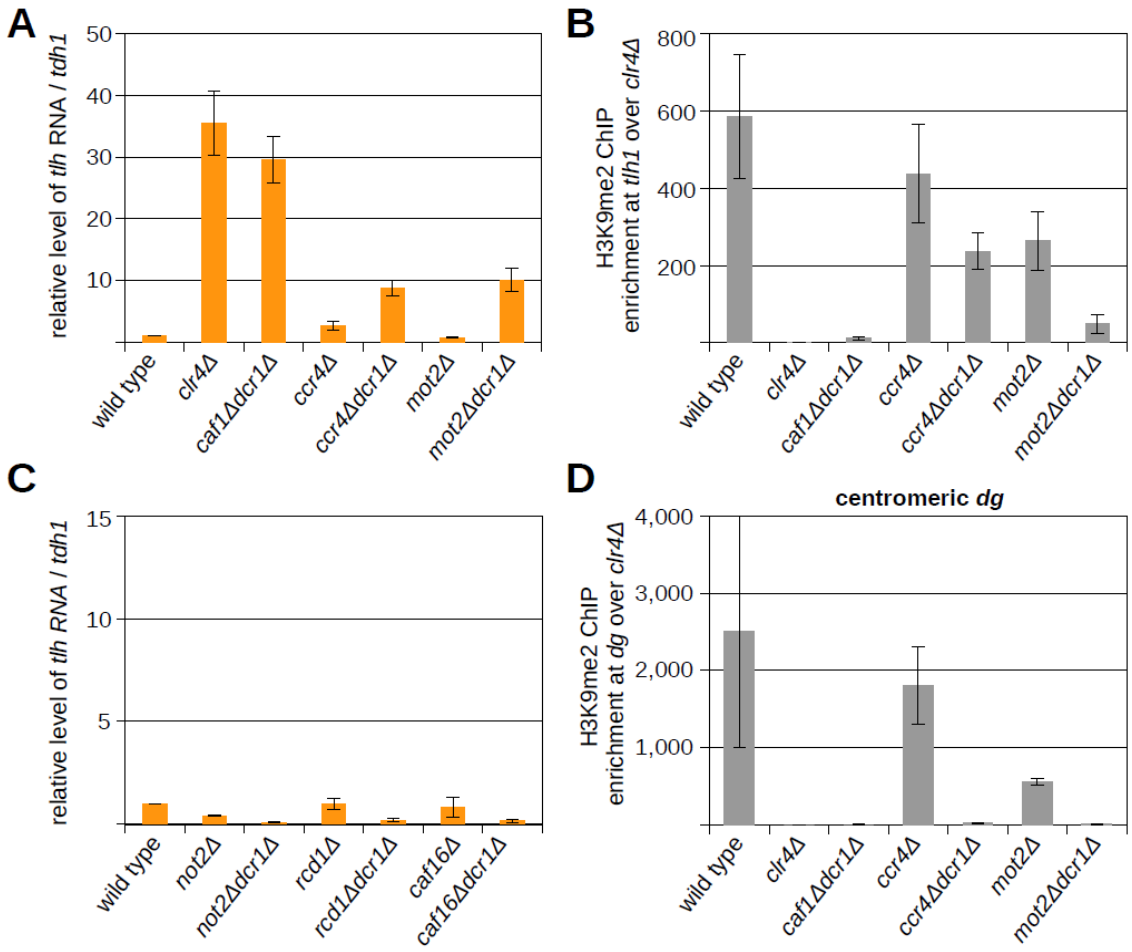

Figure 3.9 Heterochromatic silencing in mutants of Ccr4-Not complex subunits

A) Quantification of subtelomeric *tlh* transcripts in indicated strains by RT-qPCR. In *ccr4Δdcr1Δ* and *mot2Δdcr1Δ* cells, silencing of subtelomeric repeats is defective, but not as much as in *caf1Δdcr1Δ* or *clr4Δ* cells. Error bars indicate the standard error of ≥ three independent experiments. Reverse transcription was performed with specific primers; wild type was set to 1.

B) ChIP experiment showing that H3K9me2 is lost at subtelomeric *tlh* repeats in *mot2Δdcr1Δ* cells, but not in *ccr4Δdcr1Δ*. Error bars indicate the standard error of two (*mot2Δ* and *mot2Δdcr1Δ*) or more independent experiments. *clr4Δ* was set to 1.

C) Quantification of subtelomeric *tlh* transcripts in mutants of different subunits of the Ccr4-Not complex by RT-qPCR (specific primers for RT). Not2, Rcd1 and Caf16 do not contribute to *tlh* silencing. Error bars indicate standard error of three independent experiments.

D) ChIP experiment showing that H3K9me2 is lost at centromeric *dg* repeats in *mot2Δdcr1Δ* cells. Error bars indicate standard error of three independent experiments.

Of all subunits of the Ccr4-Not complex, deletion of the Caf1 had the biggest defect in silencing at subtelomeric *tlh* transcripts. We investigated if the enzymatic deadenylation activity of Caf1 and Ccr4 was required for *tlh* silencing and heterochromatin assembly. We genomically integrated Caf1* (Caf1D53AD243AD174A) and Ccr4* (H665A) activity mutants into *caf1*Δ*dcr1*Δ and *dcr1*Δ cells (Chen et al., 2002; Jonstrup et al., 2007). Introduction of the Caf1* or Ccr4* activity mutants showed only a minor silencing defect in *caf1*dcr1*Δ and *ccr4*dcr1*Δ cells (Figure 3.10 A), suggesting that both deadenylases, Caf1 and Ccr4, might act redundantly. Since Caf1 is required for Ccr4 recruitment to the Ccr4-Not complex, deletion of Caf1 eliminates the activity of both deadenylases (Basquin et al., 2012). Mutation of the active site of both Caf1 and Ccr4 resulted in a strong accumulation of subtelomeric transcripts and reduction in H3K9me2 in *caf1*ccr4*dcr1*Δ cells (Figure 3.10 A and B). Also sequencing of nascent RNA associated with RNA PolII showed an increased transcription in *caf1*ccr4*dcr1*Δ cells, similar to *caf1*Δ*dcr1*Δ cells, at the subtelomeric, *mat* and centromeric loci (Figure 3.10 C).

Our data show that deadenylation by Caf1 and Ccr4 is required for transcriptional silencing at all heterochromatic loci. We note that *caf1*ccr4*dcr1*Δ cells have a slightly weaker defect compared to *caf1*Δ*dcr1*Δ cells, suggesting that Caf1 might recruit an additional factor contributing to RNA degradation or heterochromatin formation.

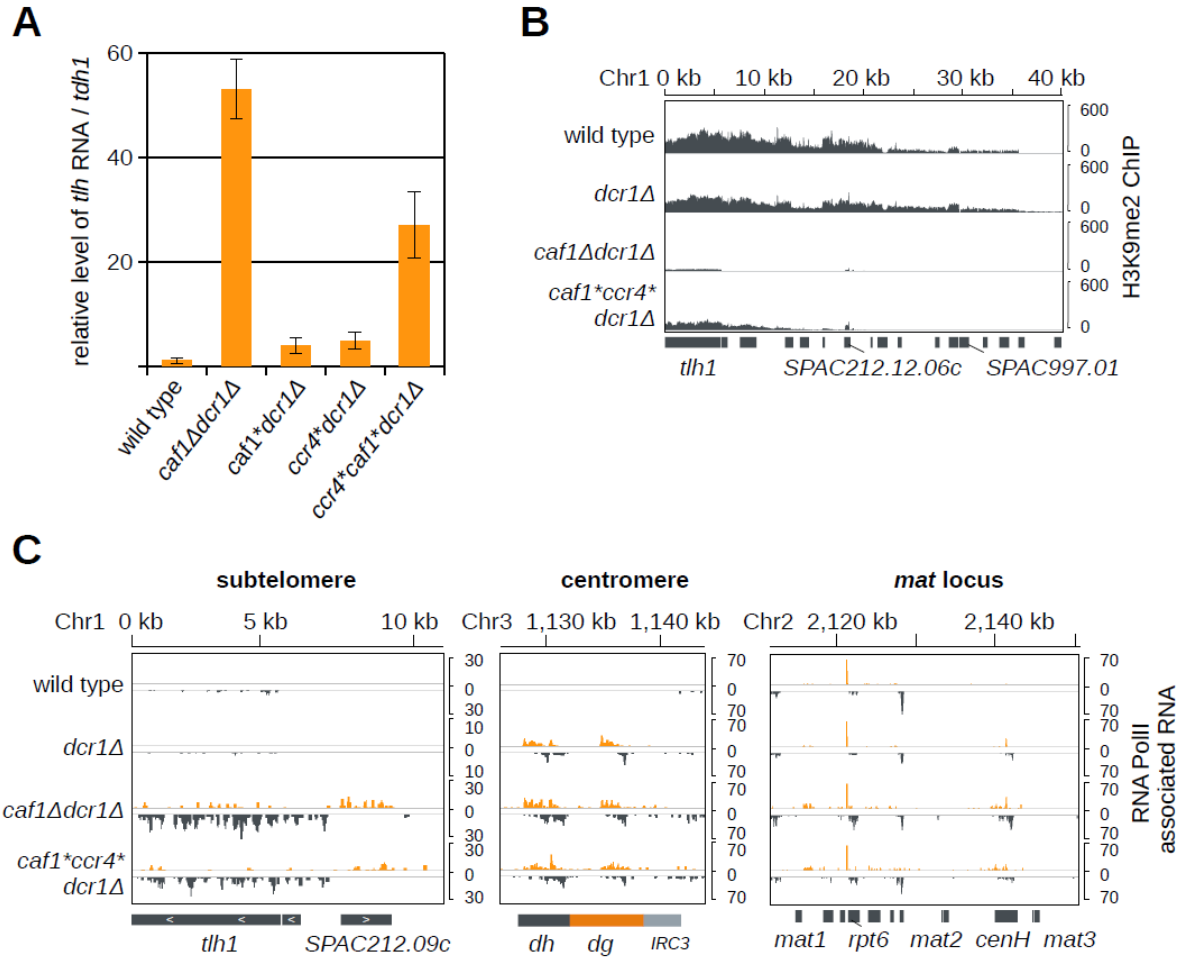

Figure 3.10 Caf1 and Ccr4 nuclease activity is required for heterochromatic silencing

A) Quantification of subtelomeric *tlh* transcripts by RT-qPCR in wild type or *caf1Δdcr1Δ* controls or in *dcr1Δ* strains expressing a Caf1* (Caf1D53AD243AD174A) or / and a Ccr4* (Ccr4H665A) activity mutant. Expression of Caf1* or Ccr4* silences *tlh*, but when both deadenylases are mutated, silencing of *tlh* is lost. Error bars indicate the standard error of three independent experiments. Reverse transcription was performed with specific primers; wild type was set to 1.

B) H3K9me2 ChIP-seq reads plotted over the whole subtelomeric region of chromosome 1 left arm in indicated strains. Scale bars on the right denote read numbers per million reads normalized to the TAS region (Chr2 4,534 kb – 4,538 kb) where H3K9me2 is not lost in the mutants (Figure 3.7).

C) Sequencing reads of RNA PolII-associated RNA in indicated cells are plotted over the subtelomeric *tlh* region, the centromeric region and the *mat* locus. In *caf1*ccr4*dcr1Δ* cells, transcription at all regions is increased compared to wild type cells or at centromeres and *mat*, also compared to *dcr1Δ* cells. Reads from + and - strands are depicted in orange and grey, respectively. Scale bars on the right denote RNA read numbers normalized to total number of reads mapping to protein coding genes.

The result, that the activity mutants had a slightly weaker defect than the deletion mutants suggested that other nucleases and RNA processing factors could also be involved in degradation of heterochromatic RNA. In addition to *caf1*Δ, deletion of the 5'-3' exonuclease Exo2 (Xrn1) showed strong accumulation of subtelomeric siRNAs (Figure 3.11 A) (see 1.4.1). Subtelomeric siRNAs were also increased in deletion of the RNA processing factor *mlo3* (Zhang et al., 2011), which was additionally reported to be involved in mRNA export (Thakurta et al., 2005) (Figure 3.11 A). In mutants with deletion of the nuclear exosome subunit *rrp6*, the TRAMP component *cid14*, the PAF complex subunit *leo1* (Sadeghi et al., 2015), HP1 protein *swi6* and in the *dis3-53* mutant, we observed only a small accumulation of subtelomeric siRNAs (Figure 3.11 A and B). There was little or no effect on siRNA generation at centromeric repeats in these mutants (Figure 3.11 A). These results suggest that the Ccr4-Not/Exo2 pathway eliminates subtelomeric transcripts and this is required for heterochromatic silencing. Cid14 is a poly(A) polymerase of the TRAMP complex which is suggested to target transcripts for exosomal degradation (LaCava et al., 2005) and is also connected to siRNA generation (Bühler et al., 2007, 2008). Dis3, like Rrp6, belongs to the nuclear exosome and was also reported to be involved in heterochromatic silencing (Wang et al., 2008). Leo1 and the PAF (RNA polymerase-associated factor) complex were recently shown by several publications to play a role in heterochromatin formation. However it is not clear if the PAF complex contributes due to transcription termination (Kowalik et al., 2015) or by having an effect on nucleosomes (Sadeghi et al., 2015; Verrier et al., 2015).

Nevertheless, *caf1*Δ and *exo2*Δ cells accumulate the highest amount of siRNA at *tlh* which suggests that the main degradation pathway important for heterochromatic silencing starts with deadenylation by the Ccr4-Not complex followed by the Exo2 dependent 5’-3’ processing.

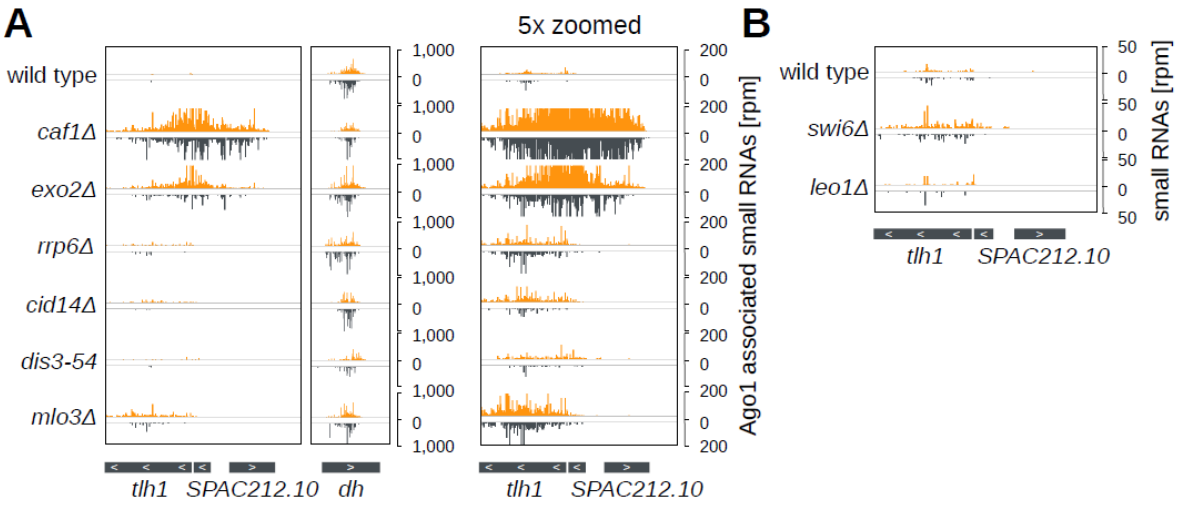

Figure 3.11 Subtelomeric siRNAs accumulate in *exo2Δ* and *caf1Δ* cells

A) Endogenously tagged Argonaute-associated small RNA reads in indicated cells were plotted over the subtelomeric region. The location of genes is indicated as grey boxes below the small RNA peaks. Reads from + and - strands are depicted in orange and grey, respectively. Scale bars on the right denote small RNA read numbers normalized per one million reads. RNAi machinery is targeting the subtelomeric region in deletion of many RNA processing factors, primarily Caf1 and Exo2. Note the 5x zoomed version on the right side. *rrp6Δ* data were processed from GSE38636, *dis3-54Δ* from GSE19734. *cid14Δ* data are from Paola Pisacane, *exo2Δ, caf1Δ* and *mlo3Δ* sRNA were done by Mario Halic.

B) Size selected small RNA reads in indicated cells were plotted over the subtelomeric region. The location of genes is indicated as grey boxes below the small RNA peaks. Reads from + and - strands are depicted in orange and grey, respectively. Scale bars on the right denote small RNA read numbers normalized per one million reads. We observe a small accumulation of subtelomeric siRNAs in *swi6Δ* and *leo1Δ* cells. *leo1Δ* data were processed from GSE66940, *swi6Δ* from GSE70945.

3.4 Heterochromatic RNA accumulates on chromatin

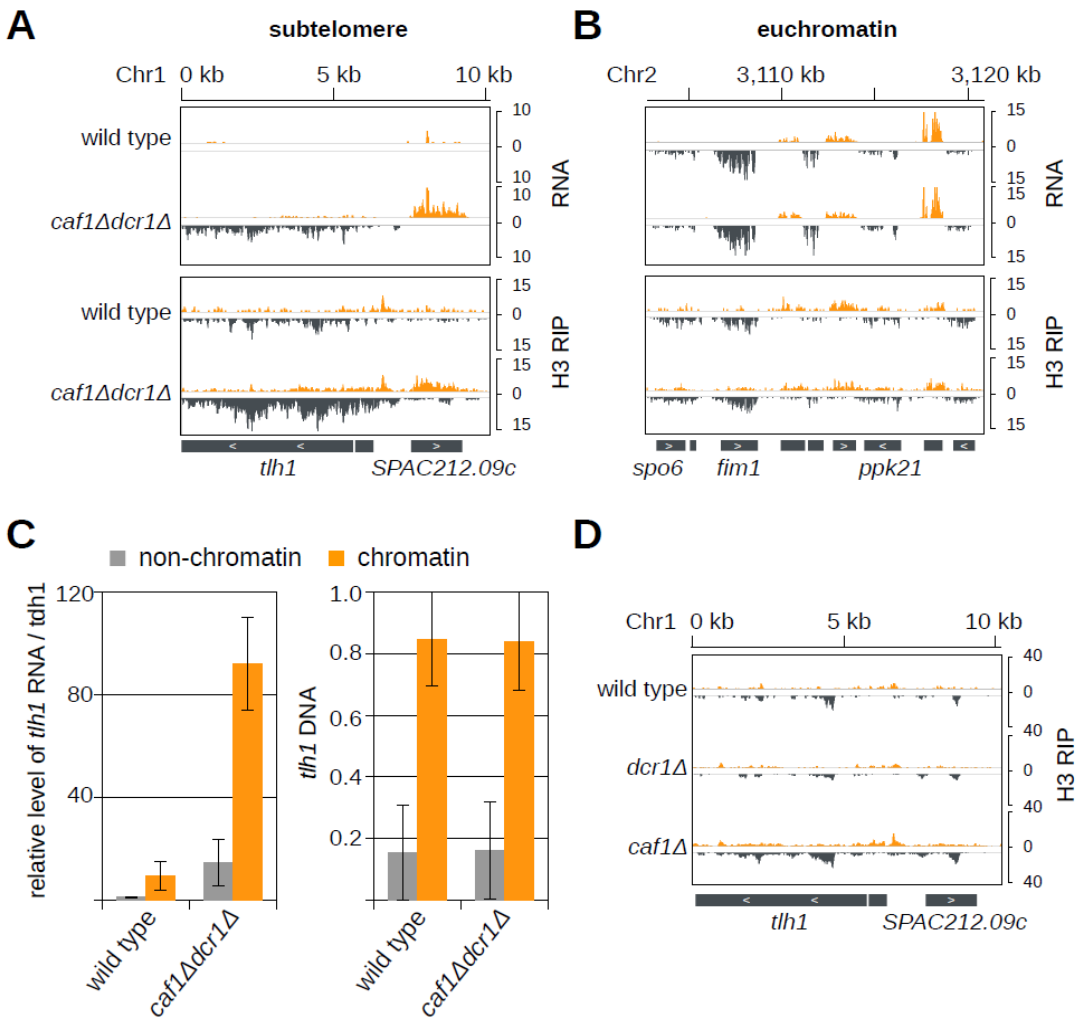

Figure 3.12 *tlh* RNA accumulates on chromatin

A + B) H3-RIP sequencing reads in indicated cells are plotted over the subtelomeric region **(A)** and a euchromatic region **(B)**. Total RNA sequencing reads on top as control. Reads from + and - strands are depicted in orange and grey, respectively. Compared to total RNA, *tlh* is enriched at the chromatin in wild type and *caf1Δdcr1Δ* cells. Scale bars on the right denote RNA read numbers normalized to total number of reads mapping to protein coding genes.

C) Chromatin fractionation assay. Left: RNA levels in indicated strains in non-chromatin or chromatin fraction. *tlh* RNA is enriched in the chromatin fraction in wild type and *caf1Δdcr1Δ* cells. Right: *tlh* DNA levels as a control for fractionation. In the chromatin fraction, DNA is enriched in the chromatin compared to the non-chromatin fraction. Error bars indicate the standard error of three independent experiments.

D) H3-RIP sequencing reads in indicated cells. Reads from + and - strands are depicted in orange and grey, respectively. Scale bars on the right denote RNA read numbers per total number of reads mapping to protein coding genes. Reads are plotted over the subtelomeric region. In *caf1Δ* cells, H3RIP signal is increased compared to wild type.

Our data show that RNA degradation is required for heterochromatic silencing. This suggests that heterochromatic transcripts might accumulate on chromatin. We performed chromatin fractionation and also sequenced histone H3-bound RNA and observed that *tlh* RNA is enriched at chromatin in wild type and even more in *caf1Δdcr1Δ* cells (Figure 3.12 A and C). In *caf1Δ* cells we already observe a small increase of *tlh* transcripts in the chromatin fraction compared to wild type cells (Figure 3.12 D). Euchromatic mRNAs are in contrast less associated with chromatin compared to their RNA level than *tlh* transcripts (Figure 3.12 B).

Genome wide comparison of histone H3-bound RNA and RNA PolII bound nascent RNA revealed that in wild type cells heterochromatic transcripts and lncRNA are more retained at chromatin than mRNAs relative to their transcription (Figure 3.13 A, B and C). We found that heterochromatic transcripts from subtelomeres, centromeres and the *mat* locus accumulate on chromatin (Figure 3.13 D). Our data suggest that heterochromatic transcripts and euchromatic lncRNA are processed less efficiently and tend to accumulate on chromatin post-transcriptionally. In euchromatin, we observed that genes that had chromatin bound RNAs were less efficiently transcribed by RNA PolII (Figure 3.14 A). The same amount of RNA PolII synthesized less nascent RNAs at these genes than at genes with no chromatin bound RNAs (Figure 3.14 A and B). These data show that in wild type cells, chromatin bound RNAs reduce transcription of euchromatic genes. In *caf1Δdcr1Δ* cells, heterochromatic transcripts from all loci and lncRNA associate even more with chromatin than in wild type cells indicating that the Ccr4-Not complex is degrading these transcripts on chromatin (Figure 3.15 A, B, and C).

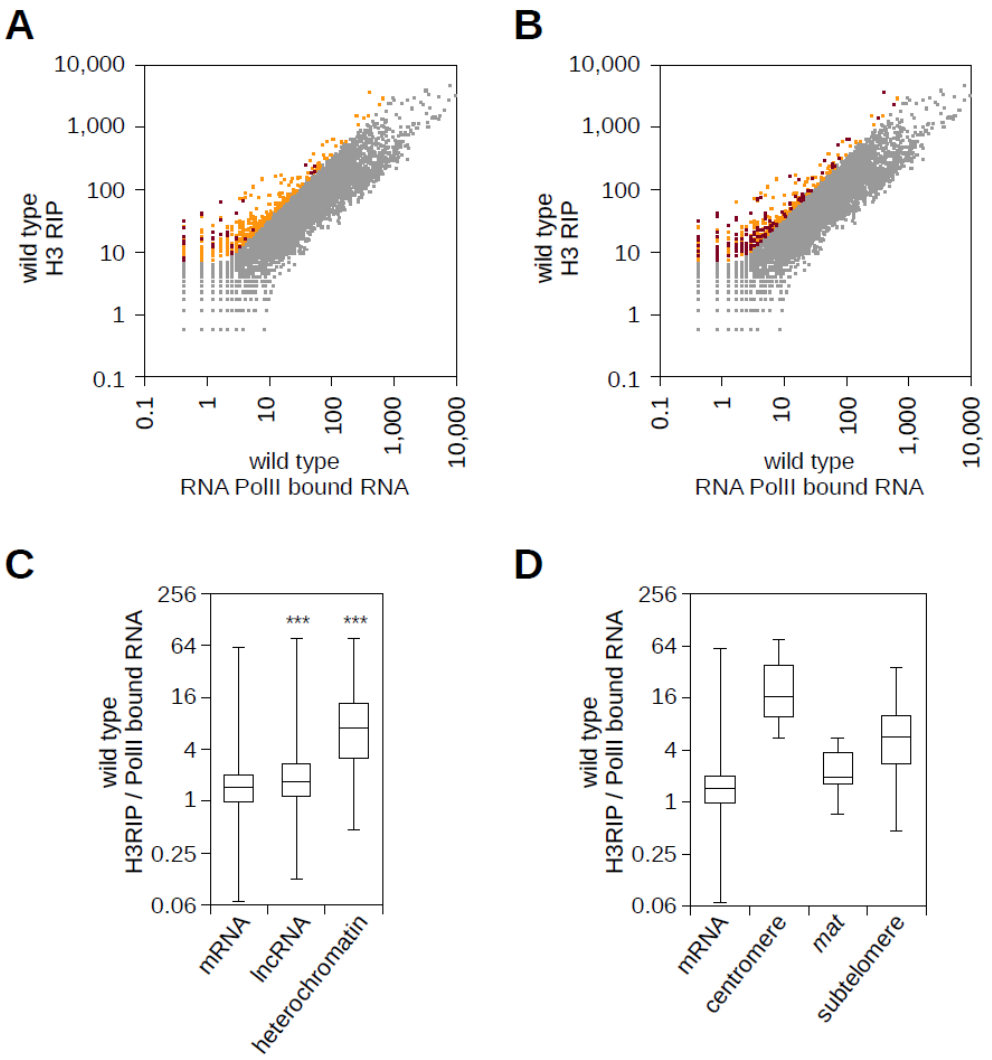

Figure 3.13 Heterochromatic RNA and lncRNA are associated with chromatin in wild type cells

A-B) Scatter plot showing H3-associated RNA relative to RNA PolII bound nascent RNA. RNAs > 4x enriched on chromatin are shown in orange or red for heterochromatic RNA **(A)** or lncRNA **(B)**. Low expressed genes show stronger enrichment on chromatin than high expressed ones.

C) Box plot analysis of H3-associated RNA relative to nascent RNA bound to RNA PolII in wild type cells. „lncRNA" (n=1354): euchromatic noncoding RNA with annotation SPNCRNA. „mRNA" (n=5014): all protein coding genes without genes in heterochromatic areas. „heterochromatic" (n=62): genes which are located in constitutive heterochromatin areas. Relative to their transcript levels, ncRNAs and especially heterochromatic RNA are more likely to be bound to chromatin than mRNA. *** $P < 0.001$.

D) Box plot analysis like C, with separation of heterochromatic transcripts in centromeric, *mat* and subtelomeric.

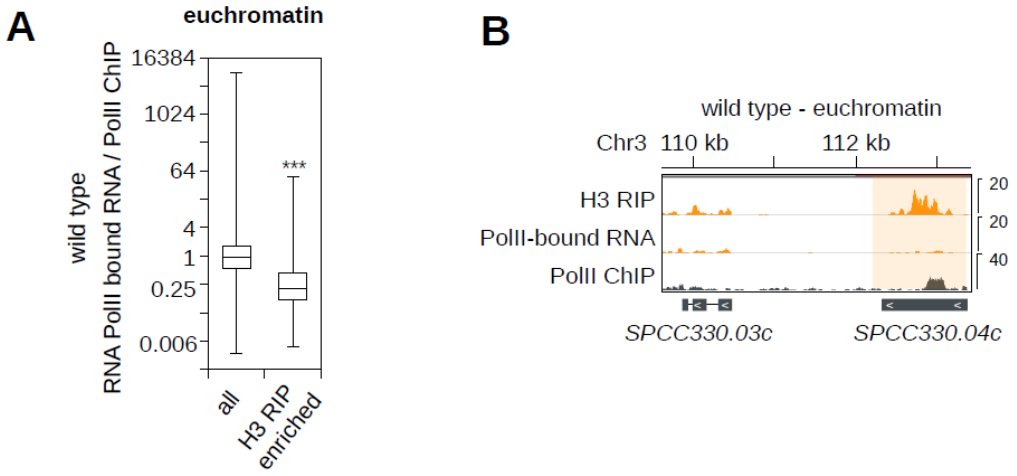

Figure 3.14 euchromatic genes enriched on chromatin are less transcribed

A) Box plot analysis of nascent RNA bound to RNA PolII relative to RNA PolII ChIP in wild type cells. Genes that have RNA enriched on chromatin show reduced transcription when compared to the quantity of RNA PolII on the chromatin. "all" (n=6345): all mRNA and lncRNA. "chromatin enriched" (n=258): euchromatic genes (mRNA and lncRNA) with > 4-fold enrichment in H3-RIP over nascent RNA. *** P < 0.001.

B) Example for a euchromatic gene which is more retained at chromatin. H3-RIP, RNA PolII nascent RNA and RNA PolII ChIP sequencing reads in indicated cells are plotted over a euchromatic region. Reads from + and - strands are depicted in orange and grey, respectively. Scale bars on the right denote RNA read numbers per million normalized to the total number of reads mapping to protein coding genes. Compared to nascent RNA, transcripts of SPCC330.04c (highlighted) are more bound to chromatin than transcripts of the SPCC330.03c gene. Compared to the amount of RNA PolII at these loci (ChIP), SPCC330.04c synthesizes less RNA (PolII-bound RNA) than SPCC330.03c.

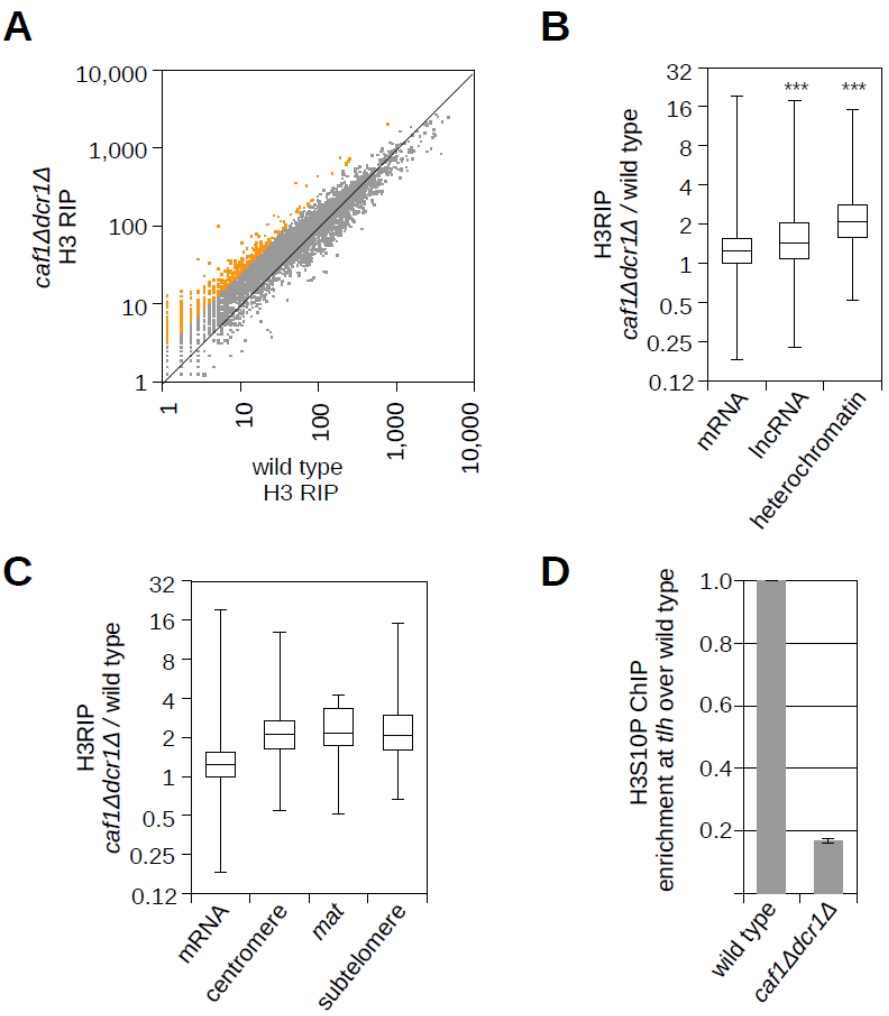

Figure 3.15 Comparison of H3RIP in *caf1Δdcr1Δ* to wild type cells

A) Scatter plot showing H3-associated RNA in *caf1Δdcr1Δ* cells compared to wild type. RNA enriched on chromatin in *caf1Δdcr1Δ* cells are shown in orange.

B) Box plot analysis of H3-associated RNA in *caf1Δdcr1Δ* cells relative to wild type cells. In *caf1Δdcr1Δ* cells, heterochromatic RNA and lncRNA are even more associated with chromatin than in wild type cells. "mRNA" (n=5058); "lncRNA" (n=1467); "heterochromatin" (n=90). *** $P < 0.001$.

C) Box plot analysis of H3-associated RNA in *caf1Δdcr1Δ* cells relative to wild type cells. All constitutive heterochromatic loci are displayed separately.

D) ChIP experiment showing that H3S10P is lost at subtelomeric *tlh* repeats in *caf1Δdcr1Δ* cells. Error bars indicate the standard error of two independent experiments. Wild type was set to 1.

Consistent with a previous observation (Nakama et al., 2012), we find low levels of DNA:RNA hybrids (= R-loops) at subtelomeres in wild type cells (Brönner et al., 2017). In *caf1Δdcr1Δ* cells, heterochromatin is lost and heterochromatic transcripts show a higher amount of DNA:RNA hybrids than in wild type cells (Brönner et al., 2017), indicating that R-loop formation is not heterochromatin dependent. This shows that in wild type cells, RNA elimination by RNAi and

Ccr4-Not prevents accumulation of heterochromatic transcripts on chromatin and formation of DNA:RNA hybrids. DNA:RNA hybrid formation was shown to induce histone 3 serine 10 phosphorylation (H3S10P) (Castellano-Pozo et al., 2013), a chromatin mark that reduces HP1 binding to H3K9 methylated nucleosomes and interferes with heterochromatin formation and silencing (Fischle et al., 2005; Kloc et al., 2008). H3S10P ChIP revealed, however, reduction of H3S10 phosphorylation at *tlh* in *caf1Δdcr1Δ* cells (Figure 3.15 D).

3.5 Caf1 eliminates heterochromatic RNA on chromatin

Our results show that heterochromatic transcripts accumulate on chromatin and suggest that Caf1 degrades them on chromatin. Using ChIP and ChIP-exo sequencing we found that Caf1 is localized at the *tlh* and *SPAC212.09c* region in wild type cells (Figure 3.16 A). This resembles the localization of Ccr4 and Not subunits that were found over open reading frames in *S. cerevisiae* (Kruk et al., 2011; Venters et al., 2011). Caf1 localization on the chromatin was weak but detectable, indicating that Caf1 is not tightly bound to the chromatin. In *clr4*Δ cells, where heterochromatin is lost, even higher amounts of Caf1 were bound to the heterochromatic regions (Figure 3.16 C). In wild type cells, Caf1 is bound to the chromatin in the same region where siRNAs were generated (Figure 3.16 A and D), in *clr4*Δ cells, Caf1 was even enriched over the larger subtelomeric region (Figure 3.16 B and E).

Our data show that the Ccr4-Not complex is associated with chromatin, but the complex is not recruited by heterochromatin. This suggests that the RNA, which is accumulating more on chromatin in *clr4*Δ mutant cells, recruits Caf1 to chromatin.

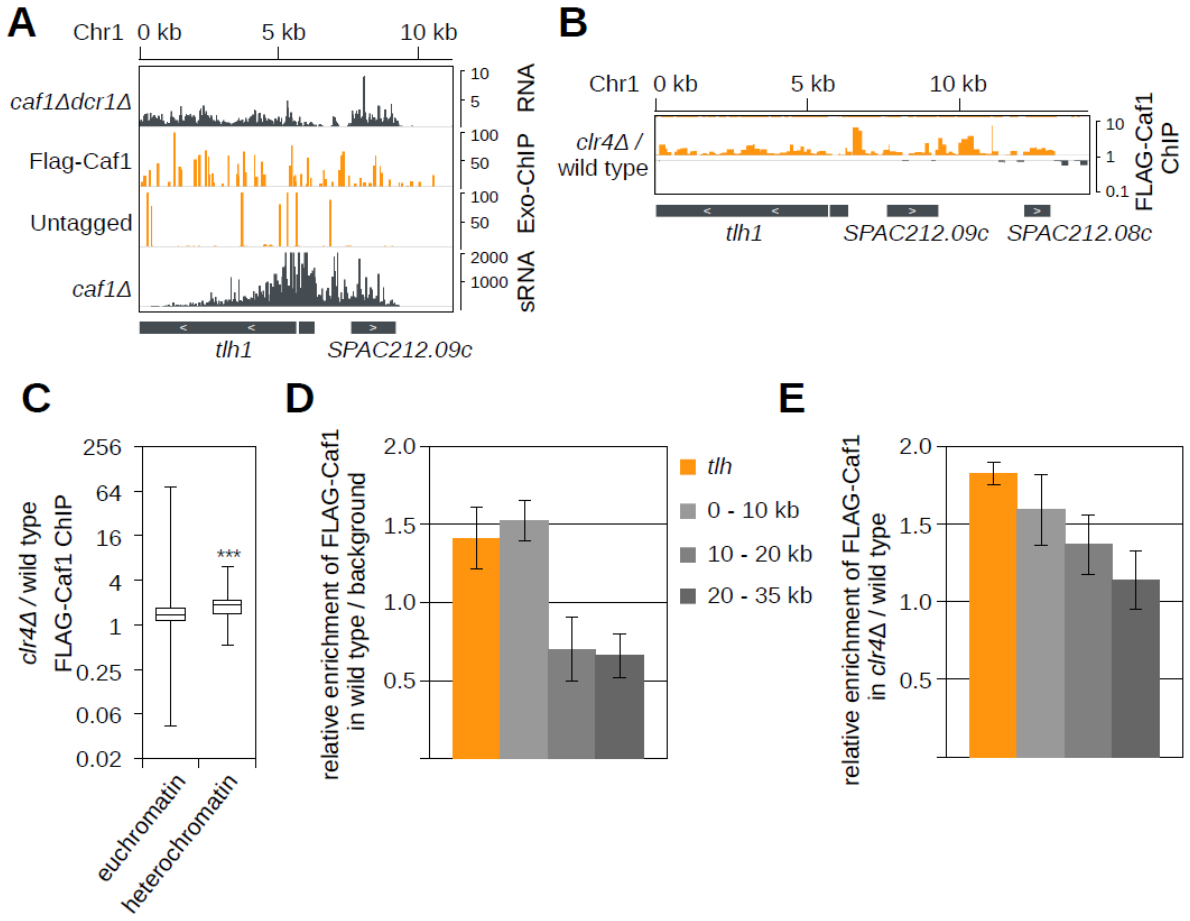

Figure 3.16 Caf1 localizes to chromatin

A) ChIP-exo (orange/ middle) sequencing of endogenously tagged FLAG-Caf1 in wild type cells and untagged cells showing that Caf1 is enriched at subtelomeric *tlh* and SPAC212.09c genes. Caf1 localization overlaps with transcription (top grey) and siRNA generation (bottom grey). Scale bars on the right denote RNA read numbers normalized to total number of reads mapping to protein coding genes (RNA), or reads per million (Exo-ChIP and sRNA). Exo-ChIP was performed by Ilaria Ugolini.

B) ChIP sequencing of endogenously tagged FLAG-Caf1 in *clr4Δ* cells over wild type cells. Caf1 is enriched at chromatin when Clr4 is deleted. Scale bars on the right denote fold change of FLAG-Caf1 ChIP in *clr4Δ* over wild type cells.

C) Box plots of FLAG-Caf1 ChIP showing that in *clr4Δ* cells, Caf1 is more localized to heterochromatic loci than in wild type cells. *** $P < 0.001$.

D, E) Quantification of FLAG-Caf1 ChIP-seq reads at indicated regions of chromosome 1 in wild type cells over background **(D)** and in *clr4Δ* over wild type cells **(E)**. Caf1 localizes at *tlh* and *SPAC212*.09c in wild type cells; in *clr4Δ* cells Caf1 is enriched over wild type at the complete subtelomeric heterochromatic region. Error bars indicate the standard error of two independent experiments.

We also performed Caf1 RNA-IP from chromatin and soluble fractions. The data show that chromatin associated Caf1 binds *tlh* more than soluble Caf1 in wild type cells, further supporting on chromatin degradation (Figure 3.17 A). Other heterochromatic transcripts from subtelomeric and *mat* regions are degraded by Caf1 on chromatin as well (Figure 3.17 B). At centromeric repeats we found that Caf1 does not degrade chromatin associated RNA in wild type cells which is consistent with RNAi being the primary degradation machinery at this locus (Figure 3.17 B). In *clr4Δ* cells, chromatin bound Caf1 associates with higher amounts of heterochromatic transcripts than soluble Caf1 (Figure 3.17 A and B). This is consistent with increased Caf1 localization to heterochromatic DNA in *clr4Δ* cells and shows that Caf1 degrades heterochromatic RNA on chromatin (Figure 3.16 B and Figure 3.17 A). Our data suggest that chromatin bound RNA is degraded by Ccr4-Not on chromatin, while mRNAs that are exported are degraded in cytosol.

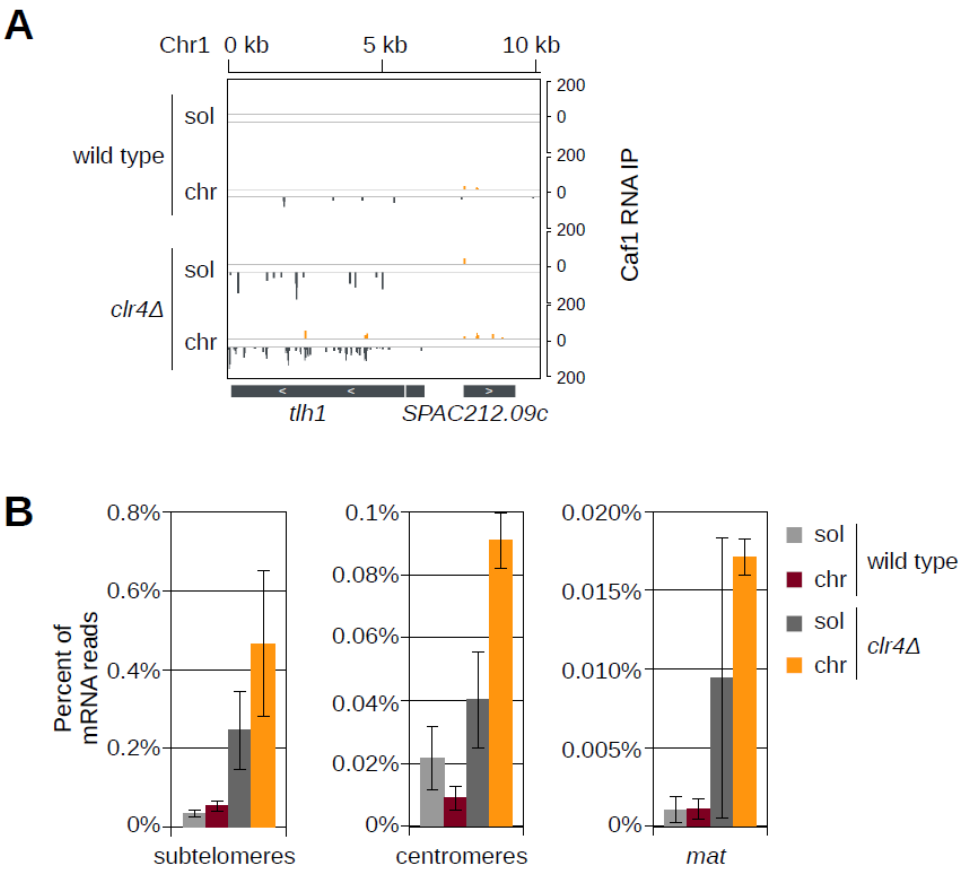

Figure 3.17 Caf1 degrades heterochromatic RNA on chromatin

A) Sequencing of FLAG-Caf1 bound RNA from soluble (sol) and chromatin (chr) fractions. *tlh* RNA associates more with Caf1 from the chromatin than the soluble fraction in both wild type and in *clr4Δ* cells. Reads from + and - strands are depicted in orange and grey, respectively. Scale bars on the right denote RNA read numbers normalized to total number of reads mapping to protein coding genes.

B) Quantification of heterochromatic transcripts bound to Caf1 in soluble (sol) and chromatin (chr) fractions in wild type and *clr4Δ* cells. Heterochromatic transcripts from subtelomeres, centromeres and *mat* locus are shown as percentage of mRNA reads.

3.6 Expression of heterochromatic *tlh* RNA leads to loss of silencing

All data presented so far show that RNA accumulation on chromatin has a negative impact on heterochromatin assembly. To test this possibility and exclude secondary effects of mutant backgrounds, we generated wild type strains expressing the heterochromatic *tlh* transcript under the thiamine repressible *nmt1* promoter at a locus 5.5 kb upstream of *tlh* (Figure 3.18 A). We split the *tlh* gene into two halves (5'*tlh* and 3'*tlh*) and inserted the 5' half into the genome at the place of *SPNCRNA.70*. As a control Luca Salvi generated the same construct with the euchromatic *LEU2*. Luca Salvi inserted also an *ade6* reporter gene 5 kb upstream of the 5'*tlh/LEU2* expressing constructs (Figure 3.18 A). When grown on low adenine medium, cells that silence the *ade6* reporter gene are red, and cells that express *ade6* are white. When grown on *nmt1* repressive low adenine medium (YE), the cells expressing the *LEU2* gene had mainly red colonies indicating that the *ade6* reporter is silenced (Figure 3.18 B). Expression of the 5'*tlh* construct showed a higher percentage of white colonies even under promoter repressive conditions (Figure 3.18 B).

When plated on EMMC low adenine media, the *nmt1* promoter is activated and RNA is transcribed at much higher levels with all constructs being expressed at similar levels (Figure 3.18 C). 5'*tlh* expressing cells showed strong loss of heterochromatin, and mainly white colonies were present on EMMC media (Figure 3.18 B). On the contrary, the *LEU2* expressing control cells did not show an increased loss of silencing on EMMC media (Figure 3.18 A). In *nmt1*-5'*tlh* expressing cells we find an increase in chromatin retention of *tlh* RNA after induction of *tlh* expression on EMMC (Figure 3.18 D). Although expressed at the same level, *LEU2* RNA shows very little enrichment on chromatin (Figure 3.18 D). In the *nmt1-LEU2* strain, we also do not observe a change in chromatin retention of endogenous *tlh* (Figure 3.18 D). The fact that *tlh* levels are enriched compared to *LEU2* RNA in H3RIP-seq is likely due to more endogenous copies.

This assay shows, that expression and chromatin retention of heterochromatic transcripts leads to loss of heterochromatin in a dose dependent way even in wild type cells.

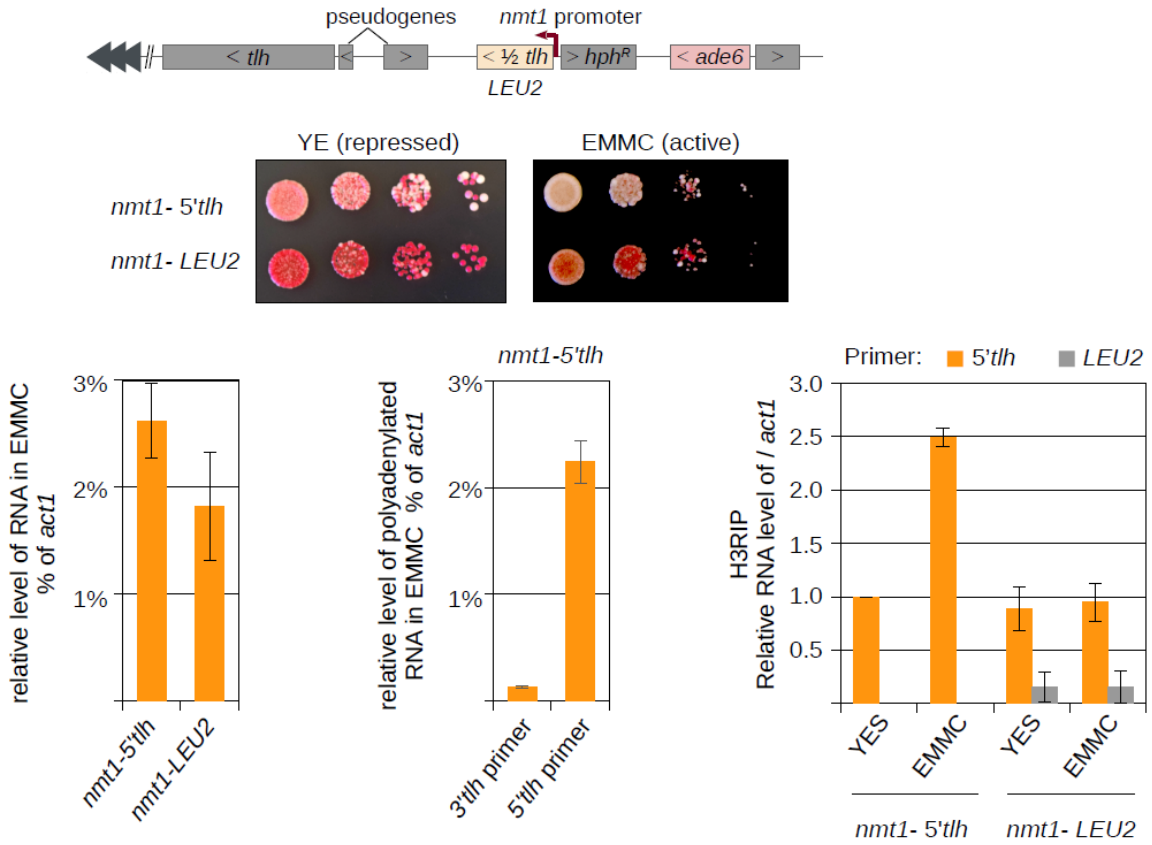

Figure 3.18 Expression of heterochromatic RNA leads to loss of silencing

A) Scheme showing the constructs used. The first half of *tlh* (5'*tlh*) or *LEU2* were inserted ~5.5 kb upstream of *tlh* under the thiamine inducible *nmt1* promoter. The *ade6* reporter gene was inserted 5 kb upstream of the inducible expression system.

B) Growth assay with *ade6* reporter gene showing *nmt1*-5'*tlh* and *nmt1-LEU2* cells. Heterochromatin maintenance of a silenced, red colony was analyzed for each strain on YE (low adenine, thiamine +) or EMMC low ade (10mg/l adenine, thiamine -) plates. Cells which silence *ade6* are red, while *ade6* expressing cells are white when grown on low adenine plates. Cells were plated in 10-fold dilutions starting with 10^5 cells. Growth assay was done by Luca Salvi.

C) Quantification of expression of 5'*tlh* in *nmt1*-5'*tlh* cells and *LEU2* in *nmt1-LEU2* cells by RT-qPCR under inducible condition (EMMC media). Expression is shown as percentage of *act1* expression. The constructs are expressed at a similar level. Error bars indicate standard error of three independent experiments.

D) The *nmt1*-5'*tlh* construct is polyadenylated. Reverse transcription of *nmt1*-5'*tlh* RNA with oligo(dT) primer and subsequent qRT-PCR with primers mapping to 3'*tlh* (not overexpressed in that strain) or 5'*tlh*. As the 5'*tlh* primer shows upregulation compared to the 3'*tlh* primer, the overexpression construct is polyadenylated although the gene is not complete.

E) Quantification of chromatin associated RNA in indicated strains and conditions by H3RIP RT-qPCR. In *nmt1*-5'*tlh* strains, 5'*tlh* RNA is enriched at chromatin in EMMC (induced) compared to YES medium (repressed). In *nmt1-LEU2* strains, neither *tlh* nor *LEU2* RNA is changed upon induction of *LEU2* expression.

3.7 Model for the impact of RNA on heterochromatin formation

Based on all results, the Ccr4-Not complex and RNAi are redundant pathways for heterochromatin maintenance in wild type cells at all constitutive heterochromatic loci. The deadenylation activity is important and degradation seems to take place on chromatin where heterochromatic RNA and the Ccr4-Not complex are localized. Loss of both degradation pathways, RNAi and Ccr4-Not, increases the amount of RNA which accumulates on chromatin. Chromatin bound RNA impairs spreading of H3K9 methylation resulting in loss of heterochromatin (Figure 3.19). In conclusion, degradation of chromatin bound RNA by the Ccr4-Not complex or RNAi is essential for heterochromatin organization.

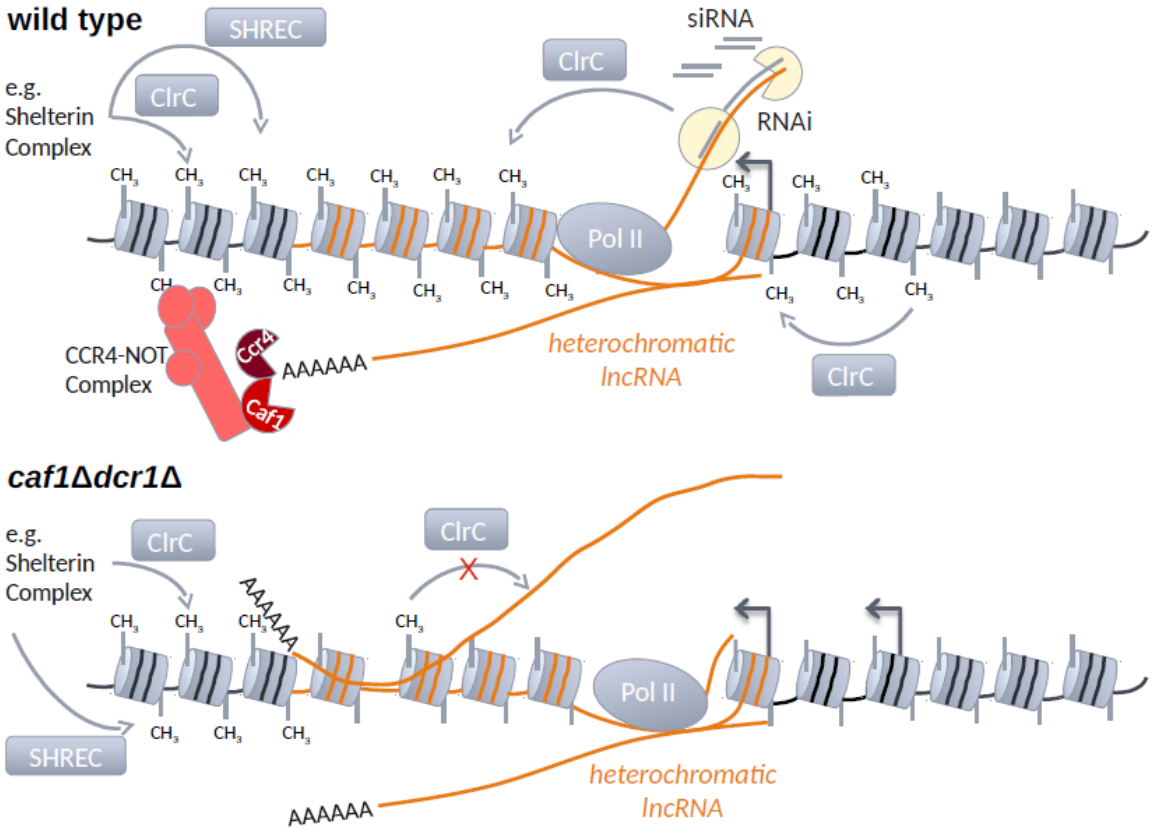

Figure 3.19 Accumulation of RNA on chromatin disrupts heterochromatin

Model: RNAi or Shelterin complex recruit the CLRC methyltransferase and SHREC deacetylase complexes to establish heterochromatin in wild type cells. CLRC and SHREC spread into repeats to establish heterochromatin. The Ccr4-Not complex eliminates heterochromatic RNA and promotes spreading of H3K9me2 over the transcribed region. In the absence of the Ccr4-Not complex and RNAi, heterochromatic transcripts accumulate on the chromatin. This leads to loss of heterochromatin. At the transcribed loci, heterochromatin is lost in *caf1Δdcr1Δ* cells, indicating that at transcribed regions RNA degradation is required for heterochromatin assembly.

4. Discussion

4.1 RNA degradation and heterochromatin

4.1.1 Comparison of current literature

Although RNA is required for heterochromatin formation, this thesis shows that RNA needs to be degraded and RNA accumulation on chromatin leads to loss of heterochromatin. Consistent with our finding, a link between various RNA degradation machineries and heterochromatin formation was recently reported. One example is H3K9me2 at so called heterochromatic islands, which comprise mainly meiotic genes (Zofall et al., 2012). Many of those meiotic genes have a determinant of selective removal (DSR) sequence, which is targeted by the protein Mmi1 for exosomal degradation (Harigaya et al., 2006). This removal of meiotic transcripts is important for suppression of meiosis (Harigaya et al., 2006). Next to Mmi1, this pathway includes the nuclear exosome subunit Rrp6, the poly(A)-binding protein Pab2 and the RNA elimination defective protein Red1 (St-André et al., 2010; Sugiyama and Sugioka-Sugiyama, 2011). Interestingly, deletion of the genes *mmi1*, *rrp6* or *red1* leads to loss of H3K9me2 at several islands (Hiriart et al., 2012; Zofall et al., 2012). Red1 is part of the NURS complex (nuclear RNA silencing complex) or also called MTREC (Mtl1-Red1 complex), which interacts with Mmi1 and directs the bound RNA to exosomal RNA degradation (Egan et al., 2014). Red1 immunoprecipitates with components of the methyltransferase complex CLRC (Zofall et al., 2012), which lead to the conclusion that CLRC is directly recruited to meiotic genes. In contrast, Hiriart et al. suggest that Mmi1 is responsible for recruitment of RNAi to meiotic genes which in return would be responsible for CLRC recruitment and methylation of H3K9 (Hiriart et al., 2012).

Another RNA degradation pathway which was connected with heterochromatin includes the essential 5'-3' exoribonuclease Dhp1 (= Rat2 or Xrn2) (Chalamcharla et al., 2015; Tucker et al., 2016). This nuclease is involved in transcription elongation and RNA PolII termination as it targets for example the downstream fragments which remain after cleavage at the poly(A) site (Brannan et al., 2012; Jimeno-González et al., 2010; Kim et al., 2004b). Depletion of *dhp1* leads to loss of H3K9 methylation at meiotic genes, as well as reduction of H3K9me2 at constitutive heterochromatin (Chalamcharla et al., 2015; Tucker et al., 2016). Both studies also showed that Dhp1 interacts with Rik1 of the CLRC complex which resulted in the conclusion that loss of Dhp1 also hinders CLRC recruitment and H3K9 methylation (Chalamcharla et al., 2015;

Tucker et al., 2016). But Tucker et al. also presented that the exonucleolytic activity of Dhp1 is important and they suggested a role in posttranscriptional gene silencing (Tucker et al., 2016). Consistent with our results, those studies clearly show a connection between RNA degradation and heterochromatin; however, they suggested mostly a direct recruitment of the H3K9 methyltransferase by different RNA degradation machineries to establish heterochromatin. It remained unclear how general RNA degradation pathways could recruit CLRC specifically to heterochromatic transcripts. We found that the main role of RNA degradation machineries, in particular the Ccr4-Not complex, is to eliminate heterochromatic transcripts on chromatin. As degradation is the common feature of those pathways, this explanation also sounds more reasonable than that all the different RNA degrading enzymes recruit heterochromatic proteins.

In fission yeast, the Ccr4-Not complex was recently shown to be also involved in H3K9 methylation at rDNA and meiotic genes (Cotobal et al., 2015; Sugiyama et al., 2016). Cotobal et al. showed that at meiotic genes, the activity of Ccr4 is important and that the Ccr4-Not complex works together with Mmi1. This was confirmed by structural studies which showed that Mmi1 is a stable subunit of the complex in *S. pombe* (Ukleja et al., 2016). In contrast to Ccr4 and Caf1, Mmi1 does not affect constitutive heterochromatin formation (Cotobal et al., 2015), suggesting an independent mechanism there. Sugiyama et al. found a connection of the Ccr4-Not complex and the protein Erh1, which together with Mmi1 is involved in suppressing meiotic mRNAs during vegetative growth. Deletion of *ccr4* as well as of *erh1* showed a defect in H3K9 methylation and integrity at rDNA repeats, respectively (Sugiyama et al., 2016), which was not further analyzed mechanistically.

Additionally, the Ccr4-Not complex was shown to play a role in silencing in higher eukaryotes. In *C. elegans* a genome-wide screen revealed enhanced RNAi in soma and germline cells in knockdowns of subunits of the Ccr4-Not complex (Fischer et al., 2013). In *D. melanogaster* germline cells, knockdown of the Ccr4-Not complex components *Not1*, *Twin* (Ccr4) and *Pop2* (Caf1) leads to nuclear accumulation of subtelomeric *HetA* transposons that are also targeted by the piRNA system (Morgunova et al., 2015). piRNAs (PIWI interacting small RNAs) target transposons in animal germline cells and establish heterochromatin in a similar way to siRNAs in fission yeast (Hirakata and Siomi, 2016). The observations in *C. elegans* and *D. melanogaster* are analogous to our findings in *S. pombe* and imply a conserved role of the Ccr4-Not complex in degradation of chromatin associated heterochromatic transcripts.

4.1.2 RNA degradation – the exclusive solution?

We show that heterochromatic transcripts are polyadenylated and that the deadenylation activity of the Ccr4-Not complex is important for heterochromatin maintenance. This indicates that degradation of polyadenylated RNA occurs on chromatin post-transcriptionally. We observed that *ccr4Δdcr1Δ* cells have less defect than *caf1Δdcr1Δ* cells, where both deadenylases are lost (Basquin et al., 2012). These data show that the activity of both, Caf1 and Ccr4, is required to silence heterochromatic transcripts and maintain heterochromatin. It has also been shown that enzyme activities of human and *S. pombe* Caf1 and Ccr4 are both required for deadenylation (Maryati et al., 2015; Stowell et al., 2016). In addition to the deadenylases Caf1 and Ccr4, deleting the E3 ubiquitin ligase Mot2 showed loss of silencing when combined with RNAi mutants. A recent study showed that ubiquitination of CNOT7, a mammalian orthologue of Caf1, was required for its deadenylation activity and mRNA degradation (Cano et al., 2015). It could be that Mot2 plays a similar role in activation of the deadenylase activity of Caf1 and Ccr4, leading to the observed defects. Mot2 might also have a distinct function.

We observed a slightly weaker defect in the activity mutants than in the knock-out strains, suggesting that the activity mutant can recruit other RNA processing enzymes, like Exo2 (Xrn1) (Collart and Panasenko, 2012; Miller and Reese, 2012). Another possibility is that other functions of the Ccr4-Not complex are impaired in the deletion mutants. Recently, the Ccr4-Not complex was shown to act as a transcription elongation factor suggested to reactivate arrested RNA PolII (Dutta et al., 2015; Kruk et al., 2011). Dicer was also implicated in release of stalled RNA PolII, which reduces DNA:RNA hybrid formation (Castel et al., 2014). These functions might contribute to heterochromatin formation additional to RNA degradation.

Double mutants of *caf1* and the HP1 protein *swi6* display a strong defect in heterochromatic silencing at *tlh*, whereas *swi6Δdcr1Δ* do not show additional transcripts compared to single mutants. Deletion of *swi6* leads to opening of the chromatin, as it is important for compaction (Bannister et al., 2001). This suggests, that the RNA degradation by RNAi alone is not as important for heterochromatin formation as RNA degradation by the Ccr4-Not complex. But this result also shows that the function of heterochromatin establishment by RNAi (which includes binding of the HP1 protein) is necessary. This is consistent with the siRNA data, which show that a low amount of RNAi is abundant at *tlh* in wild type cells, but they increase tremendously in the *caf1Δ* mutant. According to those results, the Ccr4-Not complex is the

main degradation pathway. RNAi is also degrading transcripts, but the impact of heterochromatin establishment is stronger.

4.2 One gene, two transcripts

Heterochromatin is a very effective way to silence large regions of the genome. Still, heterochromatin is not completely silence, as transcription is for example necessary for RNAi dependent heterochromatin formation (Bühler and Moazed, 2007). Looking more closely at the *tlh* gene demonstrates that heterochromatin regulates more than just the gene's status ON or OFF. In the case of *tlh*, loss of heterochromatin in *caf1Δdcr1Δ* cells leads to the opening of a second promoter resulting in a longer transcript, we called *etlh*. In contrast, in wild type cells and *caf1Δ* or *dcr1Δ* single mutants, heterochromatin could still suppress the longer transcript so that the short *tlh* was the dominant transcript detected by Northern blot. This is consistent with the meiotic gene *ssm4*. Deletion of *rrp6* results in loss of H3K9me2 as well as the detection of an additional long transcript, starting upstream of the original *ssm4* promoter (Zofall et al., 2012). In the case of *ssm4*, the upstream promoter is not covered by H3K9me2 in wild type cells, but a *pab2Δ* mutant which increases the amount of the small transcript but not loss of H3K9me2 there, did not accumulate the long transcript, whereas in concern with a *clr4* deletion the longer transcript appeared (Zofall et al., 2012). This suggests that H3K9me2 is able to regulate connected promoters, not just degradation. At *ssm4* the two transcripts are produced concurrently, for *tlh* it seems like transcription of *etlh* inhibits the promoter of the smaller product. This transcriptional interference is likely to be a general regulation mechanism, in which the transcription of the long transcript turns the downstream promoter off (Ard and Allshire, 2016; Ard et al., 2014).

4.3 Recruitment of the Ccr4-Not complex to heterochromatin

The Ccr4-Not complex was initially described as a chromatin associated complex involved in transcription (Miller and Reese, 2012), but its role on chromatin and how it should be recruited remained unclear. Our data show that chromatin bound RNA will recruit the Ccr4-Not complex to chromatin. In *clr4Δ* cells, we observe higher amounts of the Ccr4-Not complex on chromatin, than in wild type cells. Together with the result that *swi6Δcaf1Δ* mutants have a cumulative defect compared to single mutants, those data show that the Ccr4-Not complex is not recruited by H3K9me2 or HP1 proteins. It rather suggests that more RNA observed on

chromatin in *clr4Δ* mutants recruits a higher amount of the Ccr4-Not complex. Another possibility how the Ccr4-Not complex could be recruited to heterochromatin was due to RNAi. Cotobal et al. could co-immunoprecipitate Ccr4 and the RITS protein Chp1 (Cotobal et al., 2015) and in higher eukaryotes it is known that the Ccr4-Not complex is recruited to miRNA targets by interaction of CNOT9 (Rcd1) and the GW182 protein (Tas3) (Chen et al., 2014; Mathys et al., 2014). This would have fit to another publication where it looked like *chp1Δ* and *tas3Δ* had a strong increase of *tlh* transcripts compared to wild type cells (Schalch et al., 2011). Schalch et al., however, did not show controls like *clr4Δ* or *dcr1Δ* as comparison. Figure 3.9 C and Figure 3.8 D demonstrate that neither *rcd1Δdcr1Δ* nor *tas3Δ* cells lead to loss of silencing like *caf1Δdcr1Δ* mutants. This implies that these proteins cannot be considered as the ones being responsible for recruitment of the Ccr4-Not complex to heterochromatin.

We do not have a direct proof about Ccr4-Not recruitment by RNAs, but the Caf1-ChIP, Caf1-RIP and H3-RIP experiments show a high correlation for direct RNA degradation on chromatin. In human cells about 41.8% of lncRNA are not exported to the cytosol (Kapranov et al., 2007), with lncRNA being "predominantly localized in the chromatin and nucleus" (Derrien et al., 2012). A recent study suggests that in mammalian cells some lncRNAs might be degraded co-transcriptionally on chromatin, while others are degraded in the nucleoplasm (Schlackow et al., 2017). It remains to be analyzed why specific RNA are degraded already on chromatin and others in the soluble fraction. The Ccr4-Not complex is found in the cytosol and the nucleus (Collart, 2016) and our data suggest that Ccr4-Not localization is a result of RNA localization. RNAs that are predominately in the soluble fraction will recruit the Ccr4-Not complex in the soluble fraction and chromatin bound RNA recruit the complex to chromatin.

4.4 Accumulation of RNA on chromatin

4.4.1 DNA:RNA hybrids

Our data suggest that degradation of heterochromatic transcripts reduces the chance of RNA accumulation on chromatin in general and also DNA:RNA hybrid formation. The retention on the chromatin and R-loop formation was not dependent on heterochromatin, RNAi or Caf1. This also supports the previous observation that chromatin retention by DNA:RNA hybrid formation is an intrinsic property of heterochromatic transcripts in fission yeast (Castel et al., 2014; Nakama et al., 2012). Our data show that elimination of heterochromatic RNA by RNAi and the Ccr4-Not complex reduces R-loop formation and promotes heterochromatin assembly

in wild type cells. Similar to our study, *C. elegans* mutants, which cannot establish H3K9me also accumulate DNA:RNA hybrids at repeats (Zeller et al., 2016). But it has also been shown that chromatin retention and DNA:RNA hybrid formation establishes RNAi-mediated heterochromatin formation (Skourti-Stathaki et al., 2014; Sun et al., 2013; Yu et al., 2014). In contrast, deletion of RNase H reduces heterochromatin formation indicating that an excess of DNA:RNA hybrids has a negative impact on heterochromatin assembly (Nakama et al., 2012). DNA:RNA hybrids were also shown to inhibit nucleosome formation (Dunn and Griffith, 1980) or correlate with DNA damage (Keskin et al., 2014; Stirling et al., 2012), which would interfere with chromatin organization.

Depletion of RNA processing factors, such as the nuclear exosome or RNA export machinery showed increased R-loop formation on protein coding genes (Aguilera and García-Muse, 2012; Pefanis et al., 2015; Santos-Pereira and Aguilera, 2015; Stirling et al., 2012). In those mutants transcripts are retained on chromatin after transcription termination, indicating that they can induce DNA:RNA hybrids post-transcriptionally or even in *trans* (Santos-Pereira and Aguilera, 2015; Wahba et al., 2013). This fits with our finding that defects in RNA processing lead to RNA accumulation on chromatin which promotes R-loop formation and suggests that DNA:RNA hybrid formation and chromatin retention of heterochromatic RNA might be a result of low efficiency in their processing and export. As the H3-RIP signals were stronger than the DRIP result, it is also possible that RNA accumulation on chromatin interferes with assembly of functional heterochromatin in ways other than R-loops. For example the lncRNA *roX* is suggested to interact with DNA by a protein complex (Soruco et al., 2013) and recruits then chromatin modifying enzymes to increase transcript levels of the X-chromosome (Lucchesi et al., 2005; Meller and Rattner, 2002; Smith et al., 2000). All these data show that chromatin retention of RNA will interfere with chromatin organization and heterochromatin assembly.

Regarding the subtelomeres, our results suggest that the RNA accumulation at *tlh* inhibits spreading of Clr4, as H3K9me2 is still established at the TAS region but is then lost from the region on where RNA accumulates on chromatin. This might also suggest some interaction of RNA with the CLRC complex which comprises its function as methyltransferase. It seems like, although RNA retention on chromatin is necessary also for RNAi dependent heterochromatin formation, uncontrolled accumulation of RNA on chromatin disrupts heterochromatin.

4.4.2 Histone 3 serine 10 phosphorylation

R-loop formation was shown to induce H3S10 phosphorylation (Castellano-Pozo et al., 2013). Castellano-Pozo et al. linked H3S10Ph with chromatin condensation. Other studies showed that this chromatin mark reduces HP1 binding to H3K9 methylated nucleosomes and interferes with heterochromatin formation and silencing (Fischle et al., 2005; Hirota et al., 2005; Kloc et al., 2008). This might have been an explanation for loss of heterochromatin in *caf1Δdcr1Δ* cells. Our assay shows loss of H3S10Ph in the mutant where DNA:RNA hybrids are increased and H3K9me2 is lost. This is rather consistent with the result of an H3S10A mutant, which was shown to have reduced H3K9me2 levels (Kloc et al., 2008), or that H3S10Ph is connected with condensed metaphase chromosomes (Castellano-Pozo et al., 2013). These results suggest a co-dependence of the histone marks H3S10Ph and H3K9me2. More experiments would be necessary to figure out if loss of H3S10Ph is a secondary or primary effect.

4.4.3 lncRNAs on chromatin

Our data show that lncRNAs tend to accumulate on chromatin compared to mRNA. Many lncRNAs were detected to cause chromatin changes and most of them are rather connected with specific loci or chromosomes (see 1.2 Noncoding RNAs). We show, that next to heterochromatic transcripts also euchromatic lncRNAs stay on the chromatin. A current assumption is that chromatin retention of RNA, for example due to misprocessing, is enough to establish RNAi dependent heterochromatin (Kowalik et al., 2015). According to the H3RIP data, many euchromatic RNAs are retained at the chromatin and they do not recruit RNAi (Marasovic et al., 2013). Our data show that RNA localization on chromatin is not sufficient to initiate RNAi mediated heterochromatin formation. It was also shown that in mammals specific repetitive transcripts (C_0T-1 RNA) are chromatin associated exclusively in euchromatin in *cis* (Hall et al., 2014). Loss of those RNAs is connected with condensation, which would argue against a general silencing mechanism. This indicates that mutations in the PAF complex, that promote establishment of ectopic RNAi-dependent heterochromatin, interfere rather with the chromatin related functions of the Paf1 complex than with transcription elongation (Sadeghi et al., 2015; Verrier et al., 2015).

Many lncRNAs have been implicated in chromatin related processes from yeast to human cells and are overexpressed in numerous human diseases and cancer (Sánchez and Huarte, 2013). Several human lncRNAs were also suggested to be bound at chromatin (Böhmdorfer and Wierzbicki, 2015; Yamashita et al., 2016). This indicates that the degradation of chromatin

associated transcripts by the Ccr4-Not complex might be a conserved mechanism to maintain chromatin structure.

4.5 Conclusion

This thesis and several other studies showed that RNA degradation plays a strong role in heterochromatin formation: either by generating new small RNAs (Verdel et al., 2004), by trimming RNA to the right size that they can be used for RNAi (Marasovic et al., 2013), or by elimination of heterochromatic transcripts (See 4.1.1). For facultative heterochromatin loci several RNA degradation machineries were detected to be involved, however this study demonstrates, that at constitutive heterochromatin the Ccr4-Not complex followed by 5'-3' Exo2 digest is the main pathway important for heterochromatin maintenance. We show that the nuclease activity of the Ccr4-Not complex is the major contributor for heterochromatic silencing. The Ccr4-Not complex localizes to heterochromatic loci and associates with heterochromatic transcripts on chromatin. An "easy" explanation would have been that the Ccr4-Not complex recruits factors important for heterochromatin establishment while degrading transcripts. The *caf1*ccr4*dcr1Δ* activity mutants loose heterochromatic silencing, but they should still be able to recruit factors. This suggests rather an effect of the RNA itself on heterochromatin formation. Heterochromatic RNA compared to mRNA shows increased retention on chromatin which leads to strong accumulation in degradation defective mutants. At subtelomeres, spreading of heterochromatin over the region of RNA retention is impaired. If RNA recruits chromatin modifying proteins, if RNA accumulation induces secondary effects like DNA damage which interferes with heterochromatin, or if RNA affects heterochromatin formation as it interacts with heterochromatic proteins (like Clr4) reducing their function, still needs to be further analyzed. The overexpression study in wild type cells demonstrates, that RNA expression has a strong impact on heterochromatin maintenance: Important is which RNA is expressed and the amount of RNA retained. We show that heterochromatic RNA disrupts heterochromatic silencing in a dose dependent way. The more RNA accumulates on chromatin the more heterochromatic silencing is impaired.

This leads to the conclusion that heterochromatic RNA degradation by the Ccr4-Not complex is necessary to prevent accumulation of RNA on chromatin which disrupts heterochromatic silencing.

List of Abbreviations

Caf1	Ccr4p associated factor 1
Caf1*	Caf1D53AD243AD174A
Ccr4*	Ccr4H665A
Ccr4-Not	Carbon catabolite repressor protein 4 negative on TATA
ChIP	Chromatin immunoprecipitation
chr	chromatin fraction
CLRC	Clr4-Rik1-Cul4
D. melanogaster	*Drosophila melanogaster*
DSR	determinant of selective removal
etlh	extended *tlh* transcript
FLC	Flowering locus
H3K…	histone 3 lysine …
H3K27me3	Trimethylated histone 3 lysine 27
H3S10P	Histone 3 serine 10 phosphorylation
HOTAIR	HOX transcript antisense RNA
HP1	heterochromatin protein 1
imr	innermost repeats
kb	Kilo base pairs
lncRNAs	long non-coding RNAs
***mat* locus**	mating type locus
miRNAs	micro RNAs
mRNA	messenger RNA
NB	Northern Blot
ncRNAs	non-coding RNAs
nt	nucleotides
otr	outer repeat region
piRNAs	PIWI interacting small RNAs
PRC2	Polycomb repressive complex 2
priRNAs	primal small RNAs
PTM	posttranscriptional modification
qRT-PCR	quantitative real time PCR

RDRC	RNA-directed RNA polymerase complex
RIP	RNA immunoprecipitation
RITS	RNA induced transcriptional silencing
RNA PolII	RNA polymerase II
RNAi	RNA interference
rRNAs	ribosomal RNAs
RT	Reverse transcription
RT-qPCR	reverse transcription quantitative real time polymerase chain reaction
S. cerevisiae	*Saccharomyces cerevisiae*
S. pombe	*Schizosaccharomyces pombe*
SHREC	Snf2-histone deacetylase repressor complex
siRNAs	small inhibitory RNAs
snoRNAs	small nucleolar RNAs
sol	Soluble fraction
sRNAs	small RNAs
TAS	Telomere associated sequence
TE	transposable elements
tRNAs	transfer RNAs

5. List of figures

6. List of tables

7. References

Aguilera, A., and García-Muse, T. (2012). R loops: from transcription byproducts to threats to genome stability. Mol. Cell *46*, 115–124.

Albert, T.K., Hanzawa, H., Legtenberg, Y.I.A., de Ruwe, M.J., van den Heuvel, F.A.J., Collart, M.A., Boelens, R., and Timmers, H.T.M. (2002). Identification of a ubiquitin-protein ligase subunit within the CCR4-NOT transcription repressor complex. EMBO J. *21*, 355–364.

Allshire, R.C. (1995). Elements of chromosome structure and function in fission yeast. Semin. Cell Biol. *6*, 55–64.

Allshire, R.C., Javerzat, J.-P., Redhead, N.J., and Cranston, G. (1994). Position effect variegation at fission yeast centromeres. Cell *76*, 157–169.

Allshire, R.C., Nimmo, E.R., Ekwall, K., Javerzat, J.P., and Cranston, G. (1995). Mutations derepressing silent centromeric domains in fission yeast disrupt chromosome segregation. Genes Dev. *9*, 218–233.

Al-Sady, B., Madhani, H.D., and Narlikar, G.J. (2013). Division of labor between the chromodomains of HP1 and Suv39 methylase enables coordination of heterochromatin spread. Mol. Cell *51*, 80–91.

Anderson, J.S., and Parker, R.P. (1998). The 3' to 5' degradation of yeast mRNAs is a general mechanism for mRNA turnover that requires the SKI2 DEVH box protein and 3' to 5' exonucleases of the exosome complex. EMBO J. *17*, 1497–1506.

Aravin, A.A., Sachidanandam, R., Bourc'his, D., Schaefer, C., Pezic, D., Toth, K.F., Bestor, T., and Hannon, G.J. (2008). A piRNA pathway primed by individual transposons is linked to de novo DNA methylation in mice. Mol. Cell *31*, 785–799.

Ard, R., and Allshire, R.C. (2016). Transcription-coupled changes to chromatin underpin gene silencing by transcriptional interference. Nucleic Acids Res. *44*, 10619–10630.

Ard, R., Tong, P., and Allshire, R.C. (2014). Long non-coding RNA-mediated transcriptional interference of a permease gene confers drug tolerance in fission yeast. Nat. Commun. *5*, 5576.

Audergon, P.N.C.B., Catania, S., Kagansky, A., Tong, P., Shukla, M., Pidoux, A.L., and Allshire, R.C. (2015). Epigenetics. Restricted epigenetic inheritance of H3K9 methylation. Science *348*, 132–135.

Avery, O.T., Macleod, C.M., and McCarty, M. (1944). STUDIES ON THE CHEMICAL NATURE OF THE SUBSTANCE INDUCING TRANSFORMATION OF PNEUMOCOCCAL TYPES : INDUCTION OF TRANSFORMATION BY A DESOXYRIBONUCLEIC ACID FRACTION ISOLATED FROM PNEUMOCOCCUS TYPE III. J. Exp. Med. *79*, 137–158.

Bähler, J., Wu, J.-Q., Longtine, M.S., Shah, N.G., Mckenzie III, A., Steever, A.B., Wach, A., Philippsen, P., and Pringle, J.R. (1998). Heterologous modules for efficient and versatile PCR-based gene targeting inSchizosaccharomyces pombe. Yeast *14*, 943–951.

Bai, Y., Salvadore, C., Chiang, Y.C., Collart, M.A., Liu, H.Y., and Denis, C.L. (1999). The CCR4 and CAF1 proteins of the CCR4-NOT complex are physically and functionally separated from NOT2, NOT4, and NOT5. Mol. Cell. Biol. *19*, 6642–6651.

Bannister, A.J., Zegerman, P., Partridge, J.F., Miska, E.A., Thomas, J.O., Allshire, R.C., and Kouzarides, T. (2001). Selective recognition of methylated lysine 9 on histone H3 by the HP1 chromo domain. Nature *410*, 120–124.

Barber, B.A., and Rastegar, M. (2010). Epigenetic control of Hox genes during neurogenesis, development, and disease. Ann. Anat. Anat. Anz. Off. Organ Anat. Ges. *192*, 261–274.

Basquin, J., Roudko, V.V., Rode, M., Basquin, C., Séraphin, B., and Conti, E. (2012). Architecture of the nuclease module of the yeast Ccr4-not complex: the Not1-Caf1-Ccr4 interaction. Mol. Cell *48*, 207–218.

Bayne, E.H., White, S.A., Kagansky, A., Bijos, D.A., Sanchez-Pulido, L., Hoe, K.-L., Kim, D.-U., Park, H.-O., Ponting, C.P., Rappsilber, J., et al. (2010). Stc1: A Critical Link between RNAi and Chromatin Modification Required for Heterochromatin Integrity. Cell *140*, 666–677.

Beach, D.H., and Klar, A.J. (1984). Rearrangements of the transposable mating-type cassettes of fission yeast. EMBO J. *3*, 603–610.

Beelman, C.A., Stevens, A., Caponigro, G., LaGrandeur, T.E., Hatfield, L., Fortner, D.M., and Parker, R. (1996). An essential component of the decapping enzyme required for normal rates of mRNA turnover. Nature *382*, 642–646.

Bhaskar, V., Basquin, J., and Conti, E. (2015). Architecture of the ubiquitylation module of the yeast Ccr4-Not complex. Struct. Lond. Engl. 1993 *23*, 921–928.

Böhmdorfer, G., and Wierzbicki, A.T. (2015). Control of Chromatin Structure by Long Noncoding RNA. Trends Cell Biol. *25*, 623–632.

Bönisch, C., Nieratschker, S.M., Orfanos, N.K., and Hake, S.B. (2008). Chromatin proteomics and epigenetic regulatory circuits. Expert Rev. Proteomics *5*, 105–119.

Brannan, K., Kim, H., Erickson, B., Glover-Cutter, K., Kim, S., Fong, N., Kiemele, L., Hansen, K., Davis, R., Lykke-Andersen, J., et al. (2012). mRNA decapping factors and the exonuclease Xrn2 function in widespread premature termination of RNA polymerase II transcription. Mol. Cell *46*, 311–324.

Brockdorff, N. (2013). Noncoding RNA and Polycomb recruitment. RNA N. Y. N *19*, 429–442.

Brönner, C., Salvi, L., Zocco, M., Ugolini, I., and Halic, M. (2017). Accumulation of RNA on chromatin disrupts heterochromatic silencing. Genome Res. *27*, 1174–1183.

Brown, C.E., and Sachs, A.B. (1998). Poly(A) tail length control in Saccharomyces cerevisiae occurs by message-specific deadenylation. Mol. Cell. Biol. *18*, 6548–6559.

Brown, C.J., Ballabio, A., Rupert, J.L., Lafreniere, R.G., Grompe, M., Tonlorenzi, R., and Willard, H.F. (1991). A gene from the region of the human X inactivation centre is expressed exclusively from the inactive X chromosome. Nature *349*, 38–44.

Bühler, M., and Moazed, D. (2007). Transcription and RNAi in heterochromatic gene silencing. Nat. Struct. Mol. Biol. *14*, 1041–1048.

Bühler, M., Verdel, A., and Moazed, D. (2006). Tethering RITS to a nascent transcript initiates RNAi- and heterochromatin-dependent gene silencing. Cell *125*, 873–886.

Bühler, M., Haas, W., Gygi, S.P., and Moazed, D. (2007). RNAi-dependent and -independent RNA turnover mechanisms contribute to heterochromatic gene silencing. Cell *129*, 707–721.

Bühler, M., Spies, N., Bartel, D.P., and Moazed, D. (2008). TRAMP-mediated RNA surveillance prevents spurious entry of RNAs into the Schizosaccharomyces pombe siRNA pathway. Nat. Struct. Mol. Biol. *15*, 1015–1023.

Cam, H.P., Sugiyama, T., Chen, E.S., Chen, X., FitzGerald, P.C., and Grewal, S.I.S. (2005). Comprehensive analysis of heterochromatin- and RNAi-mediated epigenetic control of the fission yeast genome. Nat. Genet. *37*, 809–819.

Cano, F., Rapiteanu, R., Sebastiaan Winkler, G., and Lehner, P.J. (2015). A non-proteolytic role for ubiquitin in deadenylation of MHC-I mRNA by the RNA-binding E3-ligase MEX-3C. Nat. Commun. *6*, 8670.

Castel, S.E., Ren, J., Bhattacharjee, S., Chang, A.-Y., Sánchez, M., Valbuena, A., Antequera, F., and Martienssen, R.A. (2014). Dicer promotes transcription termination at sites of replication stress to maintain genome stability. Cell *159*, 572–583.

Castellano-Pozo, M., Santos-Pereira, J.M., Rondón, A.G., Barroso, S., Andújar, E., Pérez-Alegre, M., García-Muse, T., and Aguilera, A. (2013). R loops are linked to histone H3 S10 phosphorylation and chromatin condensation. Mol. Cell *52*, 583–590.

Chalamcharla, V.R., Folco, H.D., Dhakshnamoorthy, J., and Grewal, S.I.S. (2015). Conserved factor Dhp1/Rat1/Xrn2 triggers premature transcription termination and nucleates heterochromatin to promote gene silencing. Proc. Natl. Acad. Sci. U. S. A. *112*, 15548–15555.

Chen, J., Chiang, Y.-C., and Denis, C.L. (2002). CCR4, a 3'-5' poly(A) RNA and ssDNA exonuclease, is the catalytic component of the cytoplasmic deadenylase. EMBO J. *21*, 1414–1426.

Chen, Y., Boland, A., Kuzuoğlu-Öztürk, D., Bawankar, P., Loh, B., Chang, C.-T., Weichenrieder, O., and Izaurralde, E. (2014). A DDX6-CNOT1 complex and W-binding pockets in CNOT9 reveal direct links between miRNA target recognition and silencing. Mol. Cell *54*, 737–750.

Cheutin, T., McNairn, A.J., Jenuwein, T., Gilbert, D.M., Singh, P.B., and Misteli, T. (2003). Maintenance of stable heterochromatin domains by dynamic HP1 binding. Science *299*, 721–725.

Claverie, J.-M. (2005). Fewer genes, more noncoding RNA. Science *309*, 1529–1530.

Collart, M.A. (2016). The Ccr4-Not complex is a key regulator of eukaryotic gene expression. Wiley Interdiscip. Rev. RNA *7*, 438–454.

Collart, M.A., and Panasenko, O.O. (2012). The Ccr4--not complex. Gene *492*, 42–53.

Colmenares, S.U., Buker, S.M., Buhler, M., Dlakić, M., and Moazed, D. (2007). Coupling of Double-Stranded RNA Synthesis and siRNA Generation in Fission Yeast RNAi. Mol. Cell *27*, 449–461.

Conway, E., Healy, E., and Bracken, A.P. (2015). PRC2 mediated H3K27 methylations in cellular identity and cancer. Curr. Opin. Cell Biol. *37*, 42–48.

Cotobal, C., Rodríguez-López, M., Duncan, C., Hasan, A., Yamashita, A., Yamamoto, M., Bähler, J., and Mata, J. (2015). Role of Ccr4-Not complex in heterochromatin formation at meiotic genes and subtelomeres in fission yeast. Epigenetics Chromatin *8*, 28.

Dahlberg, A.E. (1989). The functional role of ribosomal RNA in protein synthesis. Cell *57*, 525–529.

Daugeron, M.C., Mauxion, F., and Séraphin, B. (2001). The yeast POP2 gene encodes a nuclease involved in mRNA deadenylation. Nucleic Acids Res. *29*, 2448–2455.

Davidovich, C., and Cech, T.R. (2015). The recruitment of chromatin modifiers by long noncoding RNAs: lessons from PRC2. RNA N. Y. N *21*, 2007–2022.

Deniz, E., and Erman, B. (2016). Long noncoding RNA (lincRNA), a new paradigm in gene expression control. Funct. Integr. Genomics.

Derrien, T., Johnson, R., Bussotti, G., Tanzer, A., Djebali, S., Tilgner, H., Guernec, G., Martin, D., Merkel, A., Knowles, D.G., et al. (2012). The GENCODE v7 catalog of human long noncoding RNAs: analysis of their gene structure, evolution, and expression. Genome Res. *22*, 1775–1789.

Dimitrova, L.N., Kuroha, K., Tatematsu, T., and Inada, T. (2009). Nascent peptide-dependent translation arrest leads to Not4p-mediated protein degradation by the proteasome. J. Biol. Chem. *284*, 10343–10352.

Djebali, S., Davis, C.A., Merkel, A., Dobin, A., Lassmann, T., Mortazavi, A., Tanzer, A., Lagarde, J., Lin, W., Schlesinger, F., et al. (2012). Landscape of transcription in human cells. Nature *489*, 101–108.

Dunn, K., and Griffith, J.D. (1980). The presence of RNA in a double helix inhibits its interaction with histone protein. Nucleic Acids Res. *8*, 555–566.

Dupressoir, A., Morel, A.P., Barbot, W., Loireau, M.P., Corbo, L., and Heidmann, T. (2001). Identification of four families of yCCR4- and Mg2+-dependent endonuclease-related proteins in higher eukaryotes, and characterization of orthologs of yCCR4 with a conserved leucine-rich repeat essential for hCAF1/hPOP2 binding. BMC Genomics *2*, 9.

Dutta, A., Babbarwal, V., Fu, J., Brunke-Reese, D., Libert, D.M., Willis, J., and Reese, J.C. (2015). Ccr4-Not and TFIIS Function Cooperatively To Rescue Arrested RNA Polymerase II. Mol. Cell. Biol. *35*, 1915–1925.

Egan, E.D., Braun, C.R., Gygi, S.P., and Moazed, D. (2014). Post-transcriptional regulation of meiotic genes by a nuclear RNA silencing complex. RNA N. Y. N *20*, 867–881.

Ekwall, K., Olsson, T., Turner, B.M., Cranston, G., and Allshire, R.C. (1997). Transient Inhibition of Histone Deacetylation Alters the Structural and Functional Imprint at Fission Yeast Centromeres. Cell *91*, 1021–1032.

Fabian, M.R., Frank, F., Rouya, C., Siddiqui, N., Lai, W.S., Karetnikov, A., Blackshear, P.J., Nagar, B., and Sonenberg, N. (2013). Structural basis for the recruitment of the human CCR4-NOT deadenylase complex by tristetraprolin. Nat. Struct. Mol. Biol. *20*, 735–739.

Festenstein, R., Pagakis, S.N., Hiragami, K., Lyon, D., Verreault, A., Sekkali, B., and Kioussis, D. (2003). Modulation of heterochromatin protein 1 dynamics in primary Mammalian cells. Science *299*, 719–721.

Fischer, S.E.J., Pan, Q., Breen, P.C., Qi, Y., Shi, Z., Zhang, C., and Ruvkun, G. (2013). Multiple small RNA pathways regulate the silencing of repeated and foreign genes in C. elegans. Genes Dev. *27*, 2678–2695.

Fischle, W., Tseng, B.S., Dormann, H.L., Ueberheide, B.M., Garcia, B.A., Shabanowitz, J., Hunt, D.F., Funabiki, H., and Allis, C.D. (2005). Regulation of HP1-chromatin binding by histone H3 methylation and phosphorylation. Nature *438*, 1116–1122.

Fishel, B., Amstutz, H., Baum, M., Carbon, J., and Clarke, L. (1988). Structural organization and functional analysis of centromeric DNA in the fission yeast Schizosaccharomyces pombe. Mol. Cell. Biol. *8*, 754–763.

Garcia, J.F., Dumesic, P.A., Hartley, P.D., El-Samad, H., and Madhani, H.D. (2010). Combinatorial, site-specific requirement for heterochromatic silencing factors in the elimination of nucleosome-free regions. Genes Dev. *24*, 1758–1771.

Garcia-Ramirez, M., Dong, F., and Ausio, J. (1992). Role of the histone "tails" in the folding of oligonucleosomes depleted of histone H1. J. Biol. Chem. *267*, 19587–19595.

Garneau, N.L., Wilusz, J., and Wilusz, C.J. (2007). The highways and byways of mRNA decay. Nat. Rev. Mol. Cell Biol. *8*, 113–126.

Gerace, E.L., Halic, M., and Moazed, D. (2010). The Methyltransferase Activity of Clr4Suv39h Triggers RNAi Independently of Histone H3K9 Methylation. Mol. Cell *39*, 360–372.

Goecks, J., Nekrutenko, A., Taylor, J., and Galaxy Team (2010). Galaxy: a comprehensive approach for supporting accessible, reproducible, and transparent computational research in the life sciences. Genome Biol. *11*, R86.

Goto, D.B., and Nakayama, J. (2012). RNA and epigenetic silencing: Insight from fission yeast: Epigenetic silencing in fission yeast. Dev. Growth Differ. *54*, 129–141.

Grewal, S.I., and Klar, A.J. (1997). A recombinationally repressed region between mat2 and mat3 loci shares homology to centromeric repeats and regulates directionality of mating-type switching in fission yeast. Genetics *146*, 1221–1238.

Grewal, S.I.S., and Jia, S. (2007). Heterochromatin revisited. Nat. Rev. Genet. *8*, 35–46.

Grewal, S.I.S., and Moazed, D. (2003). Heterochromatin and epigenetic control of gene expression. Science *301*, 798–802.

Halic, M., and Moazed, D. (2010). Dicer-independent primal RNAs trigger RNAi and heterochromatin formation. Cell *140*, 504–516.

Hall, I.M., Shankaranarayana, G.D., Noma, K.-I., Ayoub, N., Cohen, A., and Grewal, S.I.S. (2002). Establishment and maintenance of a heterochromatin domain. Science *297*, 2232–2237.

Hall, L.L., Carone, D.M., Gomez, A.V., Kolpa, H.J., Byron, M., Mehta, N., Fackelmayer, F.O., and Lawrence, J.B. (2014). Stable C0T-1 repeat RNA is abundant and is associated with euchromatic interphase chromosomes. Cell *156*, 907–919.

Hannon, G.J. (2002). RNA interference. Nature *418*, 244–251.

Hansen, K.R., Ibarra, P.T., and Thon, G. (2006). Evolutionary-conserved telomere-linked helicase genes of fission yeast are repressed by silencing factors, RNAi components and the telomere-binding protein Taz1. Nucleic Acids Res. *34*, 78–88.

Hanzawa, H., de Ruwe, M.J., Albert, T.K., van Der Vliet, P.C., Timmers, H.T., and Boelens, R. (2001). The structure of the C4C4 ring finger of human NOT4 reveals features distinct from those of C3HC4 RING fingers. J. Biol. Chem. *276*, 10185–10190.

Harigaya, Y., Tanaka, H., Yamanaka, S., Tanaka, K., Watanabe, Y., Tsutsumi, C., Chikashige, Y., Hiraoka, Y., Yamashita, A., and Yamamoto, M. (2006). Selective elimination of messenger RNA prevents an incidence of untimely meiosis. Nature *442*, 45–50.

Heard, E. (2006). Dosage compensation in mammals: fine-tuning the expression of the X chromosome. Genes Dev. *20*, 1848–1867.

Henikoff, S. (1990). Position-effect variegation after 60 years. Trends Genet. *6*, 422–426.

Henikoff, S. (2000). Heterochromatin function in complex genomes. Biochim. Biophys. Acta BBA - Rev. Cancer *1470*, O1–O8.

Heo, J.B., and Sung, S. (2011). Vernalization-mediated epigenetic silencing by a long intronic noncoding RNA. Science *331*, 76–79.

Hirakata, S., and Siomi, M.C. (2016). piRNA biogenesis in the germline: From transcription of piRNA genomic sources to piRNA maturation. Biochim. Biophys. Acta *1859*, 82–92.

Hiriart, E., Vavasseur, A., Touat-Todeschini, L., Yamashita, A., Gilquin, B., Lambert, E., Perot, J., Shichino, Y., Nazaret, N., Boyault, C., et al. (2012). Mmi1 RNA surveillance machinery directs RNAi complex RITS to specific meiotic genes in fission yeast. EMBO J. *31*, 2296–2308.

Hirota, T., Lipp, J.J., Toh, B.-H., and Peters, J.-M. (2005). Histone H3 serine 10 phosphorylation by Aurora B causes HP1 dissociation from heterochromatin. Nature *438*, 1176–1180.

Holoch, D., and Moazed, D. (2015). Small-RNA loading licenses Argonaute for assembly into a transcriptional silencing complex. Nat. Struct. Mol. Biol. *22*, 328–335.

Horiuchi, M., Takeuchi, K., Noda, N., Muroya, N., Suzuki, T., Nakamura, T., Kawamura-Tsuzuku, J., Takahasi, K., Yamamoto, T., and Inagaki, F. (2009). Structural basis for the antiproliferative activity of the Tob-hCaf1 complex. J. Biol. Chem. *284*, 13244–13255.

Huntzinger, E., and Izaurralde, E. (2011). Gene silencing by microRNAs: contributions of translational repression and mRNA decay. Nat. Rev. Genet. *12*, 99–110.

Ietswaart, R., Wu, Z., and Dean, C. (2012). Flowering time control: another window to the connection between antisense RNA and chromatin. Trends Genet. TIG *28*, 445–453.

James, N., Landrieux, E., and Collart, M.A. (2007). A SAGA-independent function of SPT3 mediates transcriptional deregulation in a mutant of the Ccr4-not complex in Saccharomyces cerevisiae. Genetics *177*, 123–135.

Jia, S., Noma, K., and Grewal, S.I.S. (2004a). RNAi-independent heterochromatin nucleation by the stress-activated ATF/CREB family proteins. Science *304*, 1971–1976.

Jia, S., Yamada, T., and Grewal, S.I.S. (2004b). Heterochromatin Regulates Cell Type-Specific Long-Range Chromatin Interactions Essential for Directed Recombination. Cell *119*, 469–480.

Jimeno-González, S., Haaning, L.L., Malagon, F., and Jensen, T.H. (2010). The yeast 5'-3' exonuclease Rat1p functions during transcription elongation by RNA polymerase II. Mol. Cell *37*, 580–587.

Jonstrup, A.T., Andersen, K.R., Van, L.B., and Brodersen, D.E. (2007). The 1.4-A crystal structure of the S. pombe Pop2p deadenylase subunit unveils the configuration of an active enzyme. Nucleic Acids Res. *35*, 3153–3164.

Kanoh, J., Sadaie, M., Urano, T., and Ishikawa, F. (2005). Telomere binding protein Taz1 establishes Swi6 heterochromatin independently of RNAi at telomeres. Curr. Biol. CB *15*, 1808–1819.

Kapranov, P., Cheng, J., Dike, S., Nix, D.A., Duttagupta, R., Willingham, A.T., Stadler, P.F., Hertel, J., Hackermüller, J., Hofacker, I.L., et al. (2007). RNA maps reveal new RNA classes and a possible function for pervasive transcription. Science *316*, 1484–1488.

Kelly, M., Burke, J., Smith, M., Klar, A., and Beach, D. (1988). Four mating-type genes control sexual differentiation in the fission yeast. EMBO J. *7*, 1537–1547.

Keskin, H., Shen, Y., Huang, F., Patel, M., Yang, T., Ashley, K., Mazin, A.V., and Storici, F. (2014). Transcript-RNA-templated DNA recombination and repair. Nature *515*, 436–439.

Kim, H.S., Choi, E.S., Shin, J.A., Jang, Y.K., and Park, S.D. (2004a). Regulation of Swi6/HP1-dependent heterochromatin assembly by cooperation of components of the mitogen-activated protein kinase pathway and a histone deacetylase Clr6. J. Biol. Chem. *279*, 42850–42859.

Kim, M., Krogan, N.J., Vasiljeva, L., Rando, O.J., Nedea, E., Greenblatt, J.F., and Buratowski, S. (2004b). The yeast Rat1 exonuclease promotes transcription termination by RNA polymerase II. Nature *432*, 517–522.

Klar, A.J.S. (2007). Lessons learned from studies of fission yeast mating-type switching and silencing. Annu. Rev. Genet. *41*, 213–236.

Klar, A.J.S., Ishikawa, K., and Moore, S. (2014). A Unique DNA Recombination Mechanism of the Mating/Cell-type Switching of Fission Yeasts: a Review. Microbiol. Spectr. *2*.

Kloc, A., Zaratiegui, M., Nora, E., and Martienssen, R. (2008). RNA interference guides histone modification during the S phase of chromosomal replication. Curr. Biol. CB *18*, 490–495.

Kornberg, R.D. (1974). Chromatin structure: a repeating unit of histones and DNA. Science *184*, 868–871.

Kowalik, K.M., Shimada, Y., Flury, V., Stadler, M.B., Batki, J., and Bühler, M. (2015). The Paf1 complex represses small-RNA-mediated epigenetic gene silencing. Nature *520*, 248–252.

Kruk, J.A., Dutta, A., Fu, J., Gilmour, D.S., and Reese, J.C. (2011). The multifunctional Ccr4-Not complex directly promotes transcription elongation. Genes Dev. *25*, 581–593.

Kuramochi-Miyagawa, S., Watanabe, T., Gotoh, K., Totoki, Y., Toyoda, A., Ikawa, M., Asada, N., Kojima, K., Yamaguchi, Y., Ijiri, T.W., et al. (2008). DNA methylation of retrotransposon genes is regulated by Piwi family members MILI and MIWI2 in murine fetal testes. Genes Dev. *22*, 908–917.

LaCava, J., Houseley, J., Saveanu, C., Petfalski, E., Thompson, E., Jacquier, A., and Tollervey, D. (2005). RNA degradation by the exosome is promoted by a nuclear polyadenylation complex. Cell *121*, 713–724.

Lachner, M., O'Carroll, D., Rea, S., Mechtler, K., and Jenuwein, T. (2001). Methylation of histone H3 lysine 9 creates a binding site for HP1 proteins. Nature *410*, 116–120.

de Lange, T. (2005). Shelterin: the protein complex that shapes and safeguards human telomeres. Genes Dev. *19*, 2100–2110.

Laribee, R.N., Shibata, Y., Mersman, D.P., Collins, S.R., Kemmeren, P., Roguev, A., Weissman, J.S., Briggs, S.D., Krogan, N.J., and Strahl, B.D. (2007). CCR4/NOT complex associates with the proteasome and regulates histone methylation. Proc. Natl. Acad. Sci. U. S. A. *104*, 5836–5841.

Lau, N.-C., Kolkman, A., van Schaik, F.M.A., Mulder, K.W., Pijnappel, W.W.M.P., Heck, A.J.R., and Timmers, H.T.M. (2009). Human Ccr4-Not complexes contain variable deadenylase subunits. Biochem. J. *422*, 443–453.

Lenssen, E., James, N., Pedruzzi, I., Dubouloz, F., Cameroni, E., Bisig, R., Maillet, L., Werner, M., Roosen, J., Petrovic, K., et al. (2005). The Ccr4-Not complex independently controls both Msn2-dependent transcriptional activation--via a newly identified Glc7/Bud14 type I protein phosphatase module--and TFIID promoter distribution. Mol. Cell. Biol. *25*, 488–498.

Liu, H.Y., Badarinarayana, V., Audino, D.C., Rappsilber, J., Mann, M., and Denis, C.L. (1998). The NOT proteins are part of the CCR4 transcriptional complex and affect gene expression both positively and negatively. EMBO J. *17*, 1096–1106.

Liu, H.Y., Chiang, Y.C., Pan, J., Chen, J., Salvadore, C., Audino, D.C., Badarinarayana, V., Palaniswamy, V., Anderson, B., and Denis, C.L. (2001). Characterization of CAF4 and CAF16 reveals a functional connection between the CCR4-NOT complex and a subset of SRB proteins of the RNA polymerase II holoenzyme. J. Biol. Chem. *276*, 7541–7548.

Lorentz, A., Heim, L., and Schmidt, H. (1992). The switching gene swi6 affects recombination and gene expression in the mating-type region of Schizosaccharomyces pombe. Mol. Gen. Genet. MGG *233*, 436–442.

Lucchesi, J.C., Kelly, W.G., and Panning, B. (2005). Chromatin remodeling in dosage compensation. Annu. Rev. Genet. *39*, 615–651.

Luger, K., Mäder, A.W., Richmond, R.K., Sargent, D.F., and Richmond, T.J. (1997). Crystal structure of the nucleosome core particle at 2.8 A resolution. Nature *389*, 251–260.

Maden, B.E., and Hughes, J.M. (1997). Eukaryotic ribosomal RNA: the recent excitement in the nucleotide modification problem. Chromosoma *105*, 391–400.

Maison, C., and Almouzni, G. (2004). HP1 and the dynamics of heterochromatin maintenance. Nat. Rev. Mol. Cell Biol. *5*, 296–305.

Mandell, J.G., Goodrich, K.J., Bähler, J., and Cech, T.R. (2005a). Expression of a RecQ helicase homolog affects progression through crisis in fission yeast lacking telomerase. J. Biol. Chem. *280*, 5249–5257.

Mandell, J.G., Bähler, J., Volpe, T.A., Martienssen, R.A., and Cech, T.R. (2005b). Global expression changes resulting from loss of telomeric DNA in fission yeast. Genome Biol. *6*, R1.

Mangus, D.A., Evans, M.C., and Jacobson, A. (2003). Poly(A)-binding proteins: multifunctional scaffolds for the post-transcriptional control of gene expression. Genome Biol. *4*, 223.

Marasovic, M., Zocco, M., and Halic, M. (2013). Argonaute and Triman generate dicer-independent priRNAs and mature siRNAs to initiate heterochromatin formation. Mol. Cell *52*, 173–183.

Margueron, R., and Reinberg, D. (2010). Chromatin structure and the inheritance of epigenetic information. Nat. Rev. Genet. *11*, 285–296.

Martienssen, R.A., Zaratiegui, M., and Goto, D.B. (2005). RNA interference and heterochromatin in the fission yeast Schizosaccharomyces pombe. Trends Genet. *21*, 450–456.

Maryati, M., Airhihen, B., and Winkler, G.S. (2015). The enzyme activities of Caf1 and Ccr4 are both required for deadenylation by the human Ccr4-Not nuclease module. Biochem. J. *469*, 169–176.

Mathys, H., Basquin, J., Ozgur, S., Czarnocki-Cieciura, M., Bonneau, F., Aartse, A., Dziembowski, A., Nowotny, M., Conti, E., and Filipowicz, W. (2014). Structural and biochemical insights to the role of the CCR4-NOT complex and DDX6 ATPase in microRNA repression. Mol. Cell *54*, 751–765.

Matsuda, R., Ikeuchi, K., Nomura, S., and Inada, T. (2014). Protein quality control systems associated with no-go and nonstop mRNA surveillance in yeast. Genes Cells Devoted Mol. Cell. Mech. *19*, 1–12.

Matzke, M., Aufsatz, W., Kanno, T., Daxinger, L., Papp, I., Mette, M.F., and Matzke, A.J.M. (2004). Genetic analysis of RNA-mediated transcriptional gene silencing. Biochim. Biophys. Acta *1677*, 129–141.

Mauxion, F., Faux, C., and Séraphin, B. (2008). The BTG2 protein is a general activator of mRNA deadenylation. EMBO J. *27*, 1039–1048.

Maxfield Boumil, R. (2001). Forty years of decoding the silence in X-chromosome inactivation. Hum. Mol. Genet. *10*, 2225–2232.

Meller, V.H., and Rattner, B.P. (2002). The roX genes encode redundant male-specific lethal transcripts required for targeting of the MSL complex. EMBO J. *21*, 1084–1091.

Mersman, D.P., Du, H.-N., Fingerman, I.M., South, P.F., and Briggs, S.D. (2009). Polyubiquitination of the demethylase Jhd2 controls histone methylation and gene expression. Genes Dev. *23*, 951–962.

Miller, J.E., and Reese, J.C. (2012). Ccr4-Not complex: the control freak of eukaryotic cells. Crit. Rev. Biochem. Mol. Biol. *47*, 315–333.

Mitchison, J.M. (1990). My favourite cell: The fission yeast,Schizosaccharomyces pombe. BioEssays *12*, 189–191.

Moazed, D. (2009). Small RNAs in transcriptional gene silencing and genome defence. Nature *457*, 413–420.

Moore, M.J., and Proudfoot, N.J. (2009). Pre-mRNA processing reaches back to transcription and ahead to translation. Cell *136*, 688–700.

Morgunova, V., Akulenko, N., Radion, E., Olovnikov, I., Abramov, Y., Olenina, L.V., Shpiz, S., Kopytova, D.V., Georgieva, S.G., and Kalmykova, A. (2015). Telomeric repeat silencing in germ cells is essential for early development in Drosophila. Nucleic Acids Res. *43*, 8762–8773.

Motamedi, M.R., Verdel, A., Colmenares, S.U., Gerber, S.A., Gygi, S.P., and Moazed, D. (2004). Two RNAi Complexes, RITS and RDRC, Physically Interact and Localize to Noncoding Centromeric RNAs. Cell *119*, 789–802.

Motamedi, M.R., Hong, E.-J.E., Li, X., Gerber, S., Denison, C., Gygi, S., and Moazed, D. (2008). HP1 Proteins Form Distinct Complexes and Mediate Heterochromatic Gene Silencing by Nonoverlapping Mechanisms. Mol. Cell *32*, 778–790.

Müller, J., Hart, C.M., Francis, N.J., Vargas, M.L., Sengupta, A., Wild, B., Miller, E.L., O'Connor, M.B., Kingston, R.E., and Simon, J.A. (2002). Histone methyltransferase activity of a Drosophila Polycomb group repressor complex. Cell *111*, 197–208.

Murthy, K.G., and Manley, J.L. (1995). The 160-kD subunit of human cleavage-polyadenylation specificity factor coordinates pre-mRNA 3'-end formation. Genes Dev. *9*, 2672–2683.

Nakama, M., Kawakami, K., Kajitani, T., Urano, T., and Murakami, Y. (2012). DNA-RNA hybrid formation mediates RNAi-directed heterochromatin formation. Genes Cells Devoted Mol. Cell. Mech. *17*, 218–233.

Nakayama, J., Rice, J.C., Strahl, B.D., Allis, C.D., and Grewal, S.I. (2001). Role of histone H3 lysine 9 methylation in epigenetic control of heterochromatin assembly. Science *292*, 110–113.

Nasertorabi, F., Batisse, C., Diepholz, M., Suck, D., and Böttcher, B. (2011). Insights into the structure of the CCR4-NOT complex by electron microscopy. FEBS Lett. *585*, 2182–2186.

Noller, H.F. (1993). tRNA-rRNA interactions and peptidyl transferase. FASEB J. Off. Publ. Fed. Am. Soc. Exp. Biol. *7*, 87–89.

Noma, K. -i. (2001). Transitions in Distinct Histone H3 Methylation Patterns at the Heterochromatin Domain Boundaries. Science *293*, 1150–1155.

O'Neill, L.P., and Turner, B.M. (1995). Histone H4 acetylation distinguishes coding regions of the human genome from heterochromatin in a differentiation-dependent but transcription-independent manner. EMBO J. *14*, 3946–3957.

Parker, R., and Song, H. (2004). The enzymes and control of eukaryotic mRNA turnover. Nat. Struct. Mol. Biol. *11*, 121–127.

Passarge, E. (1979). Emil Heitz and the concept of heterochromatin: longitudinal chromosome differentiation was recognized fifty years ago. Am. J. Hum. Genet. *31*, 106–115.

Pefanis, E., Wang, J., Rothschild, G., Lim, J., Kazadi, D., Sun, J., Federation, A., Chao, J., Elliott, O., Liu, Z.-P., et al. (2015). RNA exosome-regulated long non-coding RNA transcription controls super-enhancer activity. Cell *161*, 774–789.

Peng, J.C., and Karpen, G.H. (2008). Epigenetic regulation of heterochromatic DNA stability. Curr. Opin. Genet. Dev. *18*, 204–211.

Peters, A.H.F.M., O'Carroll, D., Scherthan, H., Mechtler, K., Sauer, S., Schöfer, C., Weipoltshammer, K., Pagani, M., Lachner, M., Kohlmaier, A., et al. (2001). Loss of the Suv39h Histone Methyltransferases Impairs Mammalian Heterochromatin and Genome Stability. Cell *107*, 323–337.

Petit, A.-P., Wohlbold, L., Bawankar, P., Huntzinger, E., Schmidt, S., Izaurralde, E., and Weichenrieder, O. (2012). The structural basis for the interaction between the CAF1 nuclease and the NOT1 scaffold of the human CCR4-NOT deadenylase complex. Nucleic Acids Res. *40*, 11058–11072.

Piel, M., and Tran, P.T. (2009). Cell Shape and Cell Division in Fission Yeast. Curr. Biol. *19*, R823–R827.

Portela, A., and Esteller, M. (2010). Epigenetic modifications and human disease. Nat. Biotechnol. *28*, 1057–1068.

Pray, L.A. (2008). Discovery of DNA Structure and Function: Watson and Crick. Nat. Educ. *1*.

Prieto, E., Hizume, K., Kobori, T., Yoshimura, S.H., and Takeyasu, K. (2012). Core histone charge and linker histone H1 effects on the chromatin structure of Schizosaccharomyces pombe. Biosci. Biotechnol. Biochem. *76*, 2261–2266.

Ragunathan, K., Jih, G., and Moazed, D. (2015). Epigenetics. Epigenetic inheritance uncoupled from sequence-specific recruitment. Science *348*, 1258699.

Rea, S., Eisenhaber, F., O'Carroll, D., Strahl, B.D., Sun, Z.W., Schmid, M., Opravil, S., Mechtler, K., Ponting, C.P., Allis, C.D., et al. (2000). Regulation of chromatin structure by site-specific histone H3 methyltransferases. Nature *406*, 593–599.

Reinhart, B.J., and Bartel, D.P. (2002). Small RNAs correspond to centromere heterochromatic repeats. Science *297*, 1831.

Rhee, H.S., and Pugh, B.F. (2012). ChIP-exo method for identifying genomic location of DNA-binding proteins with near-single-nucleotide accuracy. Curr. Protoc. Mol. Biol. *Chapter 21*, Unit 21.24.

Rinn, J.L., Kertesz, M., Wang, J.K., Squazzo, S.L., Xu, X., Brugmann, S.A., Goodnough, L.H., Helms, J.A., Farnham, P.J., Segal, E., et al. (2007). Functional demarcation of active and silent chromatin domains in human HOX loci by noncoding RNAs. Cell *129*, 1311–1323.

Rosa, S., and Shaw, P. (2013). Insights into Chromatin Structure and Dynamics in Plants. Biology *2*, 1378–1410.

Rountree, M.R., and Selker, E.U. (2010). DNA methylation and the formation of heterochromatin in Neurospora crassa. Heredity *105*, 38–44.

Rutenberg-Schoenberg, M., Sexton, A.N., and Simon, M.D. (2016). The Properties of Long Noncoding RNAs That Regulate Chromatin. Annu. Rev. Genomics Hum. Genet. *17*, 69–94.

Sadeghi, L., Prasad, P., Ekwall, K., Cohen, A., and Svensson, J.P. (2015). The Paf1 complex factors Leo1 and Paf1 promote local histone turnover to modulate chromatin states in fission yeast. EMBO Rep. *16*, 1673–1687.

Sánchez, Y., and Huarte, M. (2013). Long non-coding RNAs: challenges for diagnosis and therapies. Nucleic Acid Ther. *23*, 15–20.

Sandler, H., Kreth, J., Timmers, H.T.M., and Stoecklin, G. (2011). Not1 mediates recruitment of the deadenylase Caf1 to mRNAs targeted for degradation by tristetraprolin. Nucleic Acids Res. *39*, 4373–4386.

Santos-Pereira, J.M., and Aguilera, A. (2015). R loops: new modulators of genome dynamics and function. Nat. Rev. Genet. *16*, 583–597.

Santos-Rosa, H., Schneider, R., Bannister, A.J., Sherriff, J., Bernstein, B.E., Emre, N.C.T., Schreiber, S.L., Mellor, J., and Kouzarides, T. (2002). Active genes are tri-methylated at K4 of histone H3. Nature *419*, 407–411.

Schalch, T., Job, G., Shanker, S., Partridge, J.F., and Joshua-Tor, L. (2011). The Chp1-Tas3 core is a multifunctional platform critical for gene silencing by RITS. Nat. Struct. Mol. Biol. *18*, 1351–1357.

Schlackow, M., Nojima, T., Gomes, T., Dhir, A., Carmo-Fonseca, M., and Proudfoot, N.J. (2017). Distinctive Patterns of Transcription and RNA Processing for Human lincRNAs. Mol. Cell *65*, 25–38.

Schwartz, Y.B., Kahn, T.G., Nix, D.A., Li, X.-Y., Bourgon, R., Biggin, M., and Pirrotta, V. (2006). Genome-wide analysis of Polycomb targets in Drosophila melanogaster. Nat. Genet. *38*, 700–705.

Serandour, A.A., Brown, G.D., Cohen, J.D., and Carroll, J.S. (2013). Development of an Illumina-based ChIP-exonuclease method provides insight into FoxA1-DNA binding properties. Genome Biol. *14*, R147.

Sheets, M.D., and Wickens, M. (1989). Two phases in the addition of a poly(A) tail. Genes Dev. *3*, 1401–1412.

Sienski, G., Dönertas, D., and Brennecke, J. (2012). Transcriptional silencing of transposons by Piwi and maelstrom and its impact on chromatin state and gene expression. Cell *151*, 964–980.

Skourti-Stathaki, K., Kamieniarz-Gdula, K., and Proudfoot, N.J. (2014). R-loops induce repressive chromatin marks over mammalian gene terminators. Nature *516*, 436–439.

Slotkin, R.K., and Martienssen, R. (2007). Transposable elements and the epigenetic regulation of the genome. Nat. Rev. Genet. *8*, 272–285.

Smith, E.R., Pannuti, A., Gu, W., Steurnagel, A., Cook, R.G., Allis, C.D., and Lucchesi, J.C. (2000). The drosophila MSL complex acetylates histone H4 at lysine 16, a chromatin modification linked to dosage compensation. Mol. Cell. Biol. *20*, 312–318.

Smothers, J.F., and Henikoff, S. (2000). The HP1 chromo shadow domain binds a consensus peptide pentamer. Curr. Biol. CB *10*, 27–30.

Snowden, A.W., Gregory, P.D., Case, C.C., and Pabo, C.O. (2002). Gene-specific targeting of H3K9 methylation is sufficient for initiating repression in vivo. Curr. Biol. CB *12*, 2159–2166.

Soruco, M.M.L., Chery, J., Bishop, E.P., Siggers, T., Tolstorukov, M.Y., Leydon, A.R., Sugden, A.U., Goebel, K., Feng, J., Xia, P., et al. (2013). The CLAMP protein links the MSL complex to the X chromosome during Drosophila dosage compensation. Genes Dev. *27*, 1551–1556.

St-André, O., Lemieux, C., Perreault, A., Lackner, D.H., Bähler, J., and Bachand, F. (2010). Negative regulation of meiotic gene expression by the nuclear poly(a)-binding protein in fission yeast. J. Biol. Chem. *285*, 27859–27868.

Stevens, A., and Maupin, M.K. (1987). A 5'----3' exoribonuclease of human placental nuclei: purification and substrate specificity. Nucleic Acids Res. *15*, 695–708.

Stirling, P.C., Chan, Y.A., Minaker, S.W., Aristizabal, M.J., Barrett, I., Sipahimalani, P., Kobor, M.S., and Hieter, P. (2012). R-loop-mediated genome instability in mRNA cleavage and polyadenylation mutants. Genes Dev. *26*, 163–175.

Stowell, J.A.W., Webster, M.W., Kögel, A., Wolf, J., Shelley, K.L., and Passmore, L.A. (2016). Reconstitution of Targeted Deadenylation by the Ccr4-Not Complex and the YTH Domain Protein Mmi1. Cell Rep. *17*, 1978–1989.

Strahl, B.D., and Allis, C.D. (2000). The language of covalent histone modifications. Nature *403*, 41–45.

Sugiyama, T., and Sugioka-Sugiyama, R. (2011). Red1 promotes the elimination of meiosis-specific mRNAs in vegetatively growing fission yeast. EMBO J. *30*, 1027–1039.

Sugiyama, T., Cam, H., Verdel, A., Moazed, D., and Grewal, S.I.S. (2005). From The Cover: RNA-dependent RNA polymerase is an essential component of a self-enforcing loop coupling heterochromatin assembly to siRNA production. Proc. Natl. Acad. Sci. *102*, 152–157.

Sugiyama, T., Cam, H.P., Sugiyama, R., Noma, K., Zofall, M., Kobayashi, R., and Grewal, S.I.S. (2007). SHREC, an Effector Complex for Heterochromatic Transcriptional Silencing. Cell *128*, 491–504.

Sugiyama, T., Thillainadesan, G., Chalamcharla, V.R., Meng, Z., Balachandran, V., Dhakshnamoorthy, J., Zhou, M., and Grewal, S.I.S. (2016). Enhancer of Rudimentary Cooperates with Conserved RNA-Processing Factors to Promote Meiotic mRNA Decay and Facultative Heterochromatin Assembly. Mol. Cell *61*, 747–759.

Sun, Q., Csorba, T., Skourti-Stathaki, K., Proudfoot, N.J., and Dean, C. (2013). R-loop stabilization represses antisense transcription at the Arabidopsis FLC locus. Science *340*, 619–621.

Suzuki, A., Igarashi, K., Aisaki, K.-I., Kanno, J., and Saga, Y. (2010). NANOS2 interacts with the CCR4-NOT deadenylation complex and leads to suppression of specific RNAs. Proc. Natl. Acad. Sci. U. S. A. *107*, 3594–3599.

Taddei, A., Maison, C., Roche, D., and Almouzni, G. (2001). Reversible disruption of pericentric heterochromatin and centromere function by inhibiting deacetylases. Nat. Cell Biol. *3*, 114–120.

Tadeo, X., Wang, J., Kallgren, S.P., Liu, J., Reddy, B.D., Qiao, F., and Jia, S. (2013). Elimination of shelterin components bypasses RNAi for pericentric heterochromatin assembly. Genes Dev. *27*, 2489–2499.

Takeda, T., Toda, T., Kominami, K., Kohnosu, A., Yanagida, M., and Jones, N. (1995). Schizosaccharomyces pombe atf1+ encodes a transcription factor required for sexual development and entry into stationary phase. EMBO J. *14*, 6193–6208.

Temme, C., Zhang, L., Kremmer, E., Ihling, C., Chartier, A., Sinz, A., Simonelig, M., and Wahle, E. (2010). Subunits of the Drosophila CCR4-NOT complex and their roles in mRNA deadenylation. RNA N. Y. N *16*, 1356–1370.

Thakurta, A.G., Gopal, G., Yoon, J.H., Kozak, L., and Dhar, R. (2005). Homolog of BRCA2-interacting Dss1p and Uap56p link Mlo3p and Rae1p for mRNA export in fission yeast. EMBO J. *24*, 2512–2523.

Thanbichler, M., Wang, S.C., and Shapiro, L. (2005). The bacterial nucleoid: A highly organized and dynamic structure. J. Cell. Biochem. *96*, 506–521.

Thon, G., and Klar, A.J. (1992). The clr1 locus regulates the expression of the cryptic mating-type loci of fission yeast. Genetics *131*, 287–296.

Thore, S., Mauxion, F., Séraphin, B., and Suck, D. (2003). X-ray structure and activity of the yeast Pop2 protein: a nuclease subunit of the mRNA deadenylase complex. EMBO Rep. *4*, 1150–1155.

Tóth, K.F., Pezic, D., Stuwe, E., and Webster, A. (2016). The piRNA Pathway Guards the Germline Genome Against Transposable Elements. Adv. Exp. Med. Biol. *886*, 51–77.

Trojer, P., and Reinberg, D. (2007). Facultative Heterochromatin: Is There a Distinctive Molecular Signature? Mol. Cell *28*, 1–13.

Tucker, J.F., Ohle, C., Schermann, G., Bendrin, K., Zhang, W., Fischer, T., and Zhang, K. (2016). A Novel Epigenetic Silencing Pathway Involving the Highly Conserved 5'-3' Exoribonuclease Dhp1/Rat1/Xrn2 in Schizosaccharomyces pombe. PLoS Genet. *12*, e1005873.

Tucker, M., Valencia-Sanchez, M.A., Staples, R.R., Chen, J., Denis, C.L., and Parker, R. (2001). The transcription factor associated Ccr4 and Caf1 proteins are components of the major cytoplasmic mRNA deadenylase in Saccharomyces cerevisiae. Cell *104*, 377–386.

Tucker, M., Staples, R.R., Valencia-Sanchez, M.A., Muhlrad, D., and Parker, R. (2002). Ccr4p is the catalytic subunit of a Ccr4p/Pop2p/Notp mRNA deadenylase complex in Saccharomyces cerevisiae. EMBO J. *21*, 1427–1436.

Ukleja, M., Cuellar, J., Siwaszek, A., Kasprzak, J.M., Czarnocki-Cieciura, M., Bujnicki, J.M., Dziembowski, A., and Valpuesta, J.M. (2016). The architecture of the Schizosaccharomyces pombe CCR4-NOT complex. Nat. Commun. *7*, 10433.

Ulrich, A., Andersen, K.R., and Schwartz, T.U. (2012). Exponential megapriming PCR (EMP) cloning--seamless DNA insertion into any target plasmid without sequence constraints. PloS One *7*, e53360.

Venters, B.J., Wachi, S., Mavrich, T.N., Andersen, B.E., Jena, P., Sinnamon, A.J., Jain, P., Rolleri, N.S., Jiang, C., Hemeryck-Walsh, C., et al. (2011). A comprehensive genomic binding map of gene and chromatin regulatory proteins in Saccharomyces. Mol. Cell *41*, 480–492.

Verdel, A., Jia, S., Gerber, S., Sugiyama, T., Gygi, S., Grewal, S.I.S., and Moazed, D. (2004). RNAi-mediated targeting of heterochromatin by the RITS complex. Science *303*, 672–676.

Verrier, L., Taglini, F., Barrales, R.R., Webb, S., Urano, T., Braun, S., and Bayne, E.H. (2015). Global regulation of heterochromatin spreading by Leo1. Open Biol. *5*.

Volpe, T.A., Kidner, C., Hall, I.M., Teng, G., Grewal, S.I.S., and Martienssen, R.A. (2002). Regulation of heterochromatic silencing and histone H3 lysine-9 methylation by RNAi. Science *297*, 1833–1837.

Wahba, L., Gore, S.K., and Koshland, D. (2013). The homologous recombination machinery modulates the formation of RNA-DNA hybrids and associated chromosome instability. eLife *2*, e00505.

Wang, J., Cohen, A.L., Letian, A., Tadeo, X., Moresco, J.J., Liu, J., Yates, J.R., Qiao, F., and Jia, S. (2016). The proper connection between shelterin components is required for telomeric heterochromatin assembly. Genes Dev. *30*, 827–839.

Wang, L., Mizzen, C., Ying, C., Candau, R., Barlev, N., Brownell, J., Allis, C.D., and Berger, S.L. (1997). Histone acetyltransferase activity is conserved between yeast and human GCN5 and is required for complementation of growth and transcriptional activation. Mol. Cell. Biol. *17*, 519–527.

Wang, S.-W., Stevenson, A.L., Kearsey, S.E., Watt, S., and Bähler, J. (2008). Global role for polyadenylation-assisted nuclear RNA degradation in posttranscriptional gene silencing. Mol. Cell. Biol. *28*, 656–665.

Watanabe, Y., and Yamamoto, M. (1996). Schizosaccharomyces pombe pcr1+ encodes a CREB/ATF protein involved in regulation of gene expression for sexual development. Mol. Cell. Biol. *16*, 704–711.

Watson, J.D., and Crick, F.H. (1953). The structure of DNA. Cold Spring Harb. Symp. Quant. Biol. *18*, 123–131.

Wecker, E. (1959). The extraction of infectious virus nucleic acid with hot phenol. Virology *7*, 241–243.

Wilkinson, M.G., Samuels, M., Takeda, T., Toone, W.M., Shieh, J.C., Toda, T., Millar, J.B., and Jones, N. (1996). The Atf1 transcription factor is a target for the Sty1 stress-activated MAP kinase pathway in fission yeast. Genes Dev. *10*, 2289–2301.

Winkler, G.S. (2010). The mammalian anti-proliferative BTG/Tob protein family. J. Cell. Physiol. *222*, 66–72.

Wixon, J. (2002). Featured Organism: Schizosaccharomyces pombe, The Fission Yeast. Comp. Funct. Genomics *3*, 194–204.

Wood, V., Gwilliam, R., Rajandream, M.-A., Lyne, M., Lyne, R., Stewart, A., Sgouros, J., Peat, N., Hayles, J., Baker, S., et al. (2002). The genome sequence of Schizosaccharomyces pombe. Nature *415*, 871–880.

Wright, M.W., and Bruford, E.A. (2011). Naming "junk": human non-protein coding RNA (ncRNA) gene nomenclature. Hum. Genomics *5*, 90–98.

Xu, G.L., Bestor, T.H., Bourc'his, D., Hsieh, C.L., Tommerup, N., Bugge, M., Hulten, M., Qu, X., Russo, J.J., and Viegas-Péquignot, E. (1999). Chromosome instability and immunodeficiency syndrome caused by mutations in a DNA methyltransferase gene. Nature *402*, 187–191.

Xu, K., Bai, Y., Zhang, A., Zhang, Q., and Bartlam, M.G. (2014). Insights into the structure and architecture of the CCR4-NOT complex. Front. Genet. *5*, 137.

Yamada, T., Fischle, W., Sugiyama, T., Allis, C.D., and Grewal, S.I.S. (2005). The nucleation and maintenance of heterochromatin by a histone deacetylase in fission yeast. Mol. Cell *20*, 173–185.

Yamashita, A., Chang, T.-C., Yamashita, Y., Zhu, W., Zhong, Z., Chen, C.-Y.A., and Shyu, A.-B. (2005). Concerted action of poly(A) nucleases and decapping enzyme in mammalian mRNA turnover. Nat. Struct. Mol. Biol. *12*, 1054–1063.

Yamashita, A., Shichino, Y., and Yamamoto, M. (2016). The long non-coding RNA world in yeasts. Biochim. Biophys. Acta *1859*, 147–154.

Yu, R., Jih, G., Iglesias, N., and Moazed, D. (2014). Determinants of heterochromatic siRNA biogenesis and function. Mol. Cell *53*, 262–276.

Zeller, P., Padeken, J., van Schendel, R., Kalck, V., Tijsterman, M., and Gasser, S.M. (2016). Histone H3K9 methylation is dispensable for Caenorhabditis elegans development but suppresses RNA:DNA hybrid-associated repeat instability. Nat. Genet. *48*, 1385–1395.

Zeng, L., and Zhou, M.M. (2002). Bromodomain: an acetyl-lysine binding domain. FEBS Lett. *513*, 124–128.

Zentner, G.E., and Henikoff, S. (2013). Regulation of nucleosome dynamics by histone modifications. Nat. Struct. Mol. Biol. *20*, 259–266.

Zhang, K., Mosch, K., Fischle, W., and Grewal, S.I.S. (2008). Roles of the Clr4 methyltransferase complex in nucleation, spreading and maintenance of heterochromatin. Nat. Struct. Mol. Biol. *15*, 381–388.

Zhang, K., Fischer, T., Porter, R.L., Dhakshnamoorthy, J., Zofall, M., Zhou, M., Veenstra, T., and Grewal, S.I.S. (2011). Clr4/Suv39 and RNA quality control factors cooperate to trigger RNAi and suppress antisense RNA. Science *331*, 1624–1627.

Zhang, X., Virtanen, A., and Kleiman, F.E. (2010). To polyadenylate or to deadenylate: That is the question. Cell Cycle *9*, 4437–4449.

Zofall, M., Yamanaka, S., Reyes-Turcu, F.E., Zhang, K., Rubin, C., and Grewal, S.I.S. (2012). RNA elimination machinery targeting meiotic mRNAs promotes facultative heterochromatin formation. Science *335*, 96–100.

8. Acknowledgment

I would like to thank Mario Halic, for giving me the opportunity to carry out this work in an excellent scientific environment, and constantly provided incredible advice and support. I appreciate especially the great discussions which opened new insights and perspectives to different scientific topics. Additionally I would like to thank Mario for the possibilities to participate at several conferences and to be involved in teaching.

I also wish to thank all current and past members of the Halic group for their support and contribution to this work. It is great that I had the chance to work in this international team, which felt like working abroad although living at home. I've learned a lot about different languages, cultures and ways to communicate in other countries.
In particular I want to thank Manuel Zocco, Luca Salvi, Ilaria Ugolini and Paola Pisacane for contributing directly to this thesis with experiments. Furthermore I wish to thank Mirela Marasovic for introducing me to the common lab methods at the beginning of my PhD. A special thanks goes to Sigrun Jaklin for being a great help in any concerns as well as to Silvija Bilokapic for always having an open ear and great ideas to improve experiments.
I would also like to express my gratitude to Stefan Krebs from LAFUGA for all the support in sequencing my thousand libraries.
I am also grateful for the possibility to supervise several great students during my PhD. Thank you for your support: Maike Becker, Adriana Savova, Marco Rinn and Carolina Carradinha! Also thank you Alrun Basfeld for doing several initial experiments under the supervision of Manuel Zocco.

A special thank goes also to Prof. Dr. Klaus Förstemann for being my second evaluator but also for providing our lab with several protocols and material. And I would also like to thank Prof. Dr. Elena Conti, Dr. Dietmar Martin, Prof. Julien Gagneur and Prof. Dr. Ulrike Gaul for building my examination board for the oral defense.
Additionally I would like to thank all Gene Center colleagues, in particular the 4th floor people (AG Hopfner and AG Cramer), for the nice kitchen, elevator and floor discussions and support with materials or protocols. Especially "thank you" Florian Schlauderer for proofreading my thesis. Also thanks to the Gagneur lab for fantastic table soccer tournaments, it was always great fun with you!
Furthermore, I would also like to thank Frau Schams for sharing the parking lot.

The biggest and most cordially thanks goes to my family. Thanks to my parents Michaela und Rudolf Brönner and all my sisters (Elisabeth, Martina and Veronika) for endless support and

love. Thanks to my niece and nephews for showing me the things which really matter in life. And a special thanks to my husband Jojo for always being supportive and helpful and for being such a great person. I have the best family possible and I love you all!